PL-TR-92-2090 SSS-FR-92-13150

Demonstration of Regional Discrimination of Eurasian Seismic Events Using Observations at Soviet IRIS and CDSN Stations

Theron J. Bennett
Antoinette K. Campanella
James F. Scheimer
John R. Murphy

Maxwell Laboratories, Incorporated
S-CUBED Division
P.O. Box 1620
La Jolla, CA 92038-1620

March, 1992

Final Report
29 March 1989-28 March 1992

Phillips Laboratory
Air Force Systems Command
Hanscom Air Force Base, MA 01731-5000

SPONSORED BY
Defense Advanced Research Projects Agency
Nuclear Monitoring Research Office
ARPA ORDER NO. 5307

MONITORED BY
Phillips Laboratory
Contract F19628-89-C-0043

This technical report has been reviewed and is approved for publication.

JAMES F. LEWKOWICZ
Contract Manager
Solid Earth Geophysics Branch
Earth Sciences Division

JAMES F. LEWKOWICZ
Branch Chief
Solid Earth Geophysics Branch
Earth Sciences Division

DONALD H. ECKHARDT, Director
Earth Sciences Division

This report has been reviewed by the ESD Public Affairs Office (PA) and is releasable to the National Technical Information Service (NTIS).

Qualified requestors may obtain additional copies from the Defense Technical Information Center. All others should apply to the National Technical Information Service.

If your address has changed, or if you wish to be removed from the mailing list, or if the addressee is no longer employed by your organization, please notify PL/IMA, Hanscom AFB, MA 01731-5000. This will assist us in maintaining a current mailing list.

Do not return copies of this report unless contractual obligations or notices on a specific document requires that it be returned.

REPORT DOCUMENTATION PAGE

Form Approved OMB No. 0704-0188

1. AGENCY USE ONLY *(Leave blank)*	2. REPORT DATE	3. REPORT TYPE AND DATES COVERED
	March, 1992	Final Report (3/29/89 - 3/28/92)

4. TITLE AND SUBTITLE
Demonstration of Regional Discrimination of Eurasian Seismic Events Using Observations at Soviet IRIS and CDSN Stations

5. FUNDING NUMBERS
F19628-89-C-0043
PE 62714 E
PR 9A10 TA OA WU BG

6. AUTHOR(S)
Theron J. Bennett, Antoinette K. Campanella, James F. Scheimer and John R. Murphy

7. PERFORMING ORGANIZATION NAME(S) AND ADDRESS(ES)
Maxwell Laboratories, Inc.
S-CUBED Division
P.O. Box 1620
La Jolla, CA 92038-1620

8. PERFORMING ORGANIZATION REPORT NUMBER
SSS-FR-92-13150

9. SPONSORING/MONITORING AGENCY NAME(S) AND ADDRESS(ES)
Phillips Laboratory
Hanscom AFB, MA 01731-5000

Contract Manager: James Lewkowicz/GPEH

10. SPONSORING/MONITORING AGENCY REPORT NUMBER
PL-TR-92-2090

11. SUPPLEMENTARY NOTES

12a. DISTRIBUTION/AVAILABILITY STATEMENT
Approved for public release; distribution unlimited

12b. DISTRIBUTION CODE

13. ABSTRACT *(Maximum 200 words)*

This study has brought together a large, high-quality database of regional signals from Eurasian seismic events, including 38 underground nuclear explosions and 68 earthquakes, recorded at Soviet IRIS and CDSN stations. Characteristics of regional phases observed at each of the Soviet IRIS stations and their relation to propagation and source effects have been analyzed. The high quality of the signals indicates the strong potential of the stations for monitoring events throughout Eurasia. A variety of amplitude and spectral measurements have been performed on the regional signals to discern differences related to source type. We find here differences in L_g/P amplitude ratios and L_g/P spectral ratios between underground nuclear explosions and earthquakes. The fact that such differences are observed for explosions and earthquakes with practically identical propagation paths provides strong evidence that the observed behavior is dependent on source type. However, the regional phase amplitudes and spectral behavior also are affected by geologic structure along the propagation path. A

(continued on reverse)

14. SUBJECT TERMS				15. NUMBER OF PAGES
Seismic	Eurasia	Earthquakes	IRIS	122
Discrimination	Soviet Explosions	Spectra	CDSN	16. PRICE CODE
Regional Phases	Chinese Explosions			

17. SECURITY CLASSIFICATION OF REPORT	18. SECURITY CLASSIFICATION OF THIS PAGE	19. SECURITY CLASSIFICATION OF ABSTRACT	20. LIMITATION OF ABSTRACT
Unclassified	Unclassified	Unclassified	Unlimited

CLASSIFIED BY:

DECLASSIFY ON:

13. ABSTRACT (Continued)

methodology for identifying and adjusting the observations for such propagation effects is described. Similarity of signals for events of a common source type suggests that discriminants effective for some events are likely to work for others from the same general area.

Accession For	
NTIS GRA&I	☑
DTIC TAB	☐
Unannounced	☐
Justification	
By	
Distribution/	
Availability Codes	
Dist	Avail and/or Special
A-1	

Table of Contents

List of Illustrations

I. INTRODUCTION

1.1 Background

Seismic techniques have long been recognized as important tools for monitoring underground nuclear weapons testing. Teleseismic monitoring, using stations beyond about 3000 km, generally has proven to be quite adequate for detecting and identifying larger events in areas of interest where there was a potential for such testing. In fact, identification capability for seismic events in the former Soviet Union using teleseismic monitoring networks is believed to extend down to a magnitude threshold near 4.0 which corresponds to a yield threshold near one kiloton for a well-coupled nuclear explosion. In addition, a long-standing goal of the DARPA research program in nuclear explosion monitoring has been to reduce the identification magnitude threshold to lower levels through the utilization of observations at regional seismic stations. Unfortunately, this goal has proven to be elusive because of the complexity of regional signals, their dependence on propagation effects, and incomplete understanding of source influences on regional signal generation.

Over the past decade, S-CUBED has conducted a systematic research program designed to improve regional seismic discrimination capability. This research program has produced a number of significant findings derived from both empirical observations and theoretical analyses of regional seismic signals. We focus here on the latest results of the empirical investigations directed at discrimination of Eurasian seismic events recorded at regional distances by Soviet stations in the Incorporated Research Institutions for Seismology (IRIS) network and by selected stations in the Chinese Digital Seismic Network (CDSN). As described in the report, the high-quality regional data collected from these stations provide a valuable resource for monitoring seismic activity throughout much of Eurasia and for testing regional discrimination methodology in these areas.

1.2 Prior Research Findings

Over the years a variety of regional discrimination methods have been proposed as potential techniques for seismic monitoring of underground nuclear weapons testing. In many cases these methods were tested on ad hoc databases of inconsistent quality; so it was difficult to evaluate the relative merits of different techniques. Furthermore, the regional data sample used to test the methods was in most cases drawn from events in the western U.S.; and it was uncertain to what extent this experience could be extended into other regions. As part of a systematic effort to identify the most reliable regional discrimination methods and to extend them to monitoring of Eurasian events, S-CUBED began assembling more than ten years ago a high-quality digital database of explosions and earthquakes which could be used to test potential regional discriminant measures. Early investigations (cf. Murphy and Bennett, 1982; Bennett and Murphy, 1986) focused on well-controlled explosions and earthquakes from the common source area near the Nevada Test Site. The idea behind these studies was to identify the most robust regional discriminants and then to define procedures which would enable extending those discrimination methods into uncalibrated regions, such as the Soviet Union. One of the principal findings of this research was the discovery of a new discriminant based on spectral differences in the regional phase signals between nuclear explosion tests and earthquakes, which has subsequently been confirmed by other investigators. In particular, L_g signals for earthquakes were found to be relatively enriched in high frequencies compared to nearby nuclear explosions with comparable magnitude and comparable regional P spectra recorded at the VELA array stations. On the negative side, these studies also suggested that L_g/P amplitude ratios measured in the time domain were not always definitive as discriminant measures. We have subsequently concluded that this latter observation may have been controlled to some extent by limitations on the frequency band of the seismic recording instruments,

emphasizing the need for broad-band recording of regional signals for use in discrimination monitoring.

Starting in the early 1980's, S-CUBED also conducted investigations of the monitoring capability of far-regional stations in Eurasia for discrimination of events in the former Soviet Union. These studies identified the general character of regional signals and pointed out propagation factors which could potentially affect monitoring capability at those sites, including zones of blockage of regional phases associated with tectonic structures in several areas along the southern Soviet border. In addition, a number of amplitude and spectral measures of regional signals, including P and L_g, were tested on the limited data available at such far-regional stations from events in the vicinity of the principal Soviet test area near Semipalatinsk with somewhat ambiguous results. These measurements included the L_g spectral ratio discriminant which appeared to work so well for events in the western U.S. The ambiguity of the results for these early studies of Soviet events was in no small measure attributable to poor data quality and limited bandwidth of the usable signals at these relatively distant stations. More recently, S-CUBED's studies of regional discrimination capabilities for events in the former Soviet Union have focused on the utilization of data from stations installed since 1986 in the Chinese Digital Seismic Network (CDSN) and since 1988 in the Soviet IRIS network. These stations represent a significant improvement for regional monitoring from two standpoints: (1) the availability of high-quality digital data permitted reliable analysis of the frequency characteristics of the regional signals over a broad range of frequencies not previously available in analog recordings from this area; and (2) the locations of the stations at regional distances, instead of far-regional and teleseismic, enabled observation of more typical regional signals whose frequency content and signal energy had been less severely altered by propagation effects. Initial analyses of data from these new sources recorded at CDSN station WMQ revealed differences in L_g/P spectral ratios between Soviet underground nuclear explosions and earthquakes at comparable ranges (cf. Bennett *et al.*, 1989). Furthermore, these studies found that the differences were often enhanced in certain

frequency bands emphasizing again the need for broad-band recording and signal content. The results from WMQ marked L_g/P spectral ratios as a potentially valuable regional discriminant measure for Eurasian events.

An important product of the S-CUBED regional discrimination research program has been the creation of a large digital database of regional phase signals from a variety of tectonic environments. This database includes approximately 2000 waveforms extending from prior to P through the L_g window for some 400 events. Events of all seismic source types are represented in the database which includes underground nuclear explosion tests, earthquakes, mine blasts, and rockbursts in mines. The events cover a wide range of tectonic environments including the Soviet Union and neighboring countries, the western U.S., eastern and central North America, and southern Asia. The data are generally of high quality and represent well-recorded regional phase signals. The database should provide a valuable resource for testing alternative regional discriminant measures in a variety of tectonic environments.

1.3 Summary of the Current Research Program

The first phase of the current research program was directed at assembling a large database of events covering a range of tectonic environments throughout Eurasia which could be used to assess the characteristics of regional phase signals across the region. This large, carefully selected sample includes 38 underground nuclear explosion and 68 earthquakes recorded at Soviet IRIS and CDSN stations. In a previous study we described the characteristics of the regional signals at the CDSN stations in some detail. Here we have analyzed the regional phase behavior for suites of events surrounding each of the four Soviet IRIS stations, ARU, GAR, OBN and KIV. For each station we have described the characteristics of the regional P and L_g signals and have considered the evidence for possible blockage of L_g by tectonic structure, particularly in the vicinity of the Caspian and Black seas. We find that the regional signals observed at the

Soviet IRIS stations are remarkably similar for events of a common source type even if the events are somewhat separated. Overall, the good quality of the regional signals at these stations from events throughout much of Eurasia indicates they could be of great value for seismic monitoring in these areas. In addition, the database already assembled can provide an important contribution to understanding propagation and extending regional discrimination techniques into new areas.

A primary goal of this research program has been to investigate the feasibility of using high-quality regional data from stations like those in the Soviet IRIS and CDSN networks to discriminate Eurasian events. In preliminary studies, using mainly observations made at the CDSN station WMQ, we had found that Soviet nuclear explosions in the vicinity of the test site near Semipalatinsk could be separated from comparable earthquakes, located mainly along the southern Soviet border and in western China, on the basis of L_g/P amplitude ratios and L_g/P spectral ratios. However, this result remained somewhat ambiguous because of the differences in locations between the different sources analyzed and the possible effects of propagation path on the regional signals which were used in that study. Therefore, an important result of the research reported here is the finding that different event types with nearly identical propagation paths also show differences in these broadband L_g/P amplitude ratios and L_g/P spectral ratios. We found these differences for a carefully selected sample of regional phase recordings from a Lop Nor, China explosion observed at the IRIS station GAR and two earthquakes near GAR for which the path to the CDSN station WMQ is approximately reciprocal. More convincingly, similar differences in the L_g/P ratios were observed at IRIS stations GAR and ARU for Lop Nor explosions and nearly co-located earthquakes. We argue here that this evidence provides a convincing case that the differences seen in broadband L_g/P amplitude ratios and L_g/P spectral ratios between underground nuclear explosions and earthquakes can be attributed to the different source types.

In addition to these findings, we have investigated several additional aspects of the regional discrimination problem for Eurasian events. In particular, we performed a thorough analysis of the L_g/P amplitude ratios and L_g/P spectral ratios observed at station ARU for a large sample of Semipalatinsk explosions and regional earthquakes. The results indicated that earthquake L_g/P ratios were normally higher than for the explosions; and the L_g/P spectral ratios were on average greater at higher frequencies for the earthquakes than for the explosions. We also investigated regional discrimination capability for selected events in the vicinity of the Semipalatinsk test site for which we were able to assemble data from a larger regional network. The latter suggested that single station discriminant measurements may in some cases provide deceptive or ambiguous results which could be rectified by the larger network observations. Finally, the results presented here and in previous studies have indicated the significant effects propagation path differences may have on regional phase observations. We have considered in this report an approach which could be used to adjust regional discriminant measurements, such as L_g/P spectral ratios, for the effects of propagation.

1.4 Report Organization

The report is organized into six sections including this introduction. Section II contains a review of the general characteristics of the seismic waveform data at each of the Soviet IRIS stations for all the Eurasian events in the database. Properties of the regional phases, including regional P and L_g, are analyzed and possible influences of propagation path on the signals are described. In Section III we analyze more closely the regional signals from the large database of Eurasian events observed at station ARU; and we make regional discriminant measurements on the signals including L_g/P and L_g/P spectral ratios. In Section IV regional discrimination results for explosions and earthquakes with nearly common paths are presented which demonstrate that differences are associated with the source type. In addition, possible corrections to the discriminant measures to account for propagation

differences are analyzed. Section V contains the results of application of the L_g/P and L_g/P spectral ratio discriminants to events in close proximity to the Semipalatinsk test site and considers how larger regional networks might improve discrimination capability. Finally, in Section VI we summarize the main results of these studies and present some specific plans for utilizing the valuable database which has already been collected to extend and improve regional discrimination capabilities throughout Eurasia, including areas where nuclear weapons proliferation may be a cause for concern in the future.

II. THE REGIONAL DATABASE FOR EURASIAN EVENTS

2.1 The Regional Monitoring Network for Eurasia

One of the primary objectives of this research program has been to determine the characteristics of regional seismic signals for events covering a range of tectonic environments throughout Eurasia. To investigate this problem we have relied on data recorded by two high-quality digital seismic networks. The first was the Chinese Digital Seismic Network (CDSN) established in late 1986, and the second was the Soviet IRIS network initiated in the fall of 1988. Figure 1 shows the locations of stations currently operating in these two networks. The CDSN network has relied primarily on automatic triggering for recording of seismic events; although recently a few stations have been upgraded to continuous recording. In our analyses of the CDSN observations we utilized data mainly from two stations, WMQ and HIA, the stations nearest the southern Soviet border. As we have described in previous reports, these two stations are the only CDSN stations which produce good regional records through the L_g window for Soviet nuclear explosions and other events along the border. Our previous reports described in detail the characteristics of the regional signals observed at WMQ and HIA, analyzed the transmission path properties for L_g signals to these stations, and thoroughly investigated regional phase signals at WMQ for seismic discrimination of Soviet underground nuclear explosions and nearby earthquakes.

In this report we will focus on regional signal observations from the Soviet IRIS stations. In particular, we will be analyzing the signals from Eurasian seismic events recorded at four stations: ARU, GAR, OBN and KIV. The additional Soviet IRIS stations have only recently started producing data on a routine basis, so the database available from these new stations is too limited for meaningful analyses at this time. The Soviet IRIS

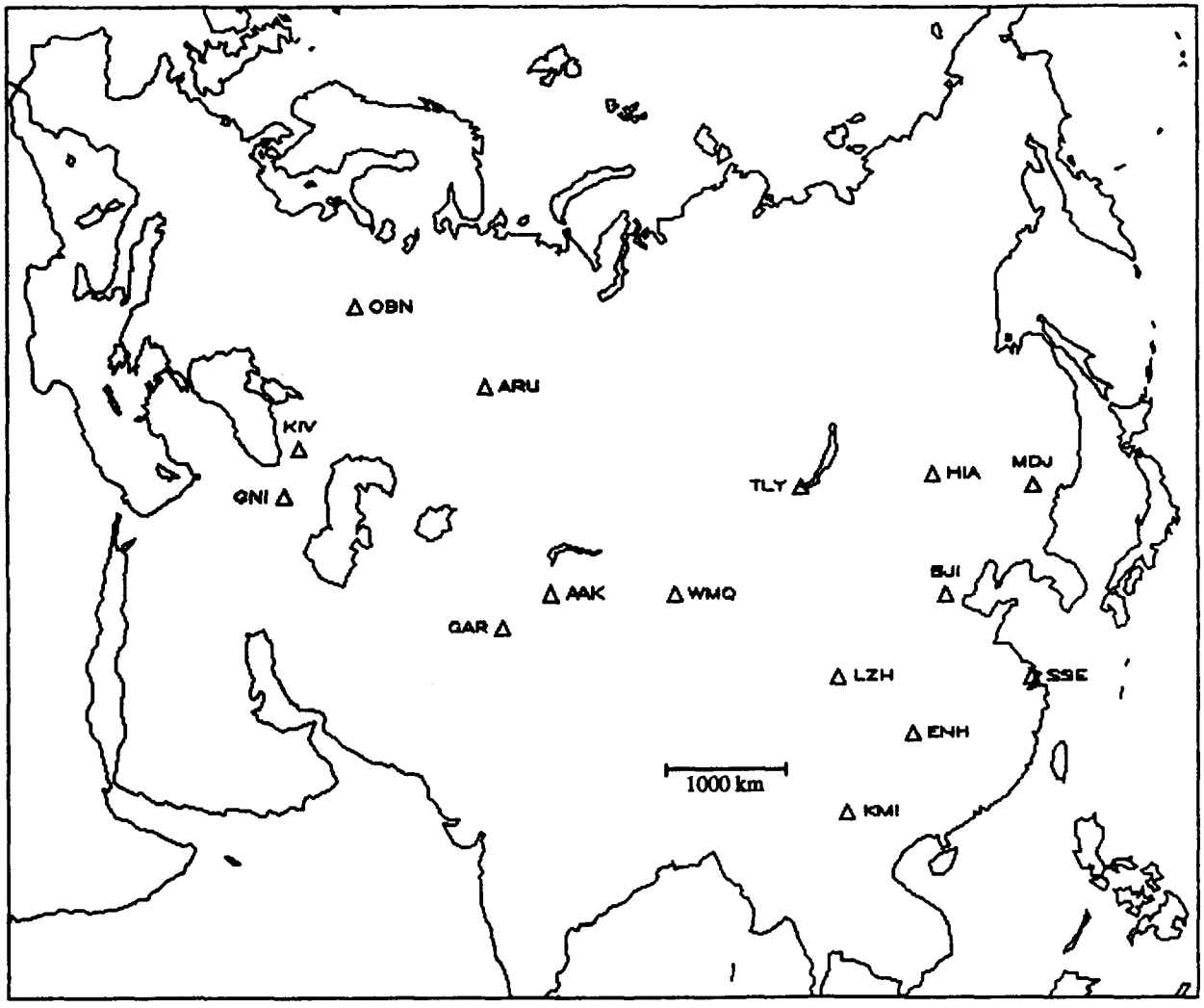

Figure 1. Currently operational stations of the Soviet IRIS and CDSN network.

stations include high-quality, broad-band three-component systems with digital recording at sampling rates of 20 samples per second. The stations also include lower-frequency elements with lower sampling rates, but these have not been used in the current study. For each of these Soviet IRIS stations, we compiled a database of regional waveforms from all available Soviet underground nuclear explosions and a large sample of well-recorded earthquakes from various tectonic environments at magnitude and epicentral distance ranges which overlap for the two different source types. In all cases we tried to select only events which produced identifiable signals extending from P through L_g on the broad-band records for at least one station in the two networks. The database thus provides an excellent source of high-quality regional signals for testing regional discrimination methods.

2.2 Overall Properties of the Database

The combined sample of regional events recorded at the CDSN and Soviet IRIS network stations includes 38 underground nuclear explosions and 68 earthquakes. The locations of these events are plotted in Figure 2. The underground nuclear explosions for which regional recordings are available were located in four different areas. The largest concentration of underground nuclear explosions with regional recordings from the Soviet IRIS and CDSN stations is the cluster near Semipalatinsk (including Shagan River and Degelen Mountain events). In addition, the database includes one underground nuclear explosion at the Novaya Zemlya test site, two explosions from the Chinese Lop Nor test site, and three PNE's in eastern Siberia.

The earthquakes in the database are located primarily in the more active tectonic areas along the southern Soviet border. The heavier concentration of events in western China are mainly events recorded at WMQ which were selected to provide comparable epicentral distances with Semipalatinsk explosions. More distant earthquakes from WMQ frequently did not produce regional L_g signals because the station often failed to remain

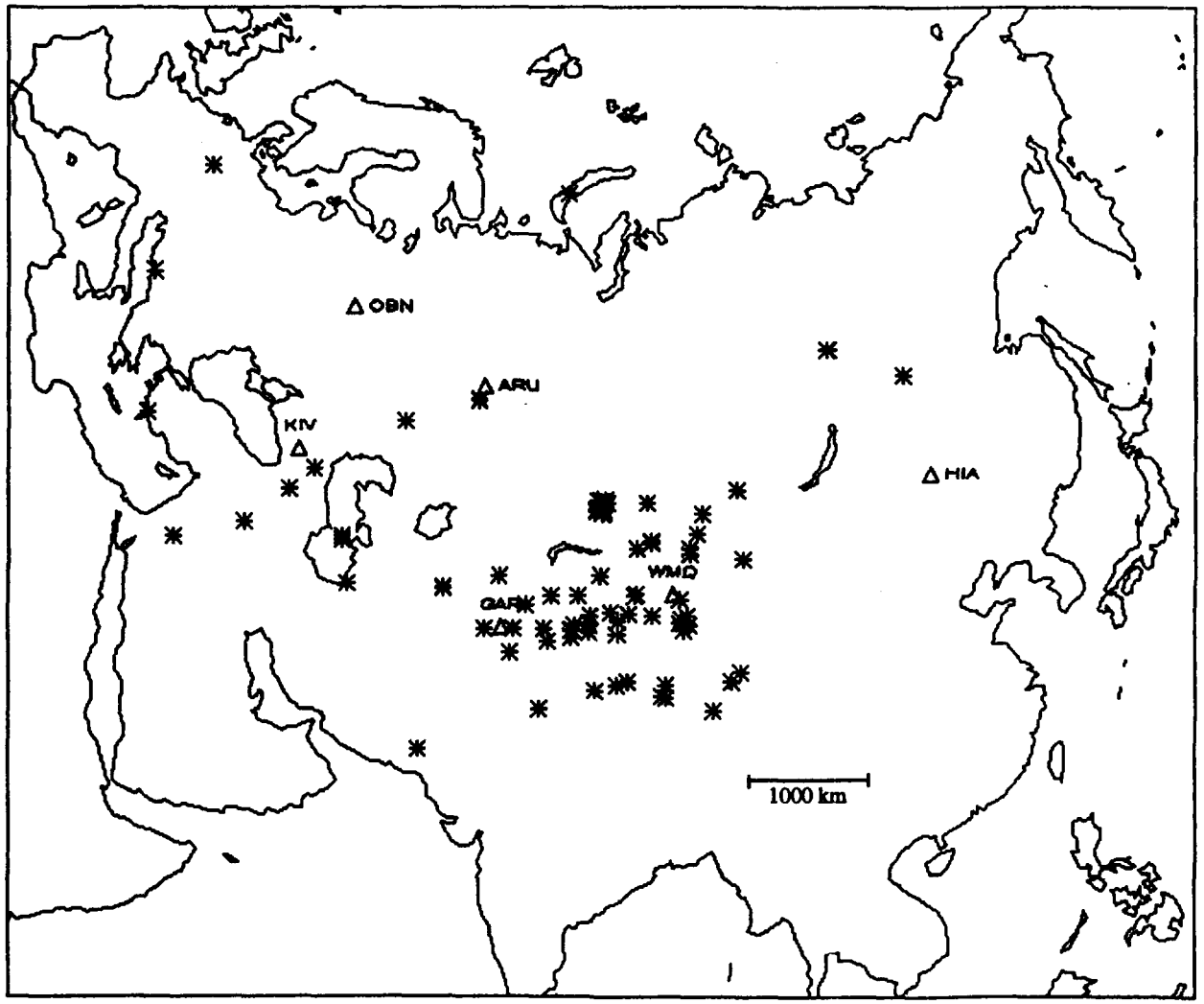

Figure 2. Eurasian events for which good regional seismic signals are currently available in the database.

triggered through the L_g window for distant events. In general, we attempted to select events from a variety of source areas to avoid potential bias in the regional signal behavior for earthquakes of like mechanism from a single area, such as might occur in an aftershock sequence. Furthermore, our objective was to select earthquakes which provided a range of epicentral distances and azimuths for each station. The resulting database includes events from some unusual source areas (e.g., the north Caspian basin, the Ural Mountains near ARU, and eastern Siberia). In addition, we sought to include events from areas which may be of interest from the standpoint of proliferation and future clandestine testing (e.g., events in Iran, Iraq, China, India and Pakistan).

Tables 1 and 2 summarize the event parameters and station availability for the underground nuclear explosions and earthquakes in the database. The nuclear explosions cover a magnitude range from 3.8 to 6.3 m_b, and the earthquakes are in the magnitude range from 4.3 to 6.4 m_b. The epicentral distance range covered by the events in the database is from near-regional (from about 100 km) out to far-regional (in excess of 4000 km). Surprisingly, rather clear L_g signals are observable even at relatively large far-regional distances for several events with propagation paths across the Eurasian continental interior, as is described in more detail below. It should be noted that waveform data may be available at additional stations to those shown in the table for some of the larger earthquakes. We generally do not show data in the table unless regional signals were clearly visible on the broad-band records at the station. Furthermore, in attempting to fill-in the coverage for individual stations, we did not always include in the database the waveforms from more distant stations if those earthquakes duplicated propagation paths at the latter stations or if the events were expected to have low signal-to-noise levels at the distant stations.

Table 1. Eurasian Nuclear Explosions - Regional Recordings

Date	Day	Origin Time	Lat.°N	Lon.°E	m_b	Stations
03/12/87	(071)	01:57:17.2	49.94	78.82	5.5	WMQ
04/03/87	(093)	01:17:08.0	49.93	78.83	6.2	WMQ,HIA
05/06/87	(126)	04:02:05.6	49.83	78.13	5.6	WMQ
06/06/87	(157)	02:37:07.0	49.86	78.11	5.3	WMQ
06/20/87	(171)	00:53:04.8	49.91	78.74	6.1	WMQ,HIA
07/06/87	(187)	23:59:56.7	61.50	112.80	5.1	HIA
07/17/87	(198)	01:17:07.0	49.80	78.11	5.8	WMQ
07/24/87	(205)	01:59:56.8	61.48	112.75	5.1	HIA
08/02/87	(214)	00:58:06.8	49.88	78.93	5.9	WMQ,HIA
08/12/87	(224)	01:29:56.8	61.46	112.76	5.0	HIA
11/15/87	(319)	03:31:06.7	49.87	78.79	6.0	WMQ,HIA
12/13/87	(347)	03:21:04.8	49.99	78.84	6.1	WMQ,HIA
12/20/87	(354)	02:55:06.7	49.83	78.00	4.8	WMQ
12/27/87	(361)	03:05:04.7	49.86	78.76	6.1	WMQ,HIA
02/06/88	(037)	04:19:06.3	49.80	78.06	5.0	WMQ
02/13/88	(044)	03:05:05.9	49.95	78.91	6.1	WMQ
04/03/88	(094)	01:33:05.8	49.92	78.95	6.1	WMQ,HIA
04/22/88	(113)	09:30:06.9	49.82	78.12	4.9	WMQ
05/04/88	(125)	00:57:06.8	49.93	78.77	6.1	WMQ
06/14/88	(166)	02:27:06.4	50.05	79.01	5.0	WMQ
09/14/88	(258)	04:00:00.0	49.87	78.82	6.3	ARU,GAR,KIV,OBN,WMQ, HIA
09/26/88	(270)	07:45:00.0	49.90	78.00	3.8	ARU
10/18/88	(292)	03:40:06.4	49.87	78.19	4.9	ARU,GAR,WMQ
11/12/88	(317)	03:30:07.2	50.64	79.15	5.8	ARU,GAR,WMQ
11/23/88	(328)	03:57:07.6	49.96	78.09	5.1	ARU,GAR,OBN,WMQ
12/04/88	(339)	05:19:53.6	73.49	54.18	5.7	No IRIS Recordings. CDSN P only
12/17/88	(352)	04:18:06.8	49.76	78.83	5.9	ARU,OBN,WMQ,HIA
12/28/88	(363)	05:28:00.0	50.00	79.00	3.9	ARU
01/22/89	(022)	03:57:06.5	49.93	78.87	6.0	ARU,HIA
02/12/89	(043)	04:15:10.6	50.67	78.31	5.8	ARU,WMQ,HIA
02/17/89	(048)	04:01:07.1	49.91	78.09	5.0	ARU,GAR,WMQ
07/08/89	(189)	03:47:01.9	50.66	78.51	5.6	ARU,GAR,KIV,OBN,WMQ, HIA
09/02/89	(245)	04:17:01.6	50.85	78.94	5.4	ARU(Only P),WMQ
10/04/89	(277)	11:29:57.6	49.75	78.01	4.6	Only OBN. Low S/N.
10/19/89	(292)	09:49:59.7	50.47	78.72	6.0	ARU,OBN,WMQ,HIA
05/26/90	(146)	07:59:57.8	41.57	88.69	5.4	ARU,KIV
08/16/90	(228)	04:59:58.7	41.76	88.77	6.2	ARU,GAR,KIV,OBN
10/24/90	(297)	14:57:54.7	72.86	54.66	5.4	ARU,GAR,OBN

Table 2. Eurasian Earthquakes - Regional Recordings

Date	Day	Origin Time	Lat.°N	Lon.°E	m_b	Stations
11/18/86	(322)	13:27:01.0	40.06	77.56	4.7	WMQ
12/14/86	(348)	03:19:17.0	47.31	83.31	5.0	WMQ
12/20/86	(354)	23:08:16.5	36.75	93.66	5.3	WMQ
01/05/87	(005)	22:52:46.5	41.96	81.32	5.9	WMQ
01/24/87	(024)	08:09:21.0	41.53	79.32	5.9	WMQ
01/24/87	(024)	13:40:40.0	41.44	79.25	5.2	WMQ
03/05/87	(064)	02:33:39.0	35.41	87.39	4.5	WMQ
04/09/87	(099)	07:25:35.7	35.50	87.07	4.8	WMQ
04/09/87	(099)	20:01:18.0	35.59	80.47	4.9	WMQ
04/30/87	(120)	05:17:37.0	39.76	74.57	5.7	WMQ
06/08/87	(159)	13:30:36.0	39.79	74.69	5.1	WMQ
08/05/87	(217)	10:24:21.0	41.36	82.11	4.8	WMQ
09/03/87	(246)	09:08:12.0	38.83	75.32	4.8	WMQ
09/16/87	(259)	17:57:26.4	52.09	95.70	4.8	WMQ
09/18/87	(261)	21:58:41.0	47.02	89.66	5.3	WMQ
10/06/87	(279)	13:06:20.3	43.44	88.55	4.8	WMQ
12/03/87	(337)	23:51:43.0	39.54	77.55	4.7	WMQ
12/06/87	(340)	16:20:45.2	37.44	94.61	4.7	WMQ
12/17/87	(351)	12:17:25.0	41.94	83.20	5.1	WMQ
12/22/87	(356)	00:16:39.0	41.36	89.64	5.9	WMQ
01/02/88	(002)	22:02:36.0	40.06	77.34	4.9	WMQ
01/09/88	(009)	03:55:05.3	39.09	71.50	5.4	WMQ
02/08/88	(039)	17:49:19.8	43.73	83.76	4.3	WMQ
03/25/88	(085)	02:37:56.0	44.71	79.60	4.5	WMQ
04/01/88	(092)	01:27:16.2	47.53	89.65	4.6	WMQ
05/02/88	(123)	02:13:26.0	40.26	82.20	4.9	WMQ
05/25/88	(146)	00:05:23.0	40.57	77.62	4.9	WMQ
05/25/88	(146)	18:21:58.0	42.01	85.69	5.2	WMQ
06/17/88	(169)	13:30:45.0	42.94	77.50	5.3	WMQ
06/30/88	(182)	15:25:15.5	50.23	91.14	5.0	WMQ
07/23/88	(205)	07:38:09.0	48.72	90.51	5.5	WMQ
09/25/88	(269)	20:52:14.7	37.18	71.81	5.5	ARU,OBN,WMQ
11/05/88	(310)	02:14:30.3	34.35	91.88	5.9	ARU
11/15/88	(320)	16:56:45.9	42.08	89.40	5.0	WMQ
12/07/88	(342)	07:41:24.2	40.99	44.19	6.2	OBN,GAR
12/15/88	(350)	06:40:51.7	46.50	95.58	5.3	ARU,OBN
12/21/88	(356)	08:21:04.0	41.22	72.30	5.4	ARU
12/27/88	(362)	23:14:07.0	36.59	83.56	5.0	ARU
01/22/89	(022)	23:02:07.1	38.47	68.69	5.3	ARU,GAR
02/12/89	(043)	23:49:17.0	51.00	84.17	4.6	ARU,GAR,WMQ
03/05/89	(064)	13:48:41.6	42.51	74.63	4.8	ARU,GAR
03/13/89	(072)	13:02:14.7	50.71	9.90	5.4	OBN rockburst
03/14/89	(073)	08:42:05.4	40.12	79.32	4.6	GAR
03/31/89	(090)	00:44:13.8	31.87	37.54	4.6	KIV
04/09/89	(099)	02:54:04.3	36.64	42.21	4.6	KIV
04/20/89	(110)	22:59:54.0	57.17	121.98	6.1	ARU,GAR,WMQ,HIA

Date	Day	Origin Time	Lat.°N	Lon.°E	m_b	Stations
04/27/89	(117)	23:06:52.2	37.03	28.18	5.3	KIV,OBN
05/10/89	(130)	20:19:21.9	33.22	75.52	4.8	GAR
05/14/89	(134)	11:46:55.9	50.84	51.24	4.5	ARU,KIV,OBN
05/16/89	(136)	09:48:50.9	43.50	83.63	4.3	ARU,GAR
05/30/89	(150)	23:15:50.3	40.43	63.39	4.7	GAR,KIV
07/21/89	(202)	06:20:47.8	40.86	79.07	5.0	GAR,KIV,OBN
08/03/89	(215)	07:42:41.0	43.59	45.36	5.0	ARU,GAR,KIV,OBN
09/13/89	(256)	07:01:31.4	37.28	54.22	5.1	ARU,OBN
09/16/89	(259)	02:05:08.9	40.34	51.53	6.4	ARU,OBN
09/17/89	(260)	00:53:39.7	40.20	51.75	6.1	ARU,OBN
10/08/89	(281)	15:49:29.5	36.25	82.58	5.1	ARU
12/28/89	(362)	14:29:28.8	40.47	63.42	4.6	ARU
01/21/90	(021)	07:53:31.9	41.53	88.73	4.6	GAR
03/28/90	(087)	21:58:31.4	36.49	87.38	4.8	GAR
04/03/90	(093)	22:02:37.1	43.42	17.39	5.1	OBN
04/09/90	(099)	08:32:09.7	42.87	68.67	4.6	ARU,GAR
05/28/90	(148)	00:35:50.7	55.26	58.70	4.5	OBN,KIV
05/28/90	(148)	02:41:28.2	55.23	58.68	4.5	OBN,KIV
06/14/90	(165)	12:47:28.8	47.87	85.08	6.1	ARU,GAR,KIV,OBN,WMQ, HIA
06/17/90	(168)	04:51:45.5	27.40	65.72	5.9	GAR
08/03/90	(215)	09:15:06.1	47.96	84.96	6.0	ARU,GAR,OBN,WMQ
11/03/90	(307)	17:25:14.0	40.88	89.07	5.1	ARU,GAR

2.3 General Noise Characteristics of the Soviet IRIS Stations

In a previous report (cf. Bennett *et al.*, 1990b) we reviewed the background noise characteristics of the Soviet IRIS stations as observed by Given (1990). Given measured the seismic background noise in different frequency bands as a function of the time of day and time of year at each of the initial four Soviet IRIS stations. Concentrating on Given's noise measurements near 1 Hz, the frequency range of most interest for regional signals, average noise levels were found to be lowest at ARU and greatest at OBN. However, the noise levels at ARU also showed large scatter, indicating that there are times when the seismic noise conditions are significantly worse there than the average values would imply. Overall the noise comparisons suggested that GAR and ARU were better sites than KIV or OBN.

Given (1990) derived detection thresholds for L_g signals at each of the Soviet IRIS stations as a function of epicentral distance using a local magnitude formula for Scandinavia to represent L_g attenuation. To develop detection thresholds at the Soviet IRIS stations which would be more representative of attenuation in the Soviet Union, Bennett *et al.* (1990b) used L_g magnitude residuals at the Soviet IRIS stations to develop an L_g attenuation model for each station and then applied that model to derive the L_g detection thresholds using the 1 Hz average noise levels measured by Given. Figure 3 shows these detection thresholds for L_g magnitudes as a function of epicentral distance. Over most regional distances the lowest detection threshold is at station ARU. Interestingly, although station OBN has a relatively high noise level, it also has very low attenuation for L_g signals; so beyond 1000 km it has the second lowest or even lowest L_g detection threshold of the IRIS stations. In contrast, GAR, which has a very low background noise level, has high attenuation; so the L_g detection threshold there is higher than at the other stations for ranges beyond about 1000 km. Thus, assuming that L_g signals at or above the noise level can be detected, the results in Figure 3 would indicate fairly low detection

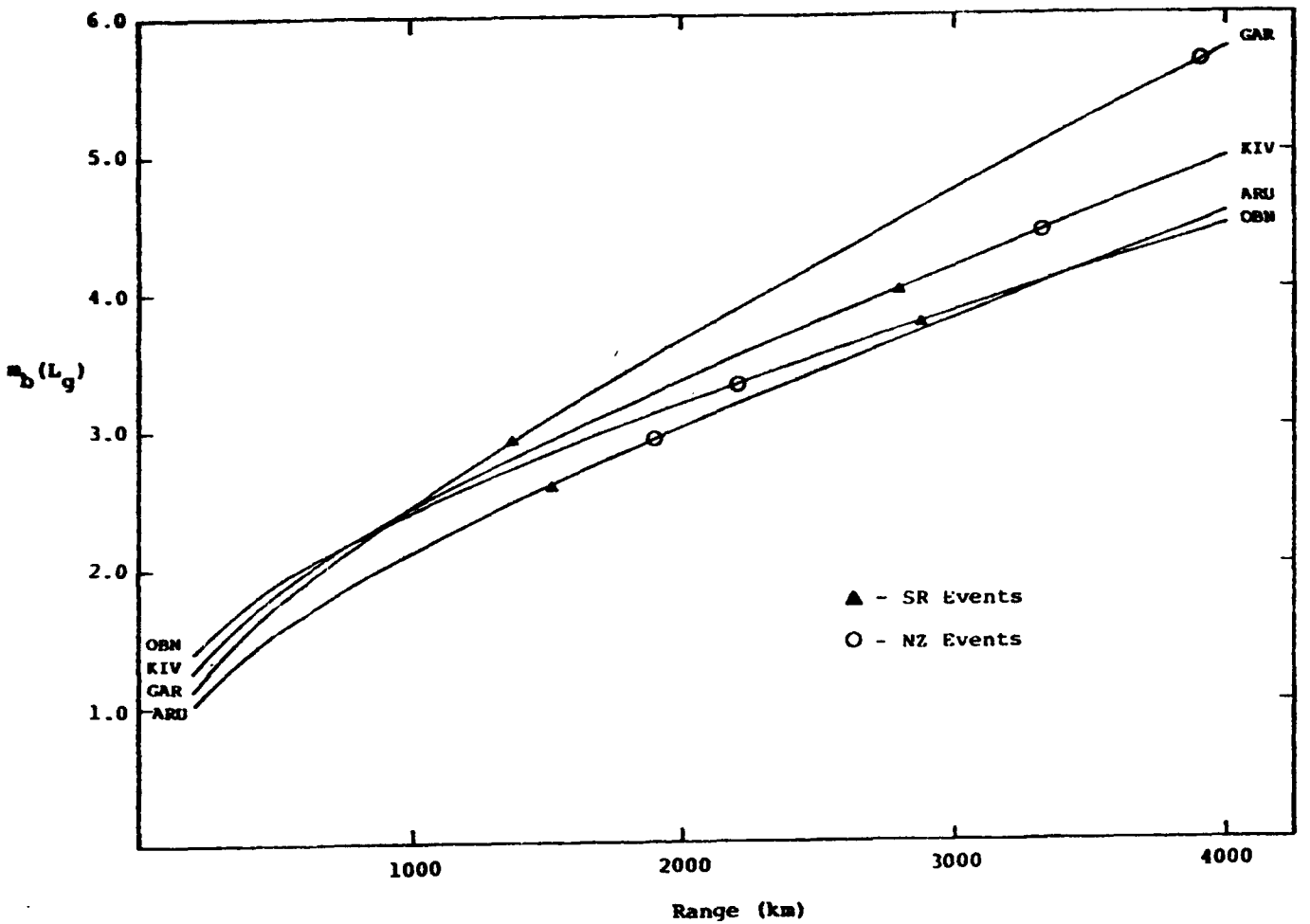

Figure 3. L_g detection thresholds (1 Hz) at the Soviet IRIS stations using the average noise levels reported by Given (1990) and L_g attenuation model developed in our previous study.

thresholds at all the Soviet IRIS stations for 1 Hz L_g signals. Out to 1000 km events with L_g magnitudes above about 2.5 should be detected. However, it is worth noting that from the standpoint of discrimination this threshold may be overly optimistic because higher frequencies required for discrimination may not be detectable. Furthermore, difficulty in observing regional signals at the Soviet IRIS stations for even some larger events (cf. Bennett *et al.*, 1990b) suggests that the L_g detection thresholds in fact may be somewhat larger than predicted on the basis of these noise measurements.

2.4 Regional Signals at Individual Soviet IRIS Stations

2.4.1 Waveforms at Arti (ARU)

Since the Soviet IRIS network was first installed, station ARU has proven to be one of the most reliable stations. This was particularly true during early stages of network operation (viz late 1988 and early 1989) when many of the underground nuclear explosions, which are included in the database, occurred. As a result ARU recorded many of these events while some of the other Soviet IRIS stations were inoperative. In addition, as described above, the L_g detection threshold for the dominant 1 Hz signals is lowest at ARU compared to the other network stations. Therefore, it is not surprising that the database includes more ARU records of Eurasian underground nuclear explosions than are available for any of the other IRIS stations. In a previous report (cf. Bennett *et al.*, 1990b) we showed that ARU recorded detectable L_g signals from Shagan River nuclear explosions with magnitudes as low as 3.8 m_b at the station range of 1500 km. ARU also records good regional signals from events in the active tectonic zone along the southern border of the Soviet Union at ranges from 1700 to 2300 km.

Figure 4 shows a map of the locations of events in the database for which good regional records are available at station ARU. These events include 16 underground nuclear explosions with magnitudes in the range from 3.8 to 6.3 m_b (cf. Table 1 above). The nuclear explosions were

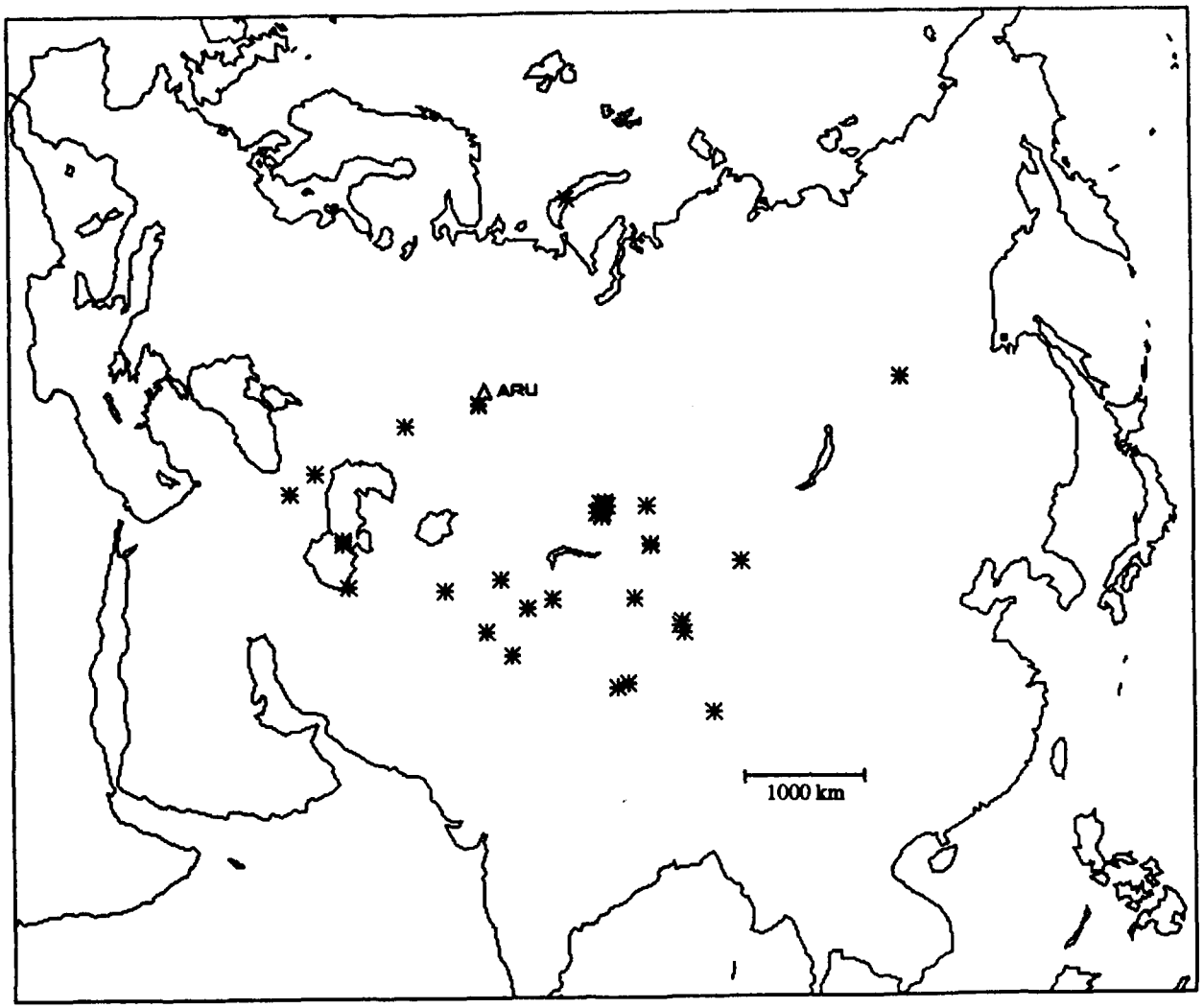

Figure 4. Regional events recorded at station ARU.

located mainly in the Semipalatinsk area (R ≈ 1500 km), but also at Novaya Zemlya (R ≈ 1850 km), and at Lop Nor (R ≈ 2710 km). The database for ARU also includes 24 earthquakes with magnitudes from 4.3 to 6.4 m_b (cf. Table 2 above). The latter events occurred primarily along the southern Soviet border but also include earthquakes in the Ural Mountains, the northern Caspian basin, eastern Siberia, and western China. The epicentral distances for the earthquakes in the database for ARU are in the range from 130 km to 3740 km. Therefore, the earthquakes in the ARU database overlap the explosions in both magnitude and distance range.

The characteristics of the regional seismic signals recorded at ARU are shown in Figure 5. This display shows a suite of vertical component records arranged approximately in order of decreasing azimuth starting from events in the west-southwest. The regional P signals are approximately aligned shortly after the beginning of the records (about 50 seconds past the start). The start time for L_g is indicated on the records by the small circle at a group velocity of 3.6 km/sec. We have displayed only one nuclear explosion record from each of the different test sites and these are denoted by asterisks. In most cases the earthquakes produce clearly identifiable L_g signals with amplitudes normally larger than the regional P on these broadband records. In a few instances the L_g are harder to identify because of large, lower-frequency noise; but closer inspection of the records and band-pass filtering of the records reveals the presence of the L_g in these cases. More problematic with regard to L_g are five events located in the vicinity of the Caspian Sea (viz 08/03/89, 12/07/88, 09/16/89, 09/17/89, and 09/13/89). In all five of these earthquakes L_g signals are not visible, apparently being buried in relatively large S coda. We attribute the lack of L_g in these events to blockage due to propagation through the north Caspian basin which previous studies have found to impede L_g transmission. This observation will be discussed more thoroughly in a subsequent section of this report.

With regard to the nuclear explosion regional signals at ARU, for both Lop Nor and Novaya Zemlya events the L_g signals are significantly

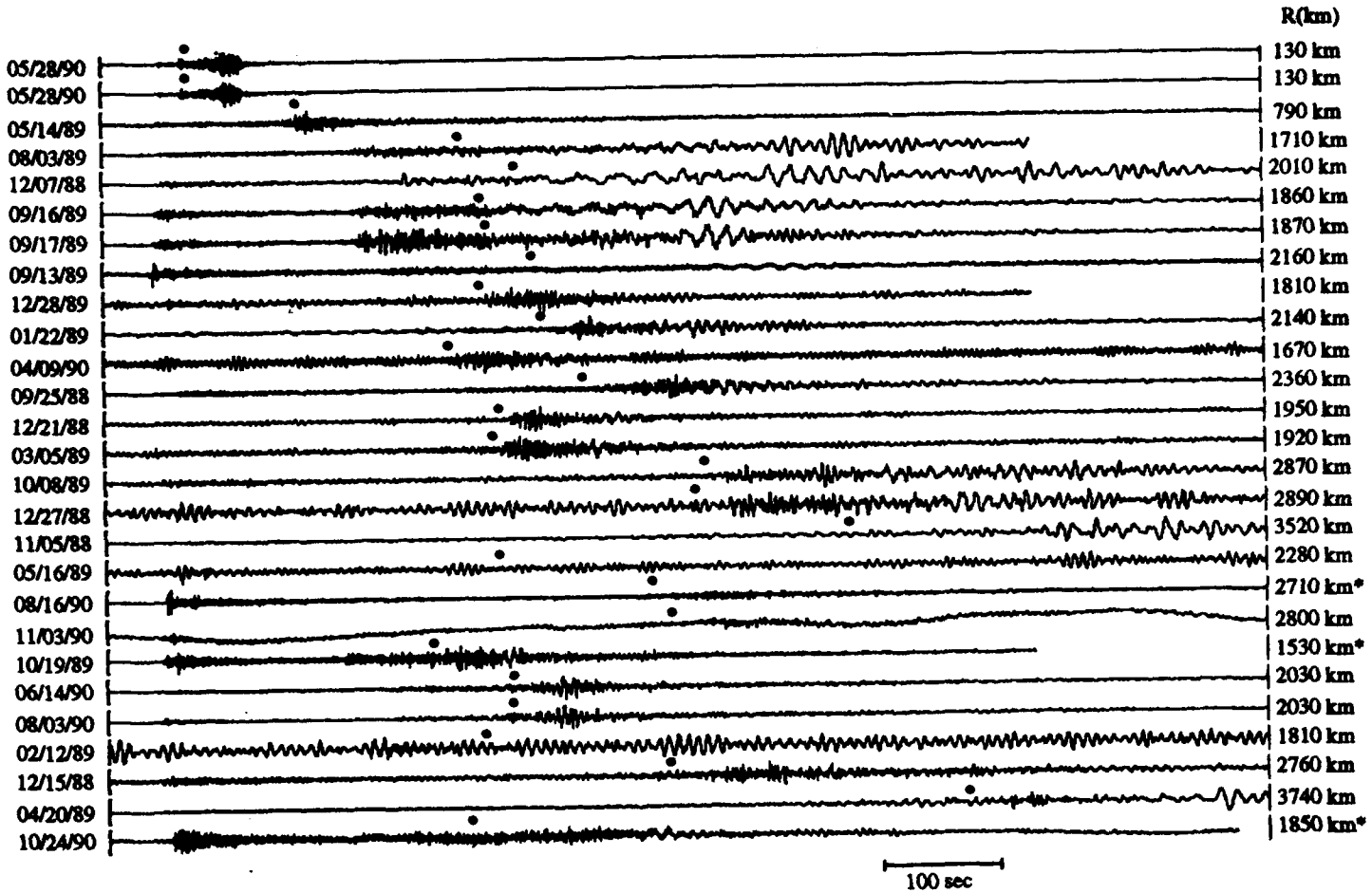

Figure 5. Vertical-component waveforms at ARU from events in the database with Lg starts indicated by solid circles.

weaker than the strong P phases. In fact, for Novaya Zemlya the L_g signal is indistinct, being buried in S coda. The record shown here for the Semipalatinsk explosion (viz 10/19/89) is typical of the waveforms from other explosions in that area recorded at ARU. On the broad-band records the L_g signals are typically about the same amplitude as the P signals. However, band-pass filtering of these signals shows the L_g/P amplitude ratios are usually much lower than one at higher frequencies. More detailed frequency analyses of the regional phase signals at ARU and the use of this observation as a discriminant is described in Section III of this report.

2.4.2 Waveforms at Garm (GAR)

In contrast to ARU, station GAR experienced numerous interruptions in service during the first year of IRIS network operation. Nevertheless, GAR recorded several Semipalatinsk nuclear explosions during late 1988. The reason for this appears to be either that the station was only turned on at the times of nuclear explosions or recordings at GAR were not always retained unless a significant signal was recorded. As described above, the background noise levels at GAR are almost as low as at ARU and lower than those at the other Soviet IRIS stations described here. However, this does not necessarily translate into a lower L_g detection threshold at GAR because of an apparent increase in attenuation in this more active tectonic region. In spite of these problems, GAR recorded good regional signals from Semipalatinsk explosions at the station range of 1390 km as well as important regional recordings from a nuclear explosion at Lop Nor, China at a range of 1590 km. GAR also provides good regional signals from earthquakes in the southern Soviet border tectonic zone and other areas to the south.

The map in Figure 6 shows the locations of the events in the database for which good regional records are available at station GAR. The GAR events include eight underground nuclear explosions having magnitudes between 4.9 and 6.3 m_b (cf. Table 1 above). Most of these explosions were

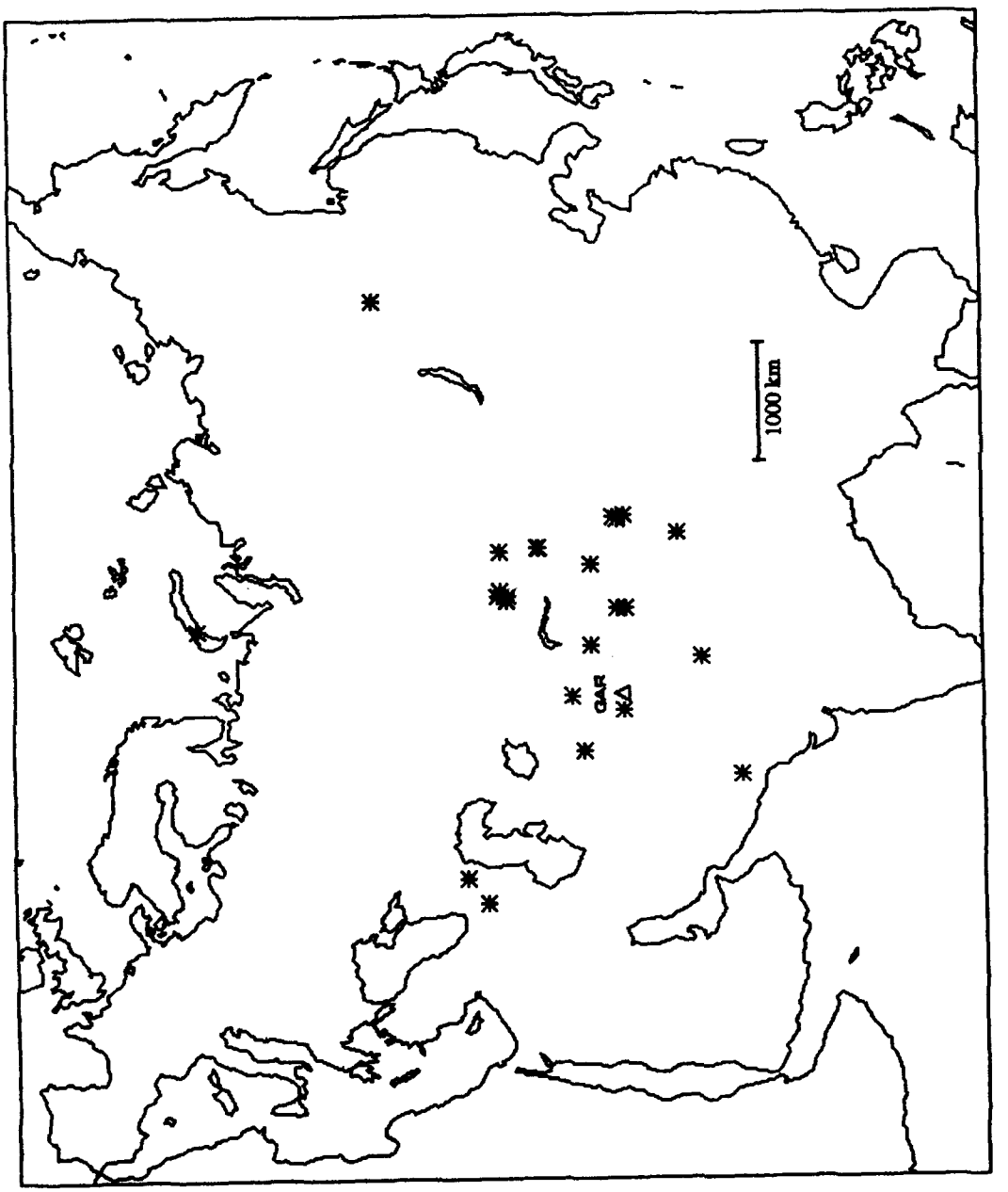

Figure 6. Regional events recorded at GAR.

located at the Semipalatinsk test site (R ≈ 1390 km); one was located at Novaya Zemlya (R ≈ 3870 km), and another at Lop Nor (R ≈ 1590 km). The earthquakes in the GAR database include 18 events with magnitudes between 4.3 and 6.2 m_b (cf. Table 2 above). Many of these earthquakes occurred in the southern Soviet border tectonic zone and in western China, although waveforms are also available from events in eastern Siberia, India, and Pakistan. The epicentral distances for the earthquakes at GAR are between 150 km and 4220 km. So again there is overlap in the magnitude and distance range of events in the GAR database.

Figure 7 shows the regional signal characteristics at GAR for a suite of vertical-component records arranged approximately in order of decreasing azimuth around the station starting with the west-northwest. In the display we again show one underground nuclear explosion from each test site, as marked by the asterisks. In nearly all cases the earthquakes recorded at GAR are observed to have strong L_g signals (L_g window start times are marked by the small circles on each waveform.). For these earthquakes the maximum amplitudes in the L_g windows are almost always larger than the corresponding regional P signals observed on these broad-band records. Exceptions again are the two earthquakes from west of the Caspian Sea (viz 08/03/89 and 12/07/88). For both of these earthquakes, the L_g signals are indistinct and appear to be buried in the coda of the regional S. This observation again appears to be associated with blockage of L_g transmission by structure in the vicinity of the Caspian Sea, which will be described more completely in a subsequent section of this report.

For the underground nuclear explosions at GAR, the L_g signals from the Lop Nor and Novaya Zemlya events (viz 08/16/90 and 10/24/90) are smaller than the corresponding P signals in these broad-band displays. In fact, the signal in the L_g window for the Novaya Zemlya explosion is very weak and practically indistinct in the S coda. On the other hand, the L_g signal from the Semipalatinsk nuclear explosion (viz 09/14/88) is fairly large and bigger than the corresponding P on the broad-band records. From the standpoint of discrimination, a valuable comparison can be made between the

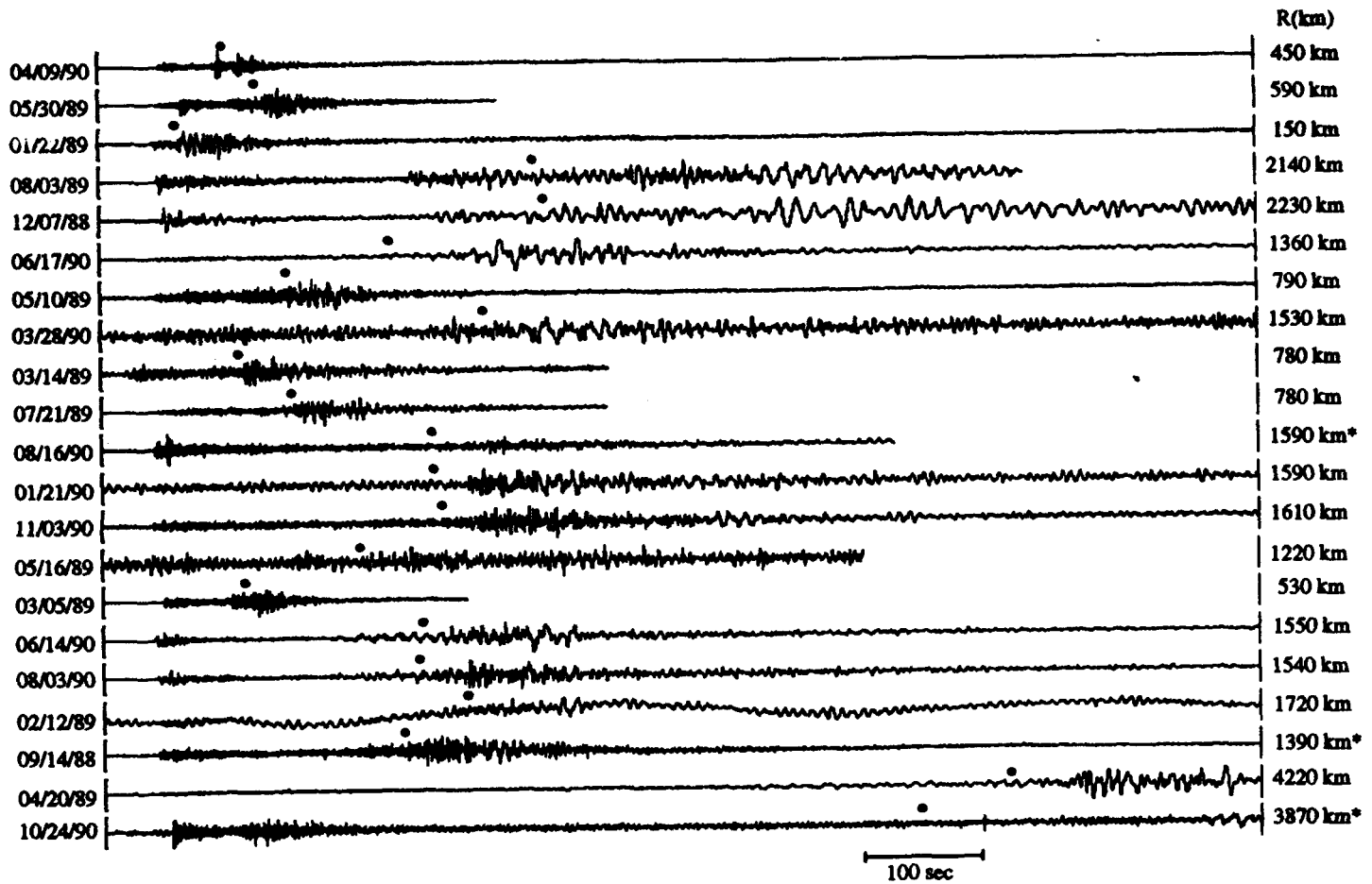

Figure 7. Vertical-component waveforms at GAR from events in the database with Lg starts indicated by solid circles.

Lop Nor explosion record and the corresponding regional signals from two nearby earthquakes (viz 01/21/90 and 11/03/90) recorded at GAR. The L_g/P amplitude ratios are much larger for the earthquakes than for the explosion. We will discuss the spectral behavior of this ratio and its potential value for regional discrimination in a subsequent section of this report.

2.4.3 Waveforms at Obninsk (OBN)

Except for the first six months of operation of the Soviet IRIS network, station OBN has been a fairly reliable station for recording Eurasian seismic events. Although OBN had a somewhat higher background noise level than those at ARU and GAR, L_g attenuation in the vicinity of OBN is smaller; so the L_g detection threshold there is still fairly low, particularly for more distant events. However, OBN is farther away from the main Soviet underground nuclear test site near Semipalatinsk and many of the more active tectonic zones along the southern Soviet border. Nevertheless, OBN manages to record identifiable regional P and L_g signals from many events in these areas as well as in other areas to the west in Europe.

Figure 8 shows a map of the locations of events in the database for which good regional signals are available at station OBN. These events include eight underground nuclear explosions with magnitudes between 4.6 and 6.3 m_b (cf. Table 1 above). These nuclear explosions were located primarily near Semipalatinsk (R ≈ 2890 km), but also at Novaya Zemlya (R ≈ 2150 km), and at Lop Nor (R ≈ 4030 km). The 16 earthquakes in the OBN database have magnitudes between 4.5 and 6.4 m_b (cf. Table 2 above) and cover ranges from 1090 km to 4140 km. Many of these earthquakes were located in the active tectonic zone along the southern Soviet border, but others were located in the northern Caspian basin, the Ural Mountains, Turkey, Yugoslavia, and Germany. The explosions and earthquakes at OBN again overlap in magnitude and epicentral distance ranges.

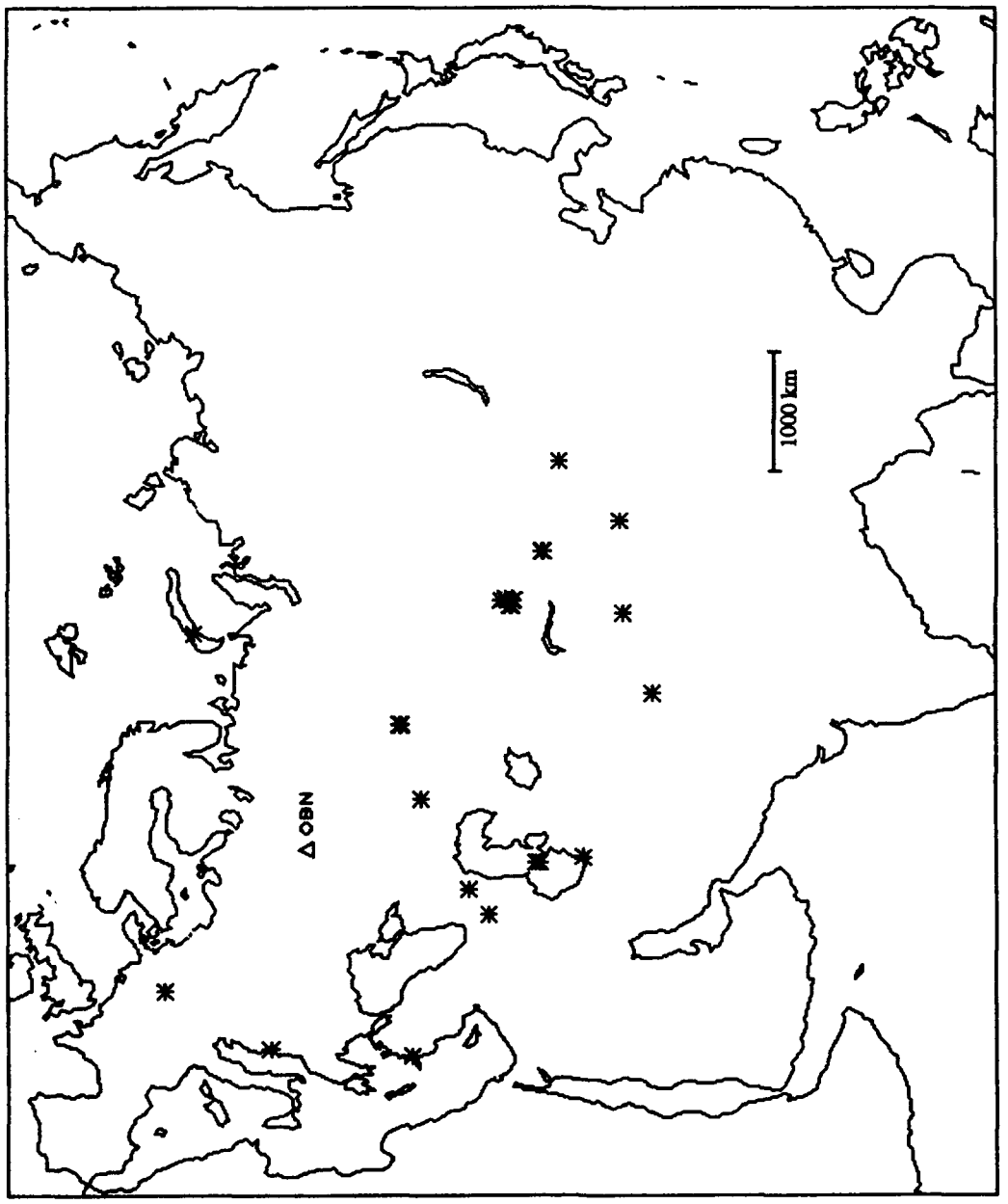

Figure 8. Regional events recorded at station OBN.

The behavior of the regional signals at OBN is shown in Figure 9. The vertical component records shown are arranged approximately in order of decreasing azimuth starting with events to the west-northwest. The first event (viz 03/13/89) is a rockburst at a mine in Germany which produced strong L_g and short-period Rayleigh waves; the signals from this event, therefore, appear to be of a more earthquake-like character. On the other hand, many of the earthquakes produce weak or indistinct L_g signals at OBN; in most cases this appears to be related to structural blockage of the signals. The earthquake in Greece (viz 04/27/89) may have L_g blocked by structures associated with the Black Sea, as some authors have previously proposed. Three events in and just east of the Caspian Sea (viz 09/16/89, 09/17/89, and 09/13/89) show little evidence of L_g at OBN possibly again related to blockage by north Caspian basin structures, as will be described in a subsequent section of the report. Interestingly, at least one of the earthquakes west of the Caspian Sea (viz 08/03/89) produces strong L_g apparently skirting whatever structure is responsible for the blockage. The remainder of the earthquakes appear to produce relatively strong L_g with amplitude larger than P on the broad-band records at OBN. L_g signals are even observed from one earthquake (viz 12/15/88) at a range of 4140 km indicating relatively efficient L_g transmission through the continental interior.

For the nuclear explosions the L_g signals are indistinct for both the Novaya Zemlya (viz 10/24/90) and Lop Nor (viz 08/16/90) explosions. The L_g signal at OBN from the explosion near Semipalatinsk (viz 10/19/89) is clearly much larger relative to the regional P amplitude than for the other two explosion source areas. We have noted a similar behavior in the relative L_g/P amplitudes for the different test sites for each of the Soviet IRIS stations (viz ARU, GAR, and OBN) described so far. This observation suggests that for some reason explosions at the Semipalatinsk test site may be more efficient in generating L_g signals than explosions in the other two source areas. Either that or the L_g signals from Novaya Zemlya and Lop Nor explosions are being blocked or more severely attenuated along the

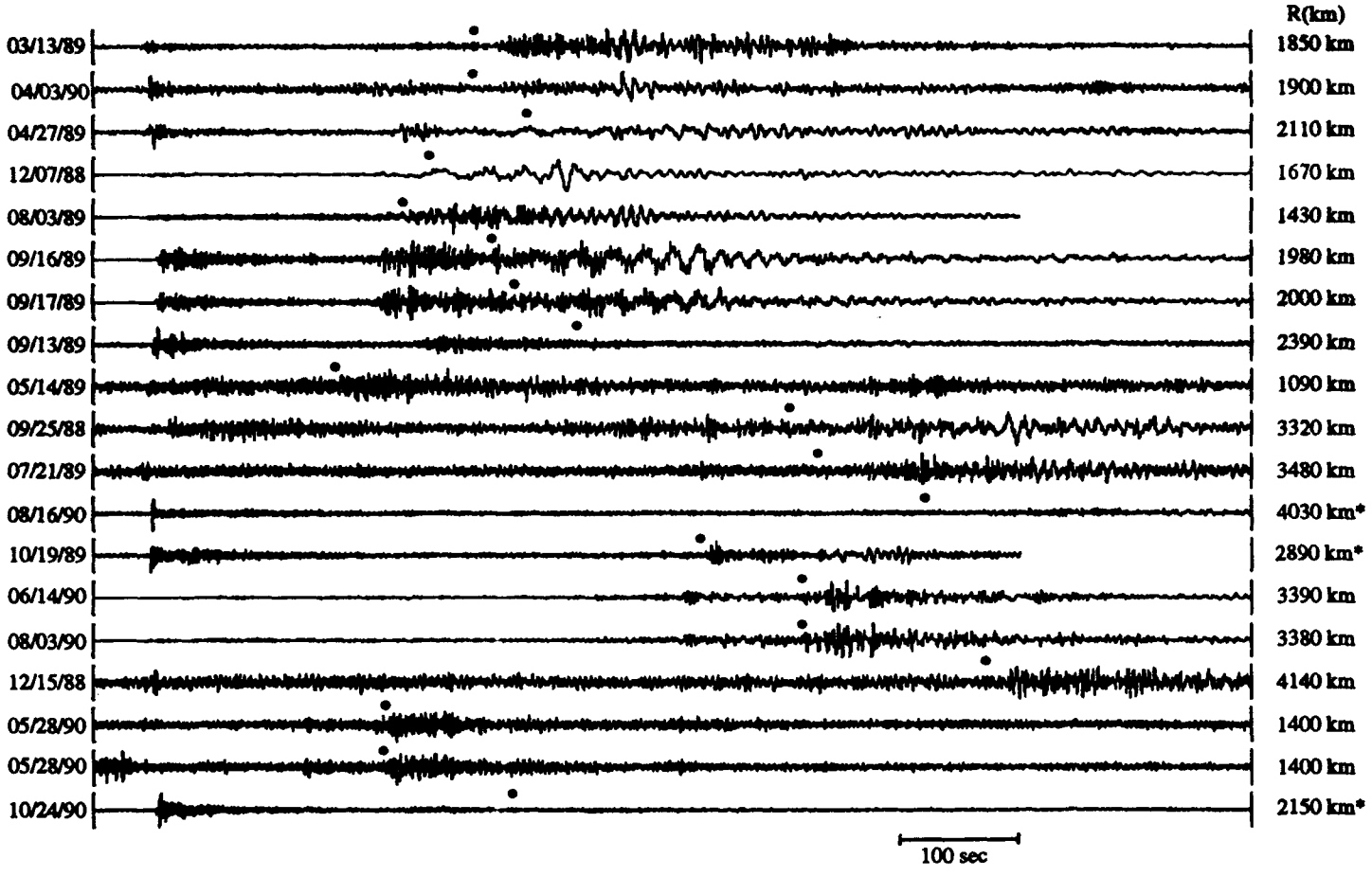

Figure 9. Vertical-component waveforms at OBN from events in the database with Lg starts indicated by solid circles.

paths to each station than are the L_g signals from Semipalatinsk explosions. The resolution of this issue will have important implications with regard to the transportability of L_g-magnitude/yield relationships and the use of L_g /P amplitude comparisons as discriminants for events in uncalibrated regions. One other noteworthy feature of the waveforms in Figure 9 is the consistency of the signals from events located in common source areas. For example, the two earthquakes beneath the Caspian Sea (viz. 09/16/89 and 09/17/89), the two earthquakes on the Soviet border southeast of Semipalatinsk (viz 06/14/90 and 08/03/90), and the two earthquakes in the Ural Mountains (viz 05/28/90 and 05/28/90) have remarkably similar regional signals. This observation suggests that tectonic sources are consistent regional signal generators. When this is combined with the observation of consistency in the regional signals from nearby explosions, it indicates that observed differences in regional signals between source types for a particular region should provide a reliable discriminant.

2.4.4 Waveforms at Kislovodsk (KIV)

Of the four Soviet IRIS stations described here KIV is probably the weakest with respect to monitoring regional events within the Soviet Union. However, because of its location KIV does provide unique capability for monitoring regional seismic events from regions to the south which may be of interest from the standpoint of proliferation. The weakness of the KIV station for monitoring Soviet events is related to several factors. One of the primary factors is its location between the Caspian and Black seas and the aforementioned L_g blockages apparently associated with tectonic structure in these areas. As a result KIV has very limited azimuthal windows for L_g signals; and these windows exclude most of the Soviet Union. Besides near regional events and a small region of the western Soviet Union, the L_g window for KIV includes some areas of interest to the south including parts of Iran and Iraq. A second factor limiting the performance of KIV is the background noise at the site. The noise level at KIV is the highest of the Soviet IRIS station sites; and as a result the detection threshold there is

relatively high. Finally, KIV has had a relatively poor level of reliability compared to the other Soviet IRIS stations particularly during the first six months of operation. This reliability problem prevented KIV from recording several significant events including a number of underground nuclear explosions during that time interval.

Figure 10 shows the locations of events in our database for which good regional records are available at KIV. These events include four underground nuclear explosions with magnitudes in the range from 5.4 to 6.3 m_b (cf. Table 1 above). Two of the nuclear explosions had sources at the Semipalatinsk test site (R ≈ 2820 km), and the other two were located at Lop Nor (R ≈ 3730 km). The ten earthquakes in the KIV database had magnitudes between 4.5 and 6.1 m_b (cf. Table 2 above) and were located at epicentral distances between 220 km and 3280 km. The earthquake database at KIV comes from scattered sources including events along the southern Soviet border, the Ural Mountains, the northern Caspian basin, Jordan, and Iraq.

The characteristics of the regional seismic signals observed at KIV are shown in Figure 11. The vertical component records shown are arranged in order of decreasing azimuth starting from the west-southwest. Several of the earthquakes show apparent L_g signals, but for others the L_g is weak or absent. In some cases this may be related to blockage or partial blockage by structures near the Black or Caspian seas, as noted above. The latter include the event in Turkey (viz 04/27/89), earthquakes east of the Caspian Sea (viz 05/30/89, 07/21/89, and 06/14/90), and earthquakes in the Ural Mountains, for which the signals must propagate through the northern Caspian basin.

The two explosions shown in Figure 11 show strong regional P phases, but the L_g signals are weak or indistinct. Whatever L_g signal may be present is buried in the S coda. This may again be related to L_g blockage by structures associated with the Caspian Sea which the paths from the two test areas cross to KIV. In spite of these problems with L_g signal blockage at KIV, the explosion records still appear unique and more similar to one

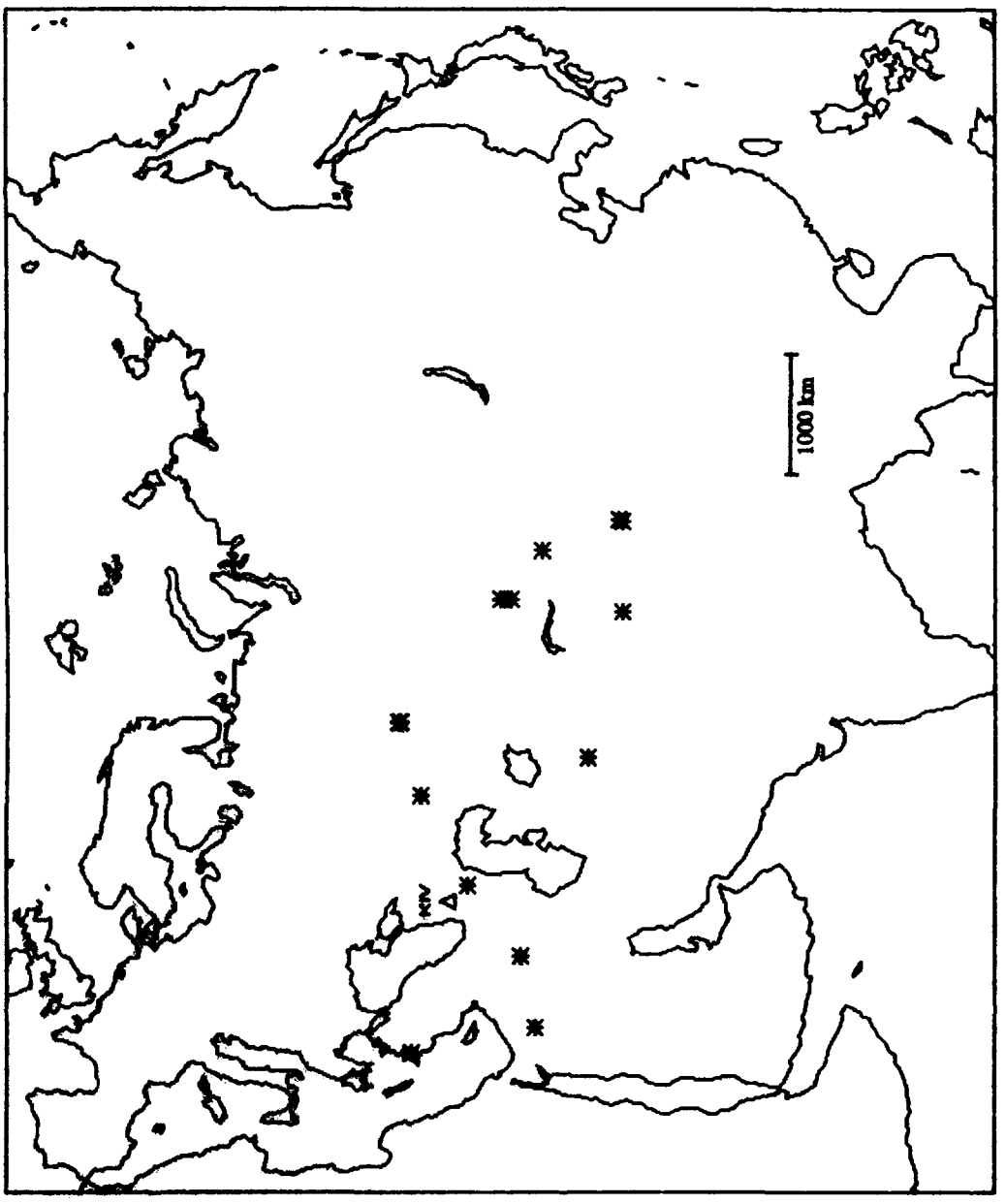

Figure 10. Regional events recorded at station KIV.

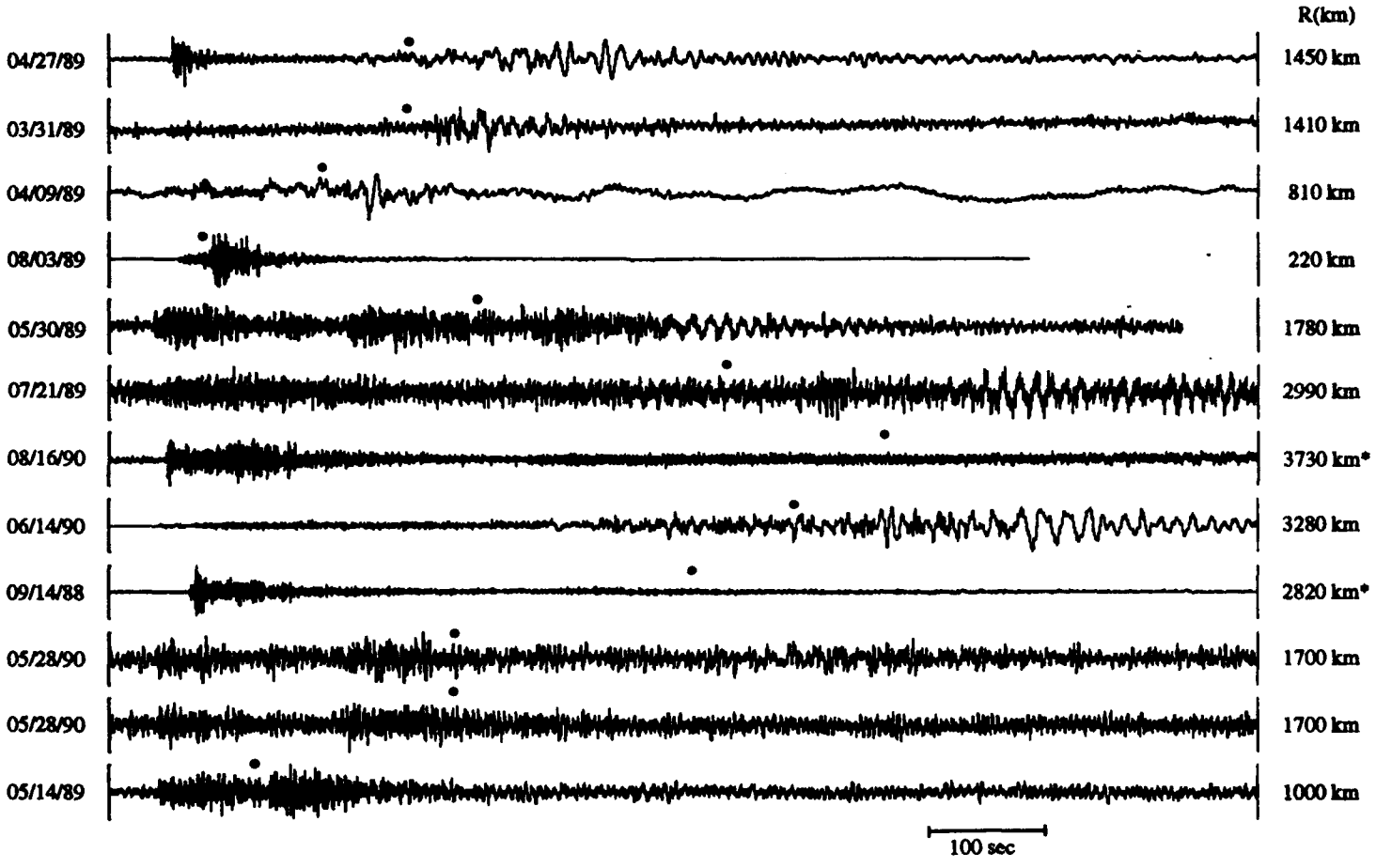

Figure 11. Vertical-component waveforms at KIV from events in the database with Lg starts indicated by solid circles.

another than to earthquakes in the database, including those which have experienced similar L_g blockage. The distinction between the explosion and earthquake records appears to lie in the fact that the seismic energy in the earthquakes is more evenly dispersed throughout a wide range of group velocities in contrast to the explosions for which most energy is confined to the P window. Thus, in comparing the two explosions and the earthquake records at nearly common azimuths (viz 08/16/90, 09/14/88, and 06/14/90), the earthquake has significantly greater post-S energy. For this and several other earthquakes in the KIV database, much of this post-S energy appears in the form of lower-frequency Rayleigh waves which are not present on the explosion records. These latter signals apparently are not interrupted by the structural blockage which affects L_g. The prominence of these signals suggests that some regional discriminant measure using these Rayleigh wave signals (e.g., regional M_s versus m_b) could provide effective discrimination in areas where problems may arise in using L_g.

2.4.5 Further Analysis of L_g Blockage by Caspian Sea Structures

It has been recognized for many years now that some areas along the southern border of the former Soviet Union appear to impede the propagation of L_g signals (cf. Ruzaikin *et al.*, 1977; Piwinskii and Springer, 1978; Nuttli, 1981; Bennett *et al.*, 1981; Kadinsky-Cade *et al.*, 1981). In particular, it was recognized in these early studies that the Caspian Sea and, possibly to a lesser extent, the Black Sea regions tended to block L_g signals crossing those areas. In these studies it was suggested that the tectonic structure in these areas might be oceanic in character and, therefore, unable to support L_g propagation (cf. Press and Ewing, 1952). More recently, Kennett and Mykkeltveit (1984) have shown that L_g propagation can be very sensitive to abrupt changes in crustal structure that deviate from horizontal stratification. Given (1991) also recently has found evidence of possible blockage of L_g signals going to the Soviet IRIS station at KIV when the propagation paths cross the Caspian or Black Seas.

In the preceding sections of this report, we have noted several instances in which records from events having propagation paths crossing the Caspian or Black Seas were relatively depleted in L_g energy. In particular, we found that earthquakes originating in the vicinity of the Caspian Sea almost never produced recognizable L_g at the Soviet IRIS stations. We also saw that the L_g signals for events in other areas with paths crossing the Caspian Sea or the Black Sea were strongly attenuated. However, it is interesting to note that in some cases events have paths which apparently do not actually cross these seas; but the L_g signals are still weak. For example, the earthquake at the southeastern corner of the Caspian Sea near the Iran border (cf. Figure 2 above) shows little recognizable L_g at ARU (cf. Figure 5 above) although the path doesn't intersect the Caspian Sea coastline. In addition, the two earthquakes near ARU (cf. Figure 2 above) show no sign of L_g at KIV (cf. Figure 11 above) even though their paths miss the Caspian Sea but do cross the northern Caspian sedimentary basin. The latter results suggest that the structures responsible for the L_g blockage may extend beyond the surface features with which they are associated. Given (1991) also described cases in which apparent L_g blockage extended south and north of the Caspian Sea.

The work by Given, as well as previous studies, indicate that it may be possible to use these kinds of observations to define the limits of the structure responsible for L_g blockage. Our preliminary results here indicate that L_g signals propagate from the earthquakes near ARU to station OBN and from the earthquake just east of KIV to station OBN (cf. Figure 2 above); so this appears to establish northern and western limits to the impeding structure. Also, the earthquake south of the Aral Sea produces strong L_g signals at station ARU thereby establishing an apparent eastern limit to the structure. Additional data are needed to establish southern limits on the structure and to further refine these boundaries. It should be noted that the southern part of the structure may tend to blend into the tectonic zone extending along the southern border of the former Soviet Union which may complicate structural interpretation in this area.

Two other features of the L_g data presented here may be helpful in understanding the effects of geologic structure on L_g propagation. First, we find that the earthquake located in the Caspian Depression, just north of the Caspian Sea (cf. Figure 2 above), is particularly interesting in this regard. This earthquake, which occurred on 05/14/89 had a body-wave magnitude of 4.5 and produced strong L_g signals at each of the surrounding Soviet IRIS stations, ARU (cf. Figure 5 above), OBN (cf. Figure 9 above), and KIV (cf. Figure 11 above). On the other hand, the two earthquakes near ARU propagating along nearly the same azimuth to KIV produced almost no L_g; and the earthquake just east of KIV, which nearly reverses the path to ARU, produced indistinct L_g at ARU. This observation suggests that L_g is not strongly disrupted by the transition from the Caspian structure to that of the surrounding region. However, L_g may be effectively blocked by the passage from the surrounding region into the Caspian structure. Theoretical analyses of wave propagation in a structural model of the Caspian basin and additional observational data from this area could provide important insight into the effects of tectonic structure on L_g propagation.

The second feature of the effects of the Caspian Sea structure on L_g propagation, which we would like to re-emphasize here, is that the blockage may to some extent be frequency dependent. In describing the regional signals recorded at KIV from the Semipalatinsk nuclear explosion and the earthquake east of the test site (cf. Figure 10 above), we noted that the two events arrive at KIV from very similar azimuths, both crossing the Caspian Sea structure. However, while L_g is apparently blocked in the explosion, there does appear to be L_g in the earthquake record. The latter seems to be dominated by relatively low frequencies, which suggests that the structure may be more effective in blocking the high frequencies while passing low frequencies in the L_g signals. Understanding of this problem would again benefit from additional analyses of these data and theoretical studies of wave propagation for structural models of this region.

2.5 Summary of General Regional Signal Characteristics at Soviet IRIS Stations

In general, then, earthquakes recorded at the Soviet IRIS stations tend to have large L_g signals relative to P in comparison to underground nuclear explosions at similar epicentral distances as measured on the broad-band records. This appears to be true over a wide range of magnitudes and, with some exceptions, at most azimuths. The most notable exceptions appear to be cases where L_g transmission may be blocked by structural features associated with the areas of the Caspian and Black seas. For even these problem cases, the broad-band regional signals for the explosions appear distinct from earthquakes with similar paths; so that some alternative regional discriminant measure may be effective. On the negative side this means that some care may be needed in deciding which regional discrimination techniques will be reliable in different areas. However, on the positive side the regional signals observed at the Soviet IRIS stations are remarkably similar for events of a common source type even if the events are somewhat separated. This suggests that regional discriminants which are effective for some events in an area are likely to be effective for others, and the extent of the geographical area over which this conclusion applies may be fairly large.

III. DISCRIMINATION ANALYSIS OF EURASIAN EVENTS USING THE REGIONAL PHASE SIGNALS AT STATION ARU

3.1 Background

In the preceding section of this report we described the general characteristics of the regional phase signals recorded at the Soviet IRIS stations and the database which has been assembled at S-CUBED to address the problem of discrimination of seismic events throughout Eurasia. The database includes high-quality digital waveforms which should provide an excellent test of the effectiveness of proposed regional discriminant measures applied to Eurasian events from a variety of tectonic and propagation environments. In a prior report we presented the results of amplitude and spectral comparisons of regional signals recorded at a single station, WMQ, for use as potential regional discriminants. In particular, we found that L_g/P spectral ratios appeared to provide effective discrimination between underground nuclear explosions and earthquakes at regional distances from WMQ for locations along the southern Soviet border and in western China. In this section we provide similar analyses of the discrimination potential of regional signal measurements obtained at the single Soviet IRIS station, ARU.

ARU was selected for these analyses because it recorded good regional signals from most of the Soviet underground nuclear tests which have occurred since the installation of the IRIS network. In addition ARU's location away from the more active tectonic zones results in a generally low-attenuation environment for regional signals. Therefore, ARU frequently records strong regional signals at ranges to 2000 km or even 3000 km, while stations in more attenuative environments may not detect such events. We were able then to put together a fairly large database of ARU regional earthquake records covering a range of azimuths and an epicentral distance

range overlapping that of the underground nuclear explosions to which they are being compared.

3.2 Further Consideration of ARU Regional Waveforms

In the preceding section of this report, we described the general characteristics of the regional signals recorded at each of the Soviet IRIS stations from suites of events surrounding each station. The suite for ARU, shown above in Figure 5, contained 27 events including three nuclear explosions, one record from each of the main Soviet test sites and one from the Chinese test site. As noted above, the total event sample for ARU includes 16 Eurasian underground nuclear explosions of which 13 were located at the Semipalatinsk test site at a range of approximately 1530 km. In Figure 12 we show the vertical-component broad-band records at ARU from all the Semipalatinsk test site explosions. The column to the right indicates the range of the station from the NEIS reported epicenters for these explosions. The epicentral distances cover a range of about 100 km (between about 1450 km and 1550 km). Some of this variation in location is real, as events in the database include explosions in different test areas (e.g., Balapan, Degelen Mountain, and Murzhik), but the NEIS locations may also include errors in some cases, particularly for the smaller events. The waveform for one event (viz 09/02/89) terminated abruptly following the P segment and missed the later L_g phase. It should also be noted that some of the events are quite small with magnitudes of 3.8 m_b and 3.9 m_b for 09/26/88 and 12/28/88, respectively. On the broad-band records in Figure 12 there is little evidence of these explosion signals at ARU. However, in our previous report (cf. Bennett *et al.*, 1990a) we showed that some signal could be detected in the ARU records for even such small magnitude events by appropriate band-pass filtering. A filter with corners at 0.8 Hz and 1.6 Hz was found to be effective in extracting the regional signals at ARU for these low-magnitude events. Figure 13 shows the band-pass filtered versions of the records in Figure 12. In nearly all cases the regional phase signals are more apparent in the filtered traces. In particular, the L_g signals stand

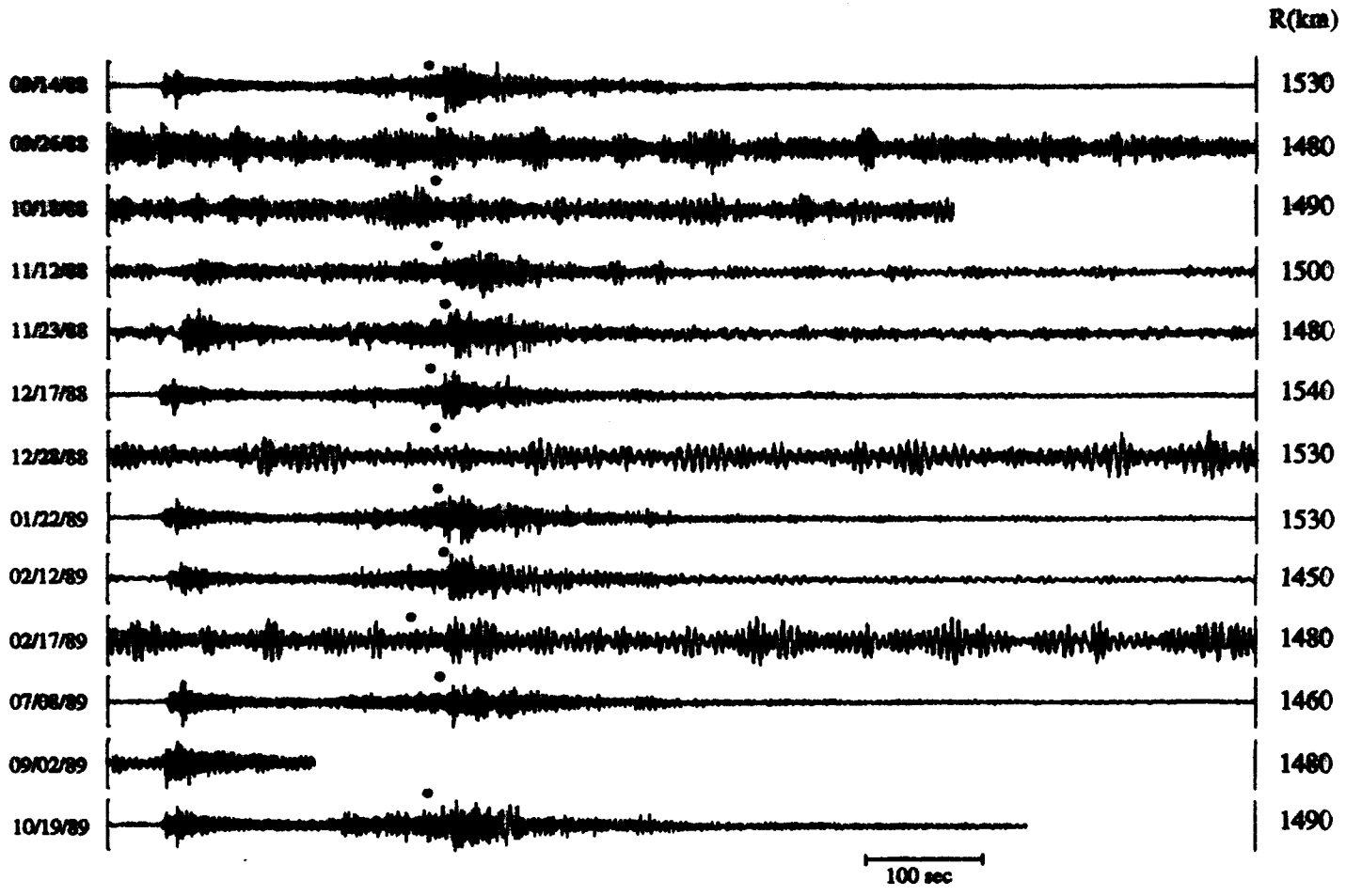

Figure 12. Unprocessed vertical-component waveforms at ARU from nuclear explosions near Semipalatinsk with Lg starts indicated by solid circles.

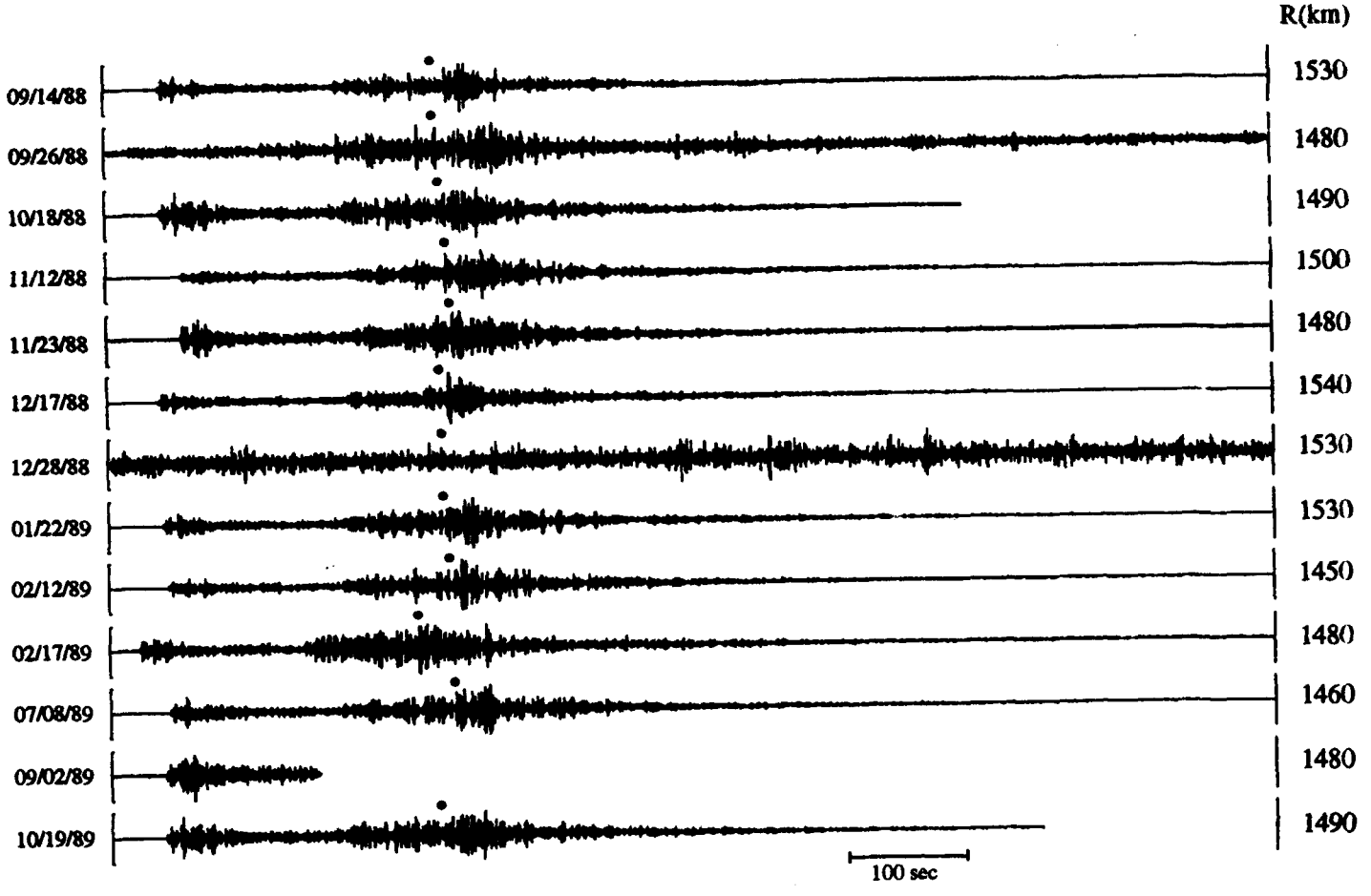

Figure 13. Band-pass filtered (0.8-1.6 Hz) vertical-component records from Figure 12 at ARU.

out on the filtered traces relative to the background especially for the smaller magnitudes. The single exception is the record from the 12/28/88 explosion for which the regional signals are still buried in the background noise. Attempts using other filters to extract these signals have proven unsuccessful, suggesting that this event ($m_b \approx 3.9$) is at or below the detection threshold for ARU.

3.3 Spectral Analyses of ARU Regional Signals

Fourier spectra were computed for the regional P and L_g signals from eighteen of the earthquake records shown above in Figure 5 and the eleven explosions in Figure 12 which included the L_g windows. We eliminated from consideration those earthquakes at epicentral distances greater than 3000 km from ARU and a few others with weaker signals. For each event the spectra were computed for a 50-second window starting just before the P and a 100-second window starting at the expected time corresponding to an L_g group velocity of 3.6 km/sec. The only exceptions were the two earthquakes nearest ARU for which we used windows half as long to avoid overlap of the signal windows. In addition, spectra were computed for a 25-second noise window preceding P for each record. In all cases the signals were demeaned and tapered prior to the spectral computation; and the spectra were smoothed to provide comparable resolution for all signals and events.

Figures 14-17 show the regional-phase amplitude spectra for some typical events recorded at ARU. Figures 14 and 15 correspond to Semipalatinsk nuclear explosions of 09/14/88 and 07/08/89 with magnitudes of 6.3 m_b and 5.6 m_b, respectively. These were located at a distance of approximately 1530 km from ARU. Figures 16 and 17 are for two earthquakes of 08/03/90 and 12/21/88 with magnitudes of 6.0 m_b and 5.4 m_b, respectively. Epicentral distances from these events to ARU were 2030 km and 1950 km, respectively. In all cases the spectra are at high levels, well-above background noise, in the frequency band near 1 Hz. In fact, the

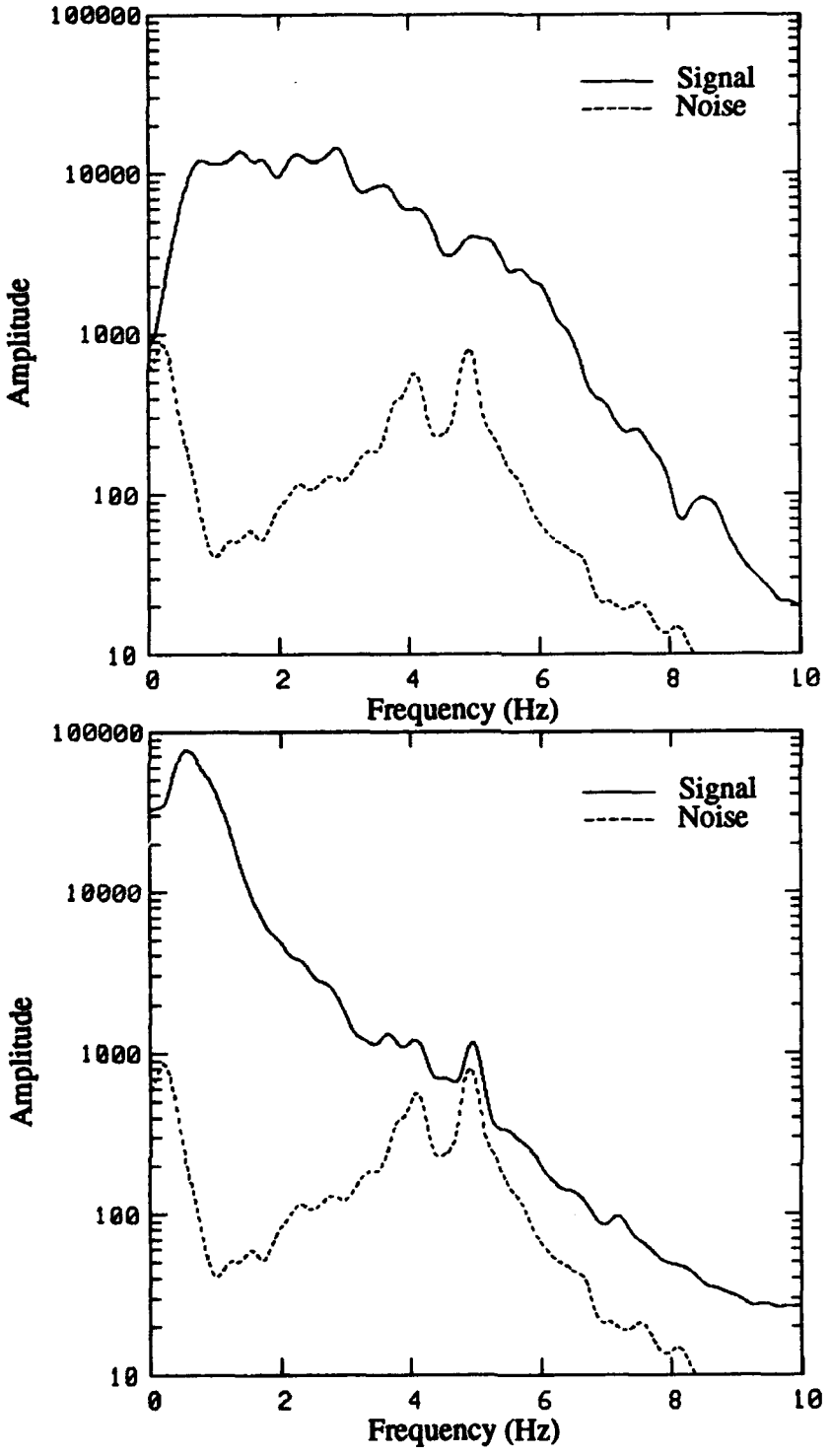

Figure 14. Regional phase spectra, P (top) and L_g (bottom), for 9/14/88 JVE explosion observed at ARU.

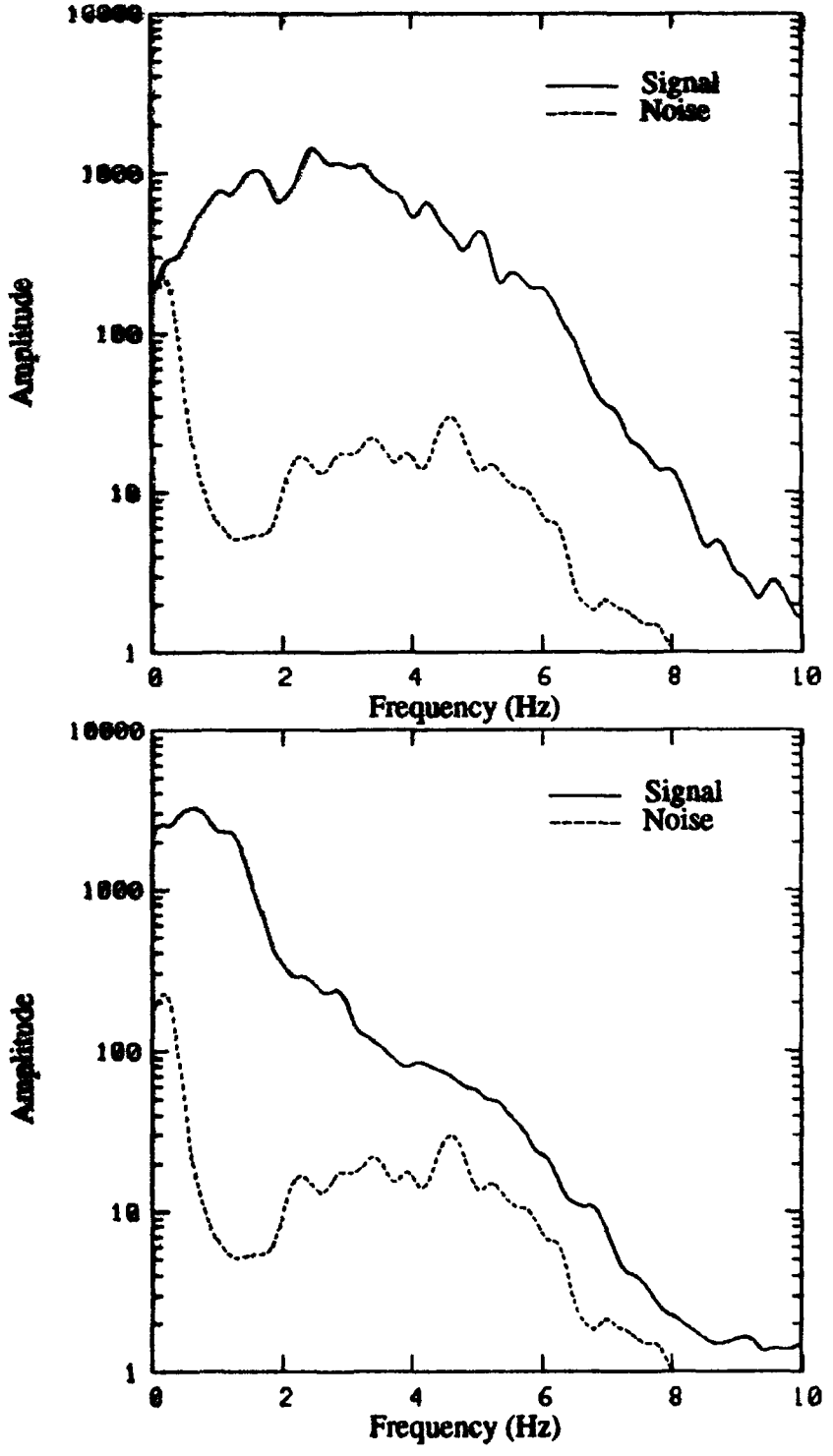

Figure 15. Regional phase spectra, P (top) and L_g (bottom), for 7/08/89 Semipalatinsk explosion observed at ARU.

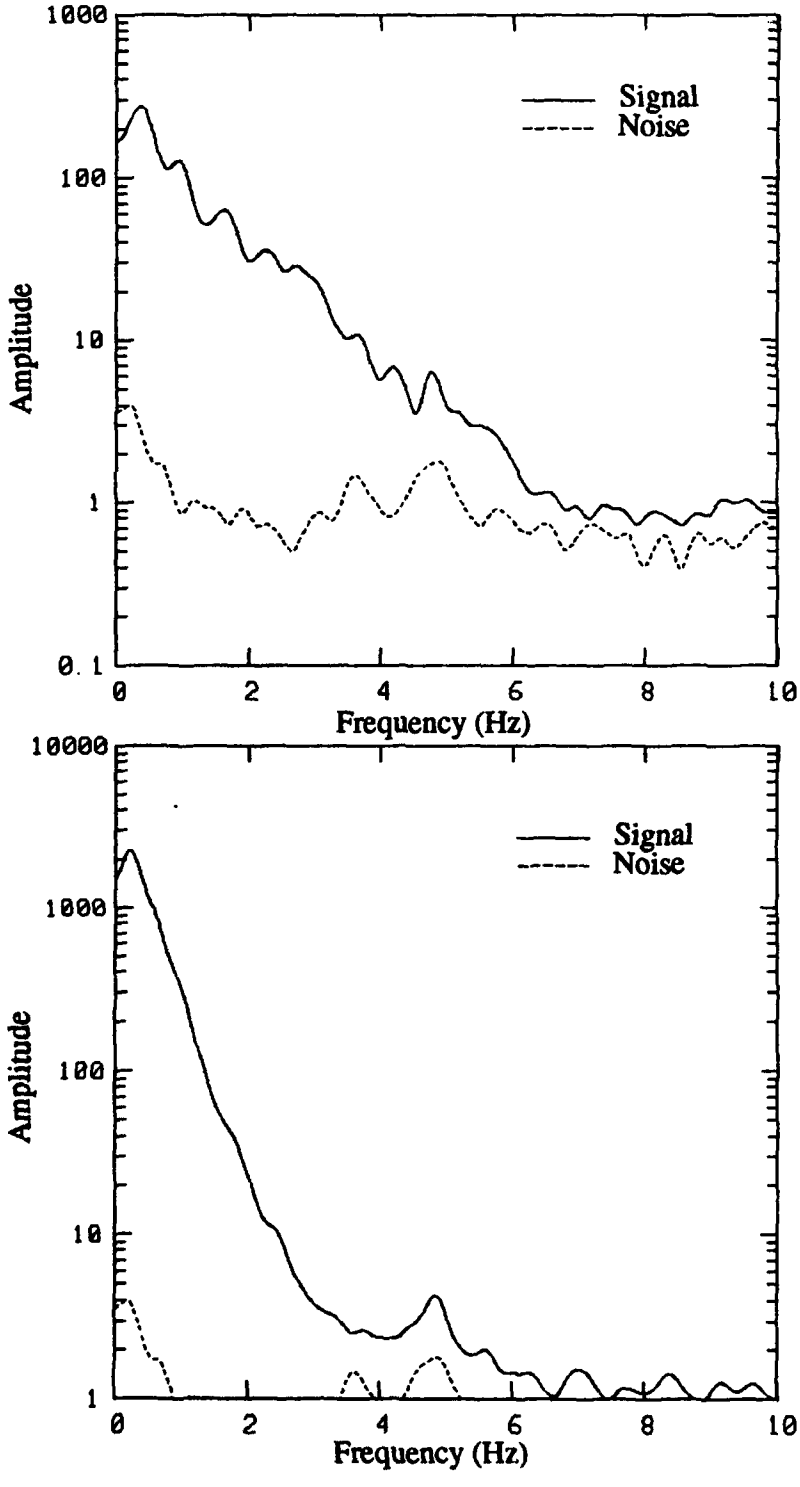

Figure 16. Regional phase spectra, P (top) and L_g (bottom), for 8/03/90 earthquake (6.0 m_b) observed at ARU.

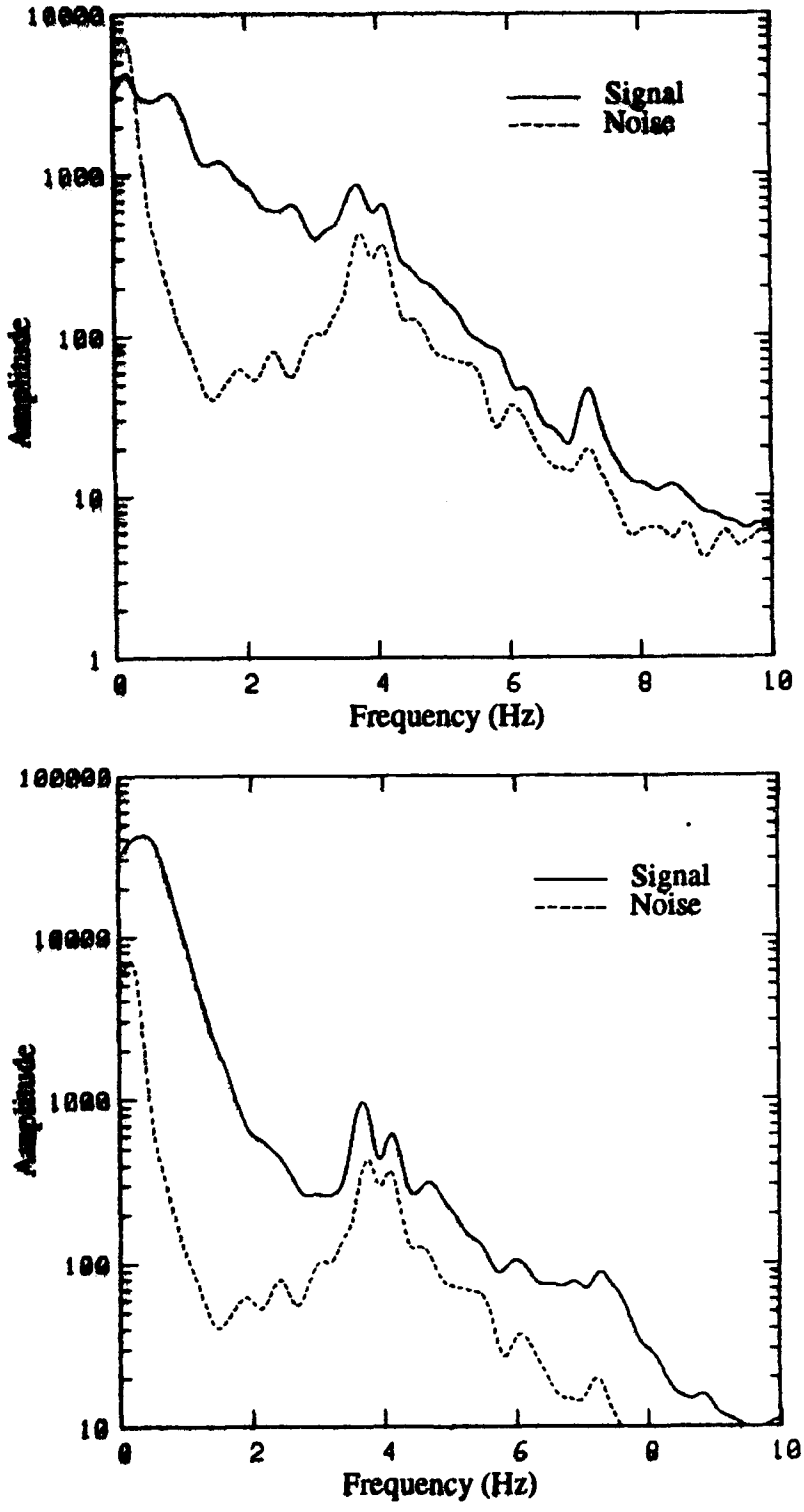

Figure 17. Regional phase spectra, P (top) and L_g (bottom), for 12/21/88 earthquake (5.4 m_b) recorded at ARU.

noise spectra for most events show minima in this same frequency band between about 1 and 2 Hz. In most cases the signal/noise ratios for these events are well above one over much of the available frequency band. However, in several instances the background noise has peaks in the band near 4 to 5 Hz producing reduced signal/noise levels in that interval. Furthermore, the signal levels frequently approach the noise at higher frequencies particularly for smaller events at larger distances.

For the explosions the regional P spectra are frequently quite broad showing a slow decay over the range from about 1 to 6 Hz. On the other hand, the explosion L_g spectra are rather sharply peaked below 1 Hz and drop-off rapidly toward higher frequencies. In contrast, for the earthquakes the regional P and L_g spectra fall-off monotonically and more rapidly from their maximum values in the frequency range below 1 Hz to the noise levels at frequencies near 6 Hz. Thus, the biggest difference in the regional phase spectra between the two source types observed at station ARU would appear to be the greater prominence of high frequencies in the explosion P signals.

3.4 L_g/P Spectral Ratios Measured at ARU

For each of the events described in the preceding section, L_g/P spectral ratios were computed. The ratio computations were limited to a frequency band from 0 to 6 Hz because of contamination of the spectra by noise at higher frequencies, particularly for the events at larger distances and smaller magnitudes. L_g/P spectral ratios for the two representative explosions and two representative earthquakes recorded at ARU are shown in Figures 18-21.

The L_g/P spectral ratios for the two Shagan River explosions in Figures 18 and 19 are remarkably similar. Both spectra have maximum values in the frequency range from 0 to 1 Hz. These maximum values are greater than ten. At larger frequencies the explosion L_g/P ratios show similar, monotonic decreases out to 3 Hz where they reach levels of about 0.2, which is maintained to higher frequencies. This result appears to be in

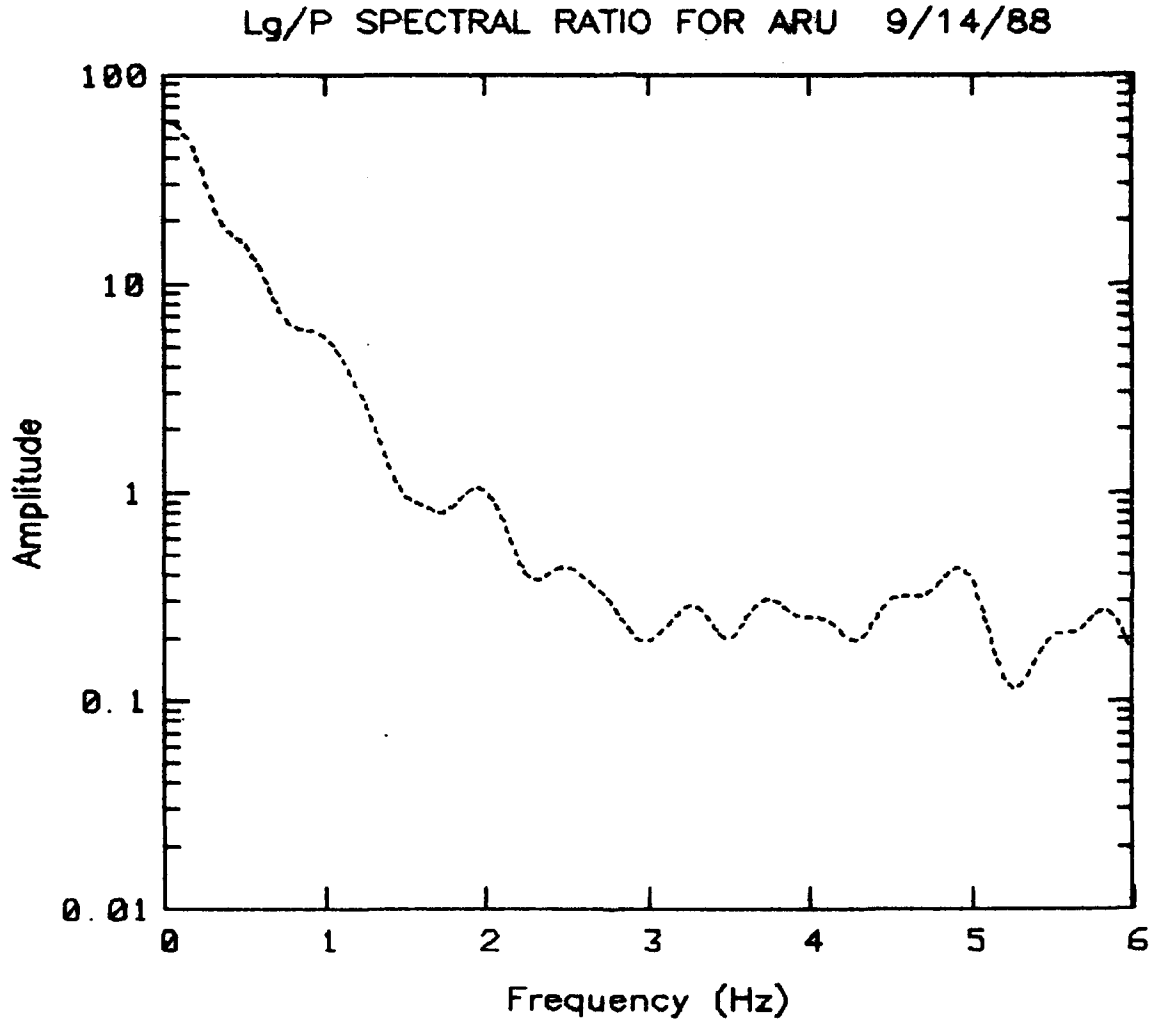

Figure 18. Lg/P spectral ratio for the JVE nuclear explosion recorded at ARU.

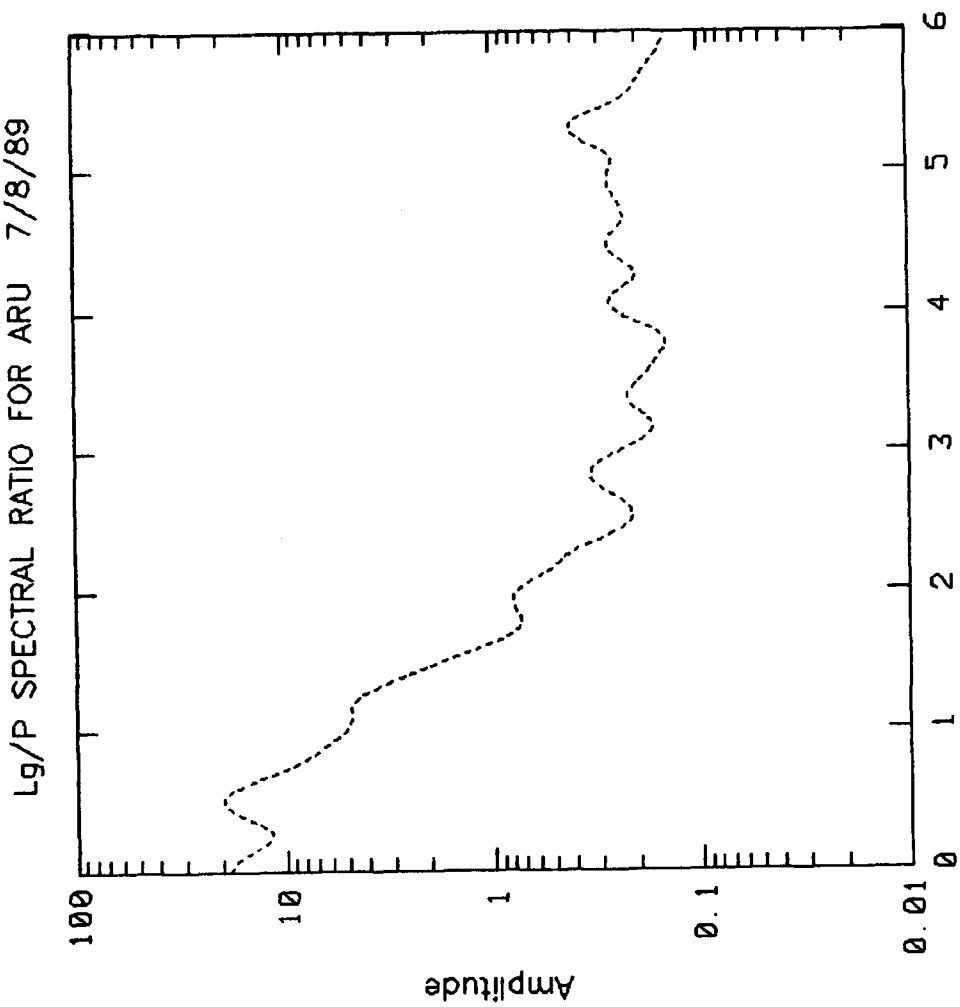

Figure 19. Lg/P spectral ratio for the 7/8/89 nuclear explosion recorded at ARU.

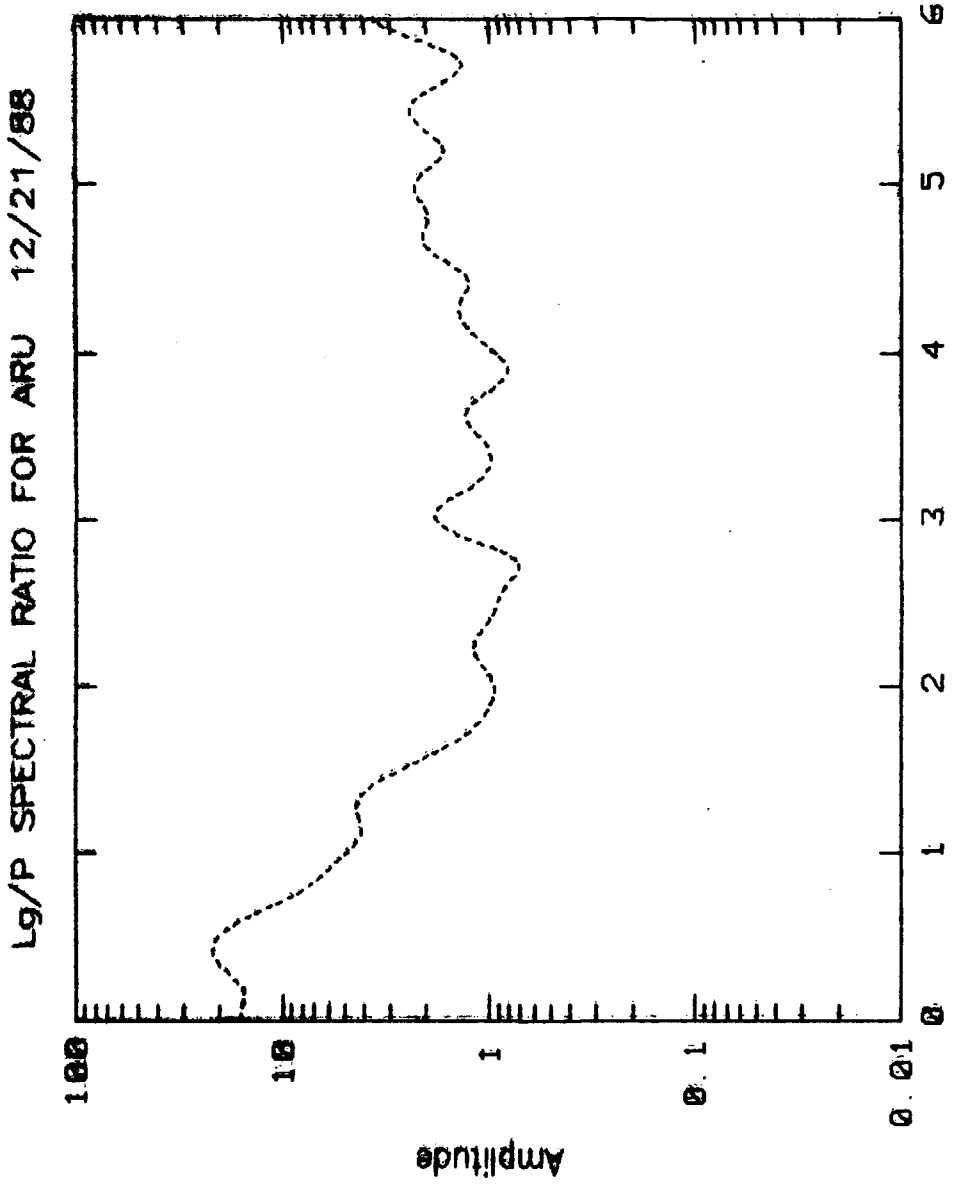

Figure 20. Lg/P spectral ratio for the 12/21/88 earthquake recorded at ARU.

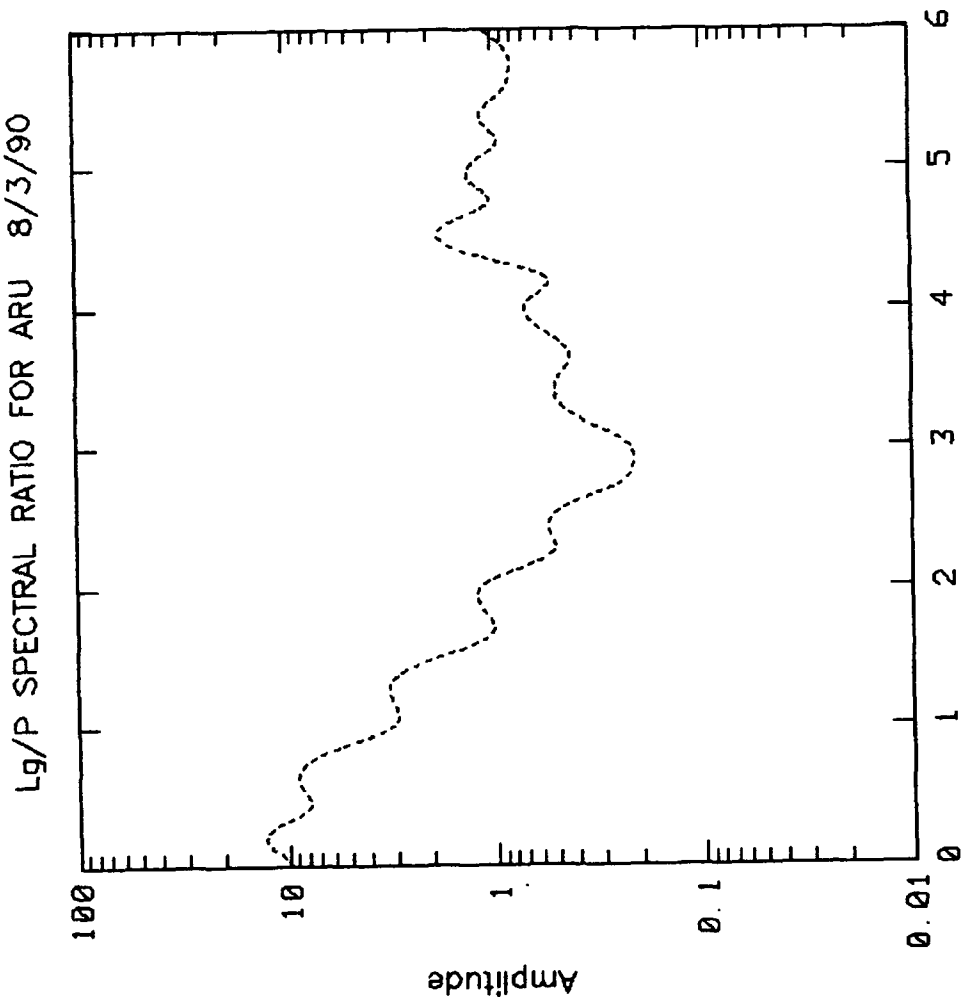

Figure 21. Lg/P spectral ratio for the 8/03/90 earthquake recorded at ARU.

close agreement with the L_g/P spectral behavior which we previously found for Semipalatinsk explosions recorded at WMQ (cf. Bennett *et al.*, 1989, 1990a).

The L_g/P spectral ratios for the two earthquakes shown in Figures 20 and 21 are also quite similar. The earthquake spectral ratios are again peaked in the frequency range from 0 to 1 Hz at maximum values somewhat greater than ten. However, the earthquake spectral ratios appear to have a slightly less steep decline and tend to reach a minimum at somewhat lower frequencies than for the explosions. In general, the earthquake L_g/P ratios are well above those of the explosions over the frequency band above about 2 Hz. This again is in agreement with our previous results for WMQ. However, as was the case there, we note that propagation paths are somewhat different for the explosions and earthquakes recorded at ARU. In particular, the two earthquakes for which the spectra are shown in Figures 20 and 21 are from 400 to 500 km farther away than the comparable explosions; and in one case (the 12/21/88 event) the azimuth is quite different. As a result, propagation effects may contribute to some of the observed differences in the L_g/P spectral ratios. However, we believe for reasons presented here and in subsequent sections of this report that propagation differences are not the sole cause of these observations.

To minimize the influences of propagation paths for particular earthquakes, we determined the average L_g/P spectral ratio for all the earthquakes and explosions recorded at ARU for which the regional phase spectra were computed. These are shown in Figure 22 accompanied by one-sigma bounds about the average ratios. The average results are seen to be quite similar to the observations for the individual events at ARU. In particular, for the nuclear explosions the average L_g/P ratio is peaked at a value between ten and twenty near 0.5 Hz and decreases monotonically above the peak out to a frequency near 3 Hz, where the spectral ratio tends to level off at a value of about 0.3. It should also be noted that the one-sigma bounds on the L_g/P ratios for the nuclear explosions are rather tight at all frequencies indicating a remarkable consistency from event to event. For

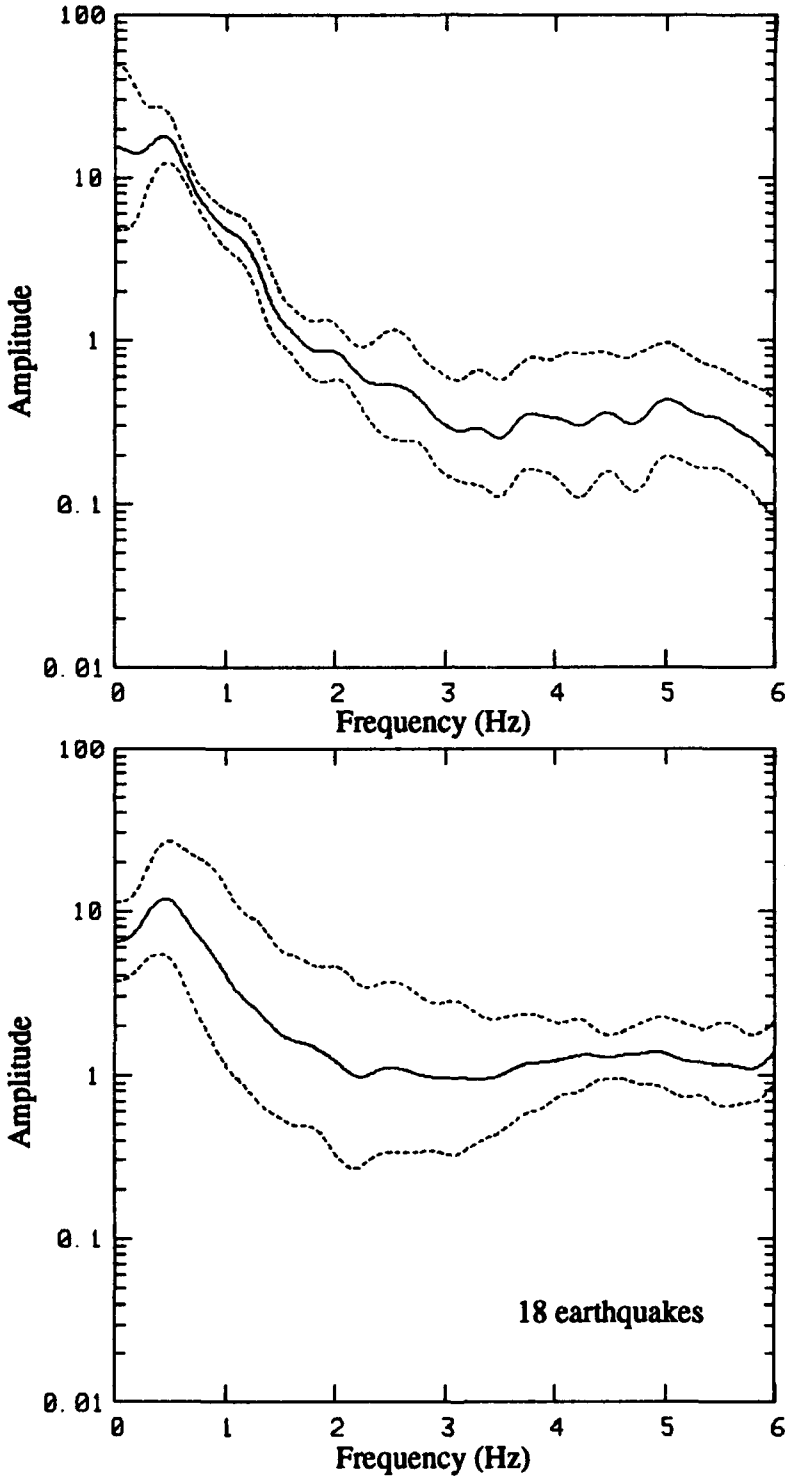

Figure 22. Mean and ± 1σ bounds on L_g/P spectral ratios for Semipalatinsk explosions (top) and 18 earthquakes (bottom) observed at ARU.

the 18 earthquakes at ARU, the average L_g/P ratio (at the bottom of Figure 22) is peaked at about the same frequency (viz 0.5 Hz) as for the explosions; and the maximum value is again somewhat greater than ten. Above the peak the L_g/P spectral ratio again decreases but at a somewhat slower rate than for the explosion average. The average earthquake ratio levels off above about 2 Hz at a value near one. The scatter in the earthquake ratios indicated by the one-sigma bounds is somewhat greater possibly indicating variations in the ratios associated with propagation path differences in the individual events.

We computed a second average earthquake L_g/P spectral ratio for ARU focusing on earthquakes with paths more comparable to those of the nuclear explosions. In particular, we eliminated some of the close-in events to ARU and the earthquakes with sources in the Caspian Sea region. This new average L_g/P spectral ratio included 12 earthquakes and is shown at the bottom of Figure 23 where it is compared with the same average explosion ratio for ARU. The results in Figure 23 show very little difference from those in Figure 22. The earthquake L_g/P ratios again level off at a value near one at higher frequencies. The scatter seems to be about the same.

Overall, from the standpoint of seismic discrimination the results at station ARU again indicate promise for L_g/P spectral ratios. In particular, at frequencies above about 2 Hz there appear to be significant differences in the L_g/P ratios between nuclear explosions and earthquakes. There remain two areas of caution with regards to this discriminant. First, propagation effects on regional phases are likely to have some influence on the spectral ratios; but, as we show in the following section, we believe they are not the cause of the discriminant. Second, the discriminant requires signal information at higher frequencies (above 2 Hz); and, therefore, it may be less effective for ranges beyond about 2000 km and for smaller events where the signal levels at these higher frequencies are approaching the detection threshold. The latter is a general problem for all areas of seismic discrimination. In this case the extent of the problem could be defined by determining the detection threshold as a function of frequency for the

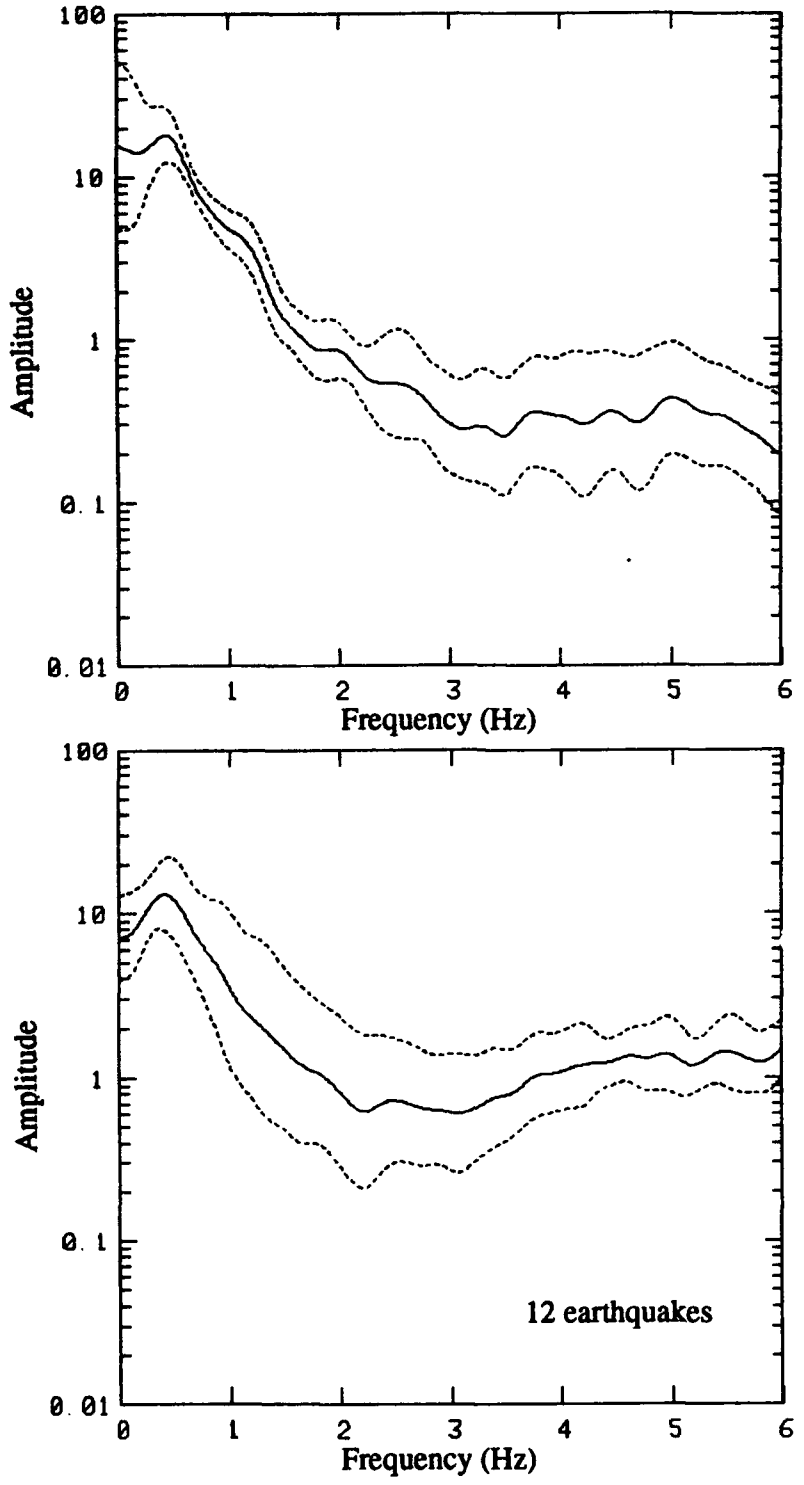

Figure 23. Mean and $\pm 1\sigma$ bounds on L_g/P spectral ratios for Semipalatinsk explosion (top) and 12 earthquakes (bottom) observed at ARU.

regional phases in the areas of interest at the stations to be used for seismic monitoring.

IV. REGIONAL DISCRIMINATION ANALYSES OF LOP NOR EXPLOSIONS AND EARTHQUAKES WITH NEARLY COMMON PATHS

4.1 Background

In prior studies of regional seismic data recorded at station WMQ, we found consistent differences in the L_g/P spectral ratios between underground nuclear explosions near Semipalatinsk and the regional earthquakes in the database (cf. Bennett *et al.* 1989, 1990a). This observation was in agreement with previous experience for NTS nuclear explosions and nearly co-located earthquakes recorded at regional distances (cf. Murphy and Bennett, 1982; Bennett and Murphy, 1986; Taylor *et al.* 1988) and also with the experience of others for non-nuclear explosions and nearby earthquakes recorded at Norwegian regional arrays (cf. Dysart and Pulli, 1990). Nevertheless, some questions were raised about the extent to which the results obtained for WMQ might have been influenced by propagation path differences, because many of the earthquakes used for comparison were located along the southern Soviet border somewhat removed from the nuclear explosion test site. Therefore, to test the degree to which observed differences in the L_g/P spectral ratios was controlled by source type, independent of propagation effects, we sought to identify Eurasian events with nearly common paths which could be used for analyses. We describe here the results of two analyses of regional phase spectra for nuclear explosions at Lop Nor, China and earthquakes with approximately the same propagation paths.

4.2 Reciprocal Relation Between Lop Nor Explosions and Earthquakes Near Garm

The Chinese nuclear test site at Lop Nor is located approximately at 41.7°N 88.7°E (cf. Table 1 above). Although the nuclear testing program in the People's Republic of China is not particularly active, there appear to

have been two tests at Lop Nor which occurred since the Soviet IRIS network became operational. These took place on 05/26/90 and 08/16/90 and had magnitudes of 5.4 and 6.2 m_b, respectively. CDSN data are apparently not available for either of these events, although the latter was well recorded at the Soviet IRIS stations, and in particular at GAR (R ≈ 1590 km). The CDSN station at WMQ is located at 43.8°N 87.7°E, less than 250 km from the Lop Nor test site, and has recorded several earthquakes from the vicinity of GAR (R ≈ 1530 km). We picked two earthquakes (viz 01/09/88 and 09/25/88) with epicenters within about 230 km of GAR which were well recorded at WMQ from our database (cf. Table 2 above).

As can be seen in Figure 24, the Lop Nor explosion recorded at GAR and the earthquakes near GAR recorded at WMQ form an approximately reciprocal relationship between source and receiver. The propagation paths between the sources and receivers in these events are nearly coincident, so the paths are approximately common for these events. Therefore, differences in the regional signals between the events should represent differences in the sources.

Figure 25 shows the broad-band vertical-component waveforms for these three events. Differences between the signals related to instrumentation differences between stations are believed to be insignificant. The major difference observed in these broad-band signals is the much larger L_g amplitudes relative to P in the earthquake records compared to the explosion. Thus, L_g/P ratios for the earthquakes are about 4:1 compared to a ratio of only about 1:2 for the explosion. The records in Figure 25 suggest that there may be some frequency differences in the regional signals between event types. The most notable difference is the prominence of the relatively low frequencies in the earthquake records. In addition, the explosion regional P signal appears to be enriched in high frequencies compared to the earthquakes. To analyze the spectral contents of these signals in more detail, Fourier spectra were computed from a 25-second sample of the initial P and a 100-second sample of the L_g window for each

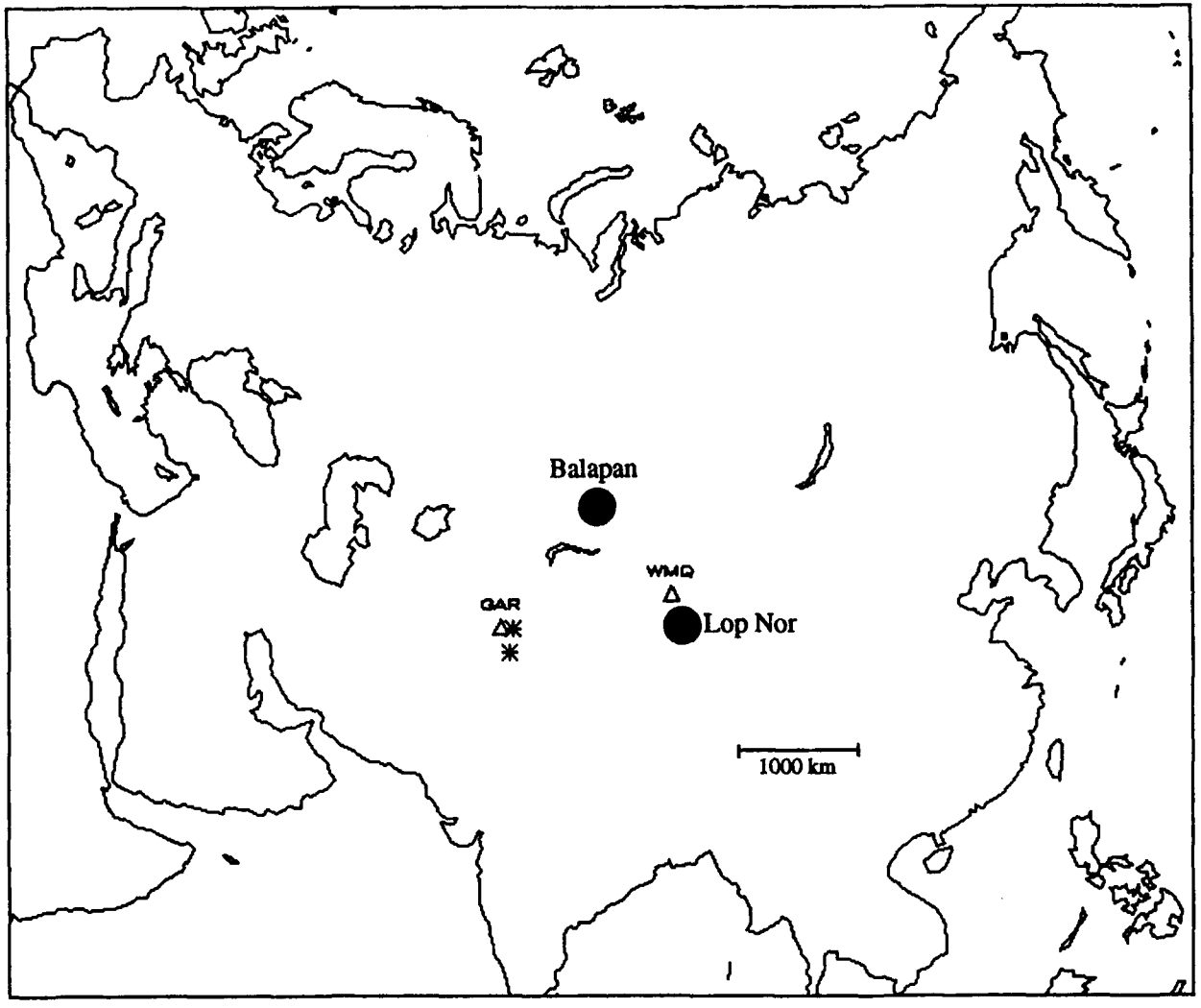

Figure 24. Approximate reciprocal relationship between Lop Nor nuclear explosion recorded at GAR and near-Gar earthquakes recorded at WMQ.

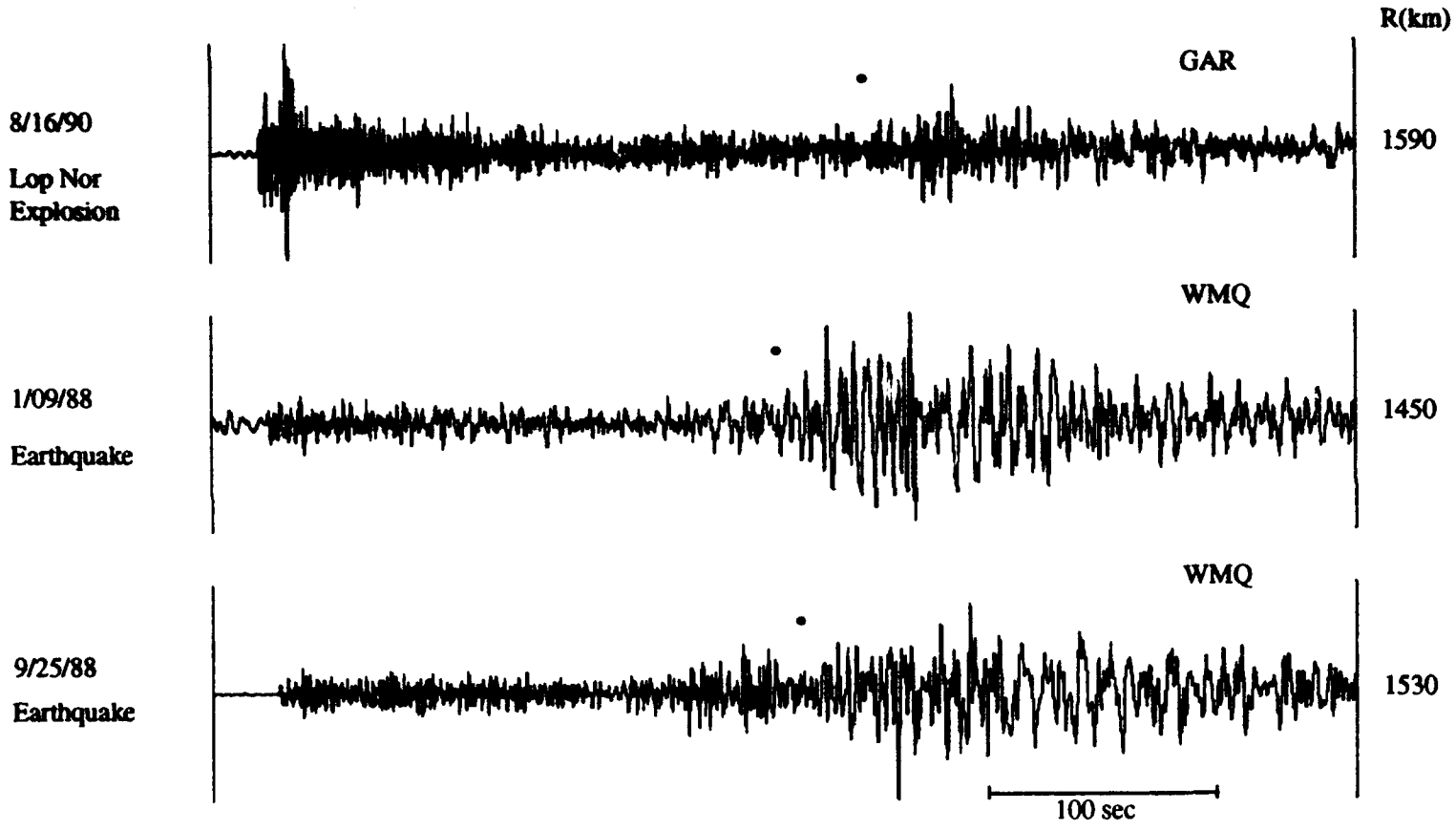

Figure 25. Vertical-component, broadband records for approximately reciprocal nuclear explosions and earthquakes.

record. The spectra were computed over a frequency band from 0 to 10 Hz and smoothed and interpolated to provide spectral estimates at the same frequencies for both P and L_g. L_g/P spectral ratios were then computed and are shown in Figure 26. The L_g/P spectral ratios for the explosion (plotted as the dashed line) appears to be significantly different from the two reciprocal earthquakes (plotted as dotted and combination dotted-and-dashed lines). For both types of events the spectral ratios are high (above one) at frequencies below about 1.0 Hz, with the earthquake ratios being slightly higher than the explosion ratio. However, the explosion ratio drops off much more rapidly toward higher frequencies than the corresponding earthquake ratios. The two earthquakes are seen to have fairly consistent L_g/P ratios which lie well above those of the Lop Nor explosion over a broad frequency band. In fact, the differences are up to a factor of ten in a frequency band between 2 and 3 Hz. At frequencies above 7 Hz the spectral ratios overlap, but the system response and noise characteristics at the stations are such that spectral estimates above about 5 Hz may not be representative of the signal amplitudes. We would conclude from the observations in Figure 26 that the earthquakes and explosions produce significantly different L_g/P spectral ratios for approximately reciprocal paths which we would attribute to source differences in the excitation of the regional seismic phases.

We also show in Figure 26 for comparison purposes the L_g/P spectral ratio for the JVE explosion (viz 09/14/88) at the Semipalatinsk test site also recorded at GAR ($R \approx 1390$ km). The magnitude of this explosion was approximately the same as that of the Lop Nor explosion. However, the L_g/P spectral ratios for the two events are notably different. Over the frequency band from less than 1 Hz to more than 3 Hz, the spectral ratio for the Semipalatinsk explosion is up to a factor of eight larger than for the Lop Nor explosion. This appears mainly to be due to the occurrence of more L_g energy in that frequency band for the GAR recording of the Semipalatinsk explosion. The path from Lop Nor to GAR seems to be more attenuative than the path from Semipalatinsk to GAR; a more complete discussion of this problem follows in a later subsection. This latter result suggests that some

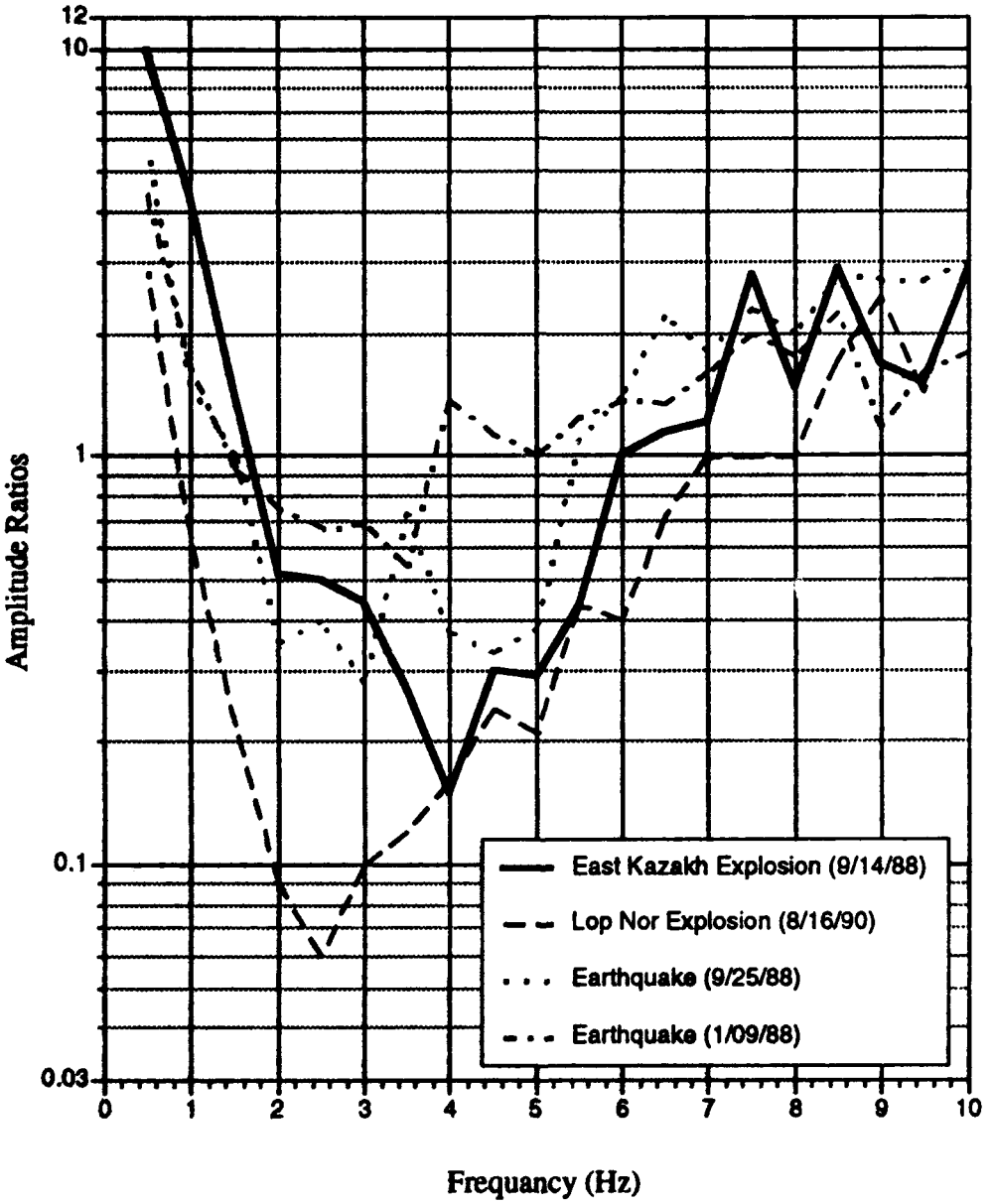

Figure 26. Lg/P spectral ratios for approximately reciprocal events from Figure 25 and 9/14/88 JVE explosion at Semipalatinsk observed at GAR.

care needs to be exercised in comparing spectral differences in regional signals for events with different propagation paths.

4.3 Nearly Co-Located Nuclear Explosions and Earthquakes Near Lop Nor

In addition to the above analysis of approximately reciprocal events, a more direct comparison of regional signals for underground nuclear explosions and earthquakes with nearly common paths can be obtained using the Lop Nor explosions and nearby earthquakes recorded at the Soviet IRIS stations. The map in Figure 27 shows the locations of two Lop Nor nuclear explosions (viz 05/26/90 and 08/16/90) and two nearby earthquakes (viz 01/21/90 and 11/03/90) for which good regional signals were recorded at stations GAR and ARU. The approximate epicentral distances of GAR and ARU from the source area of these events are 1590 km and 2710 km, respectively. The distance between individual explosion and earthquake sources is between 5 and 100 km depending on the event pair selected. In fact, the close proximity of the 01/21/90 earthquake and the 05/26/90 nuclear explosion (viz a separation distance of only about 5 km) is well within the uncertainty bounds on the event locations and makes the former event somewhat suspect. The nuclear explosion magnitudes were 5.4 and 6.2 m_b (cf. Table 1 above), while the earthquake magnitudes were 4.6 and 5.1 m_b (cf. Table 2 above).

4.3.1 General Properties of the Time-Domain Signals

Figure 28 shows the broad-band vertical-component records at stations GAR and ARU which were available for the four events near the Lop Nor test site. Unfortunately, each station recorded only three of the four possible events. In agreement with our previous findings, the waveforms show rather large L_g/P ratios for the earthquakes and smaller ratios for the nuclear explosion tests. Both regional P and L_g signals for the

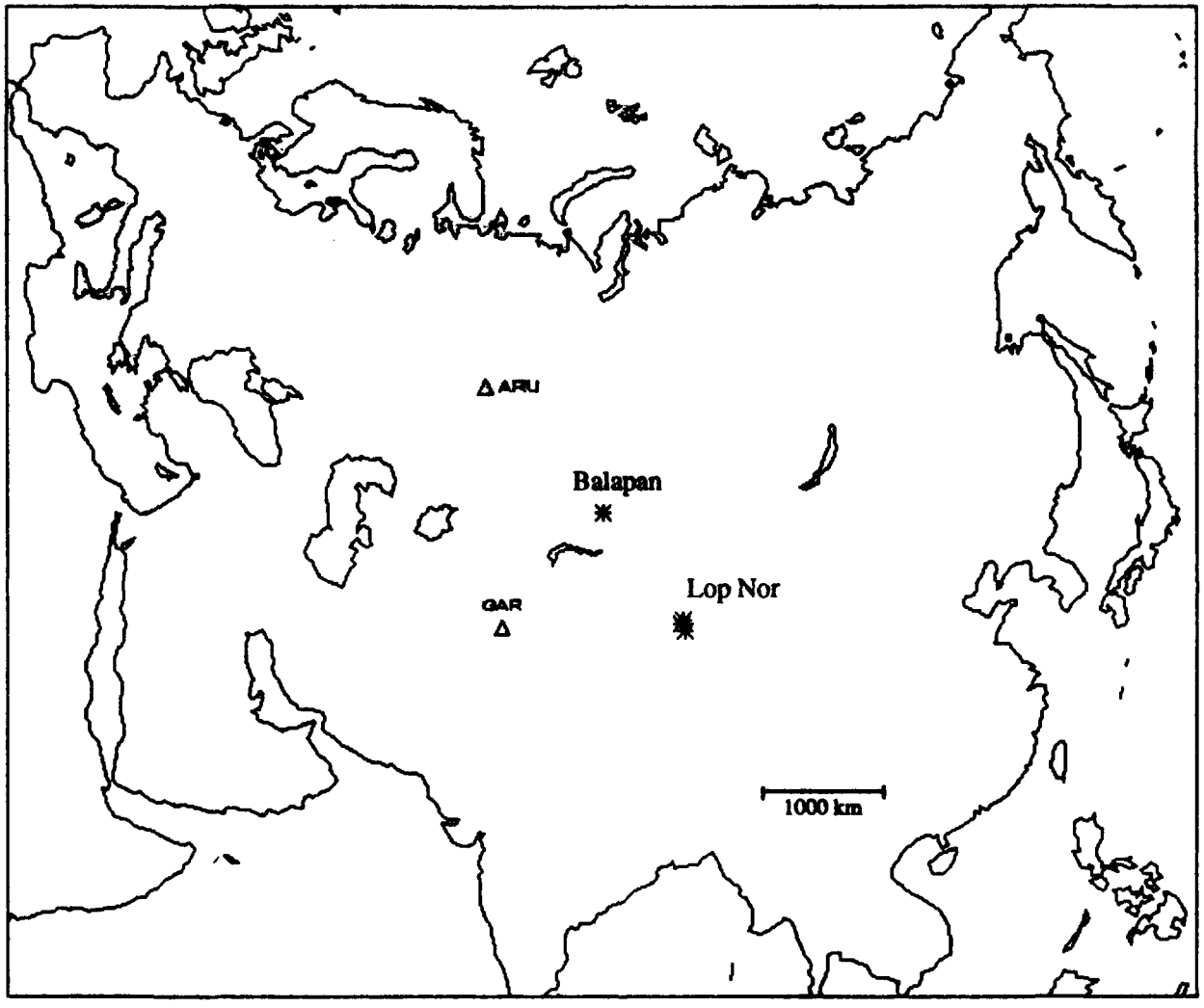

Figure 27. Locations of Lop Nor nuclear explosions and nearby earthquakes recorded at GAR and ARU.

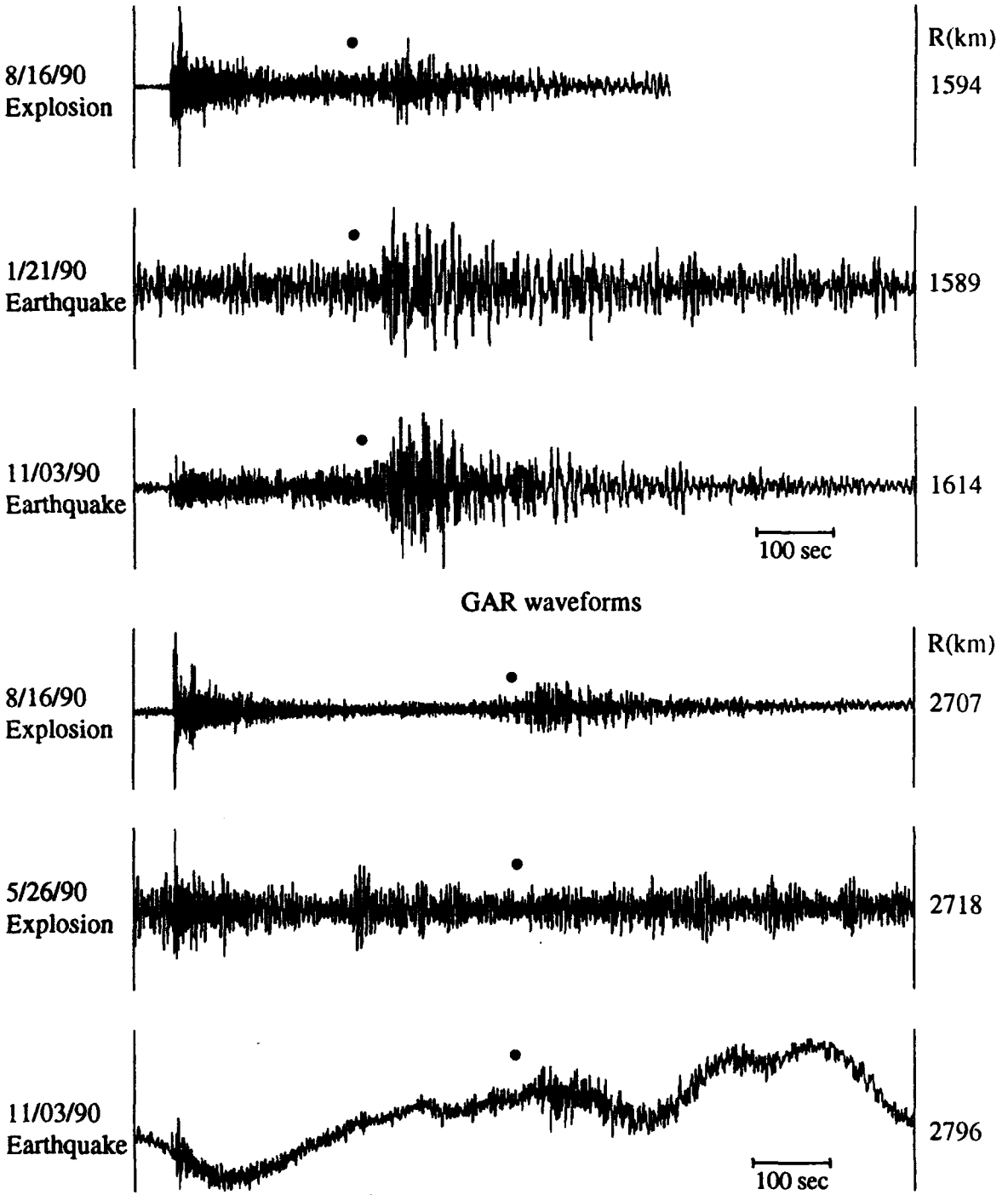

Figure 28. Unprocessed vertical-component, broadband records at GAR (top) and ARU (bottom) for nearly co-located Lop Nor explosions and earthquakes.

explosion records are enhanced at high frequencies relative to the earthquakes. Furthermore, lower-frequency Rayleigh waves appear to be somewhat more prominent relative to the other regional phases in the GAR records for the earthquakes than for the explosion. The records clearly include some unwanted noise which interferes with identification of the regional signals particularly for the smaller events. To enhance the signal-to-noise for these events, we applied a high-pass filter with a corner at 0.2 Hz to remove the microseismic background noise. These filtered records are plotted in Figure 29. Although not necessarily optimal, the filter clearly improves the signal-to-noise characteristics of the records especially for the smaller magnitude events. This filter also retains very well the amplitude levels and relation between the principal regional phases. The only negative aspect of the filtering is the apparent loss of some of the lower frequency Rayleigh wave energy which is in approximately the same frequency band as the background noise.

Considering first the GAR records in Figure 29, the two earthquake records show a remarkable consistency in the regional signals and are notably different from the record of the nearby underground nuclear explosion. The L_g/P ratios differ by almost a factor of ten; ratios are about 4:1 for the earthquakes and only about 1:2 for the explosion. The regional P signals consist of multiple phases which appear to be repeated in both the explosion and earthquake records; however, in the explosion the second P arrival has a much larger relative amplitude. With regard to L_g the earthquake records appear to have considerably longer duration with larger amplitudes extending into the latter part of the L_g window. There may also be some differences in the frequency content of the regional signals; these will be described more completely below. The ARU records in Figure 29 also show high consistency in the regional signals for the two explosions and one earthquake. However, even though the L_g/P amplitude ratio is larger for the earthquake than for the two explosions, the distinction is not as great as it was for the nearer station. Thus, the L_g/P ratio is slightly greater than 1:2 for the earthquake and less than 1:3 for the explosions. It's possible that

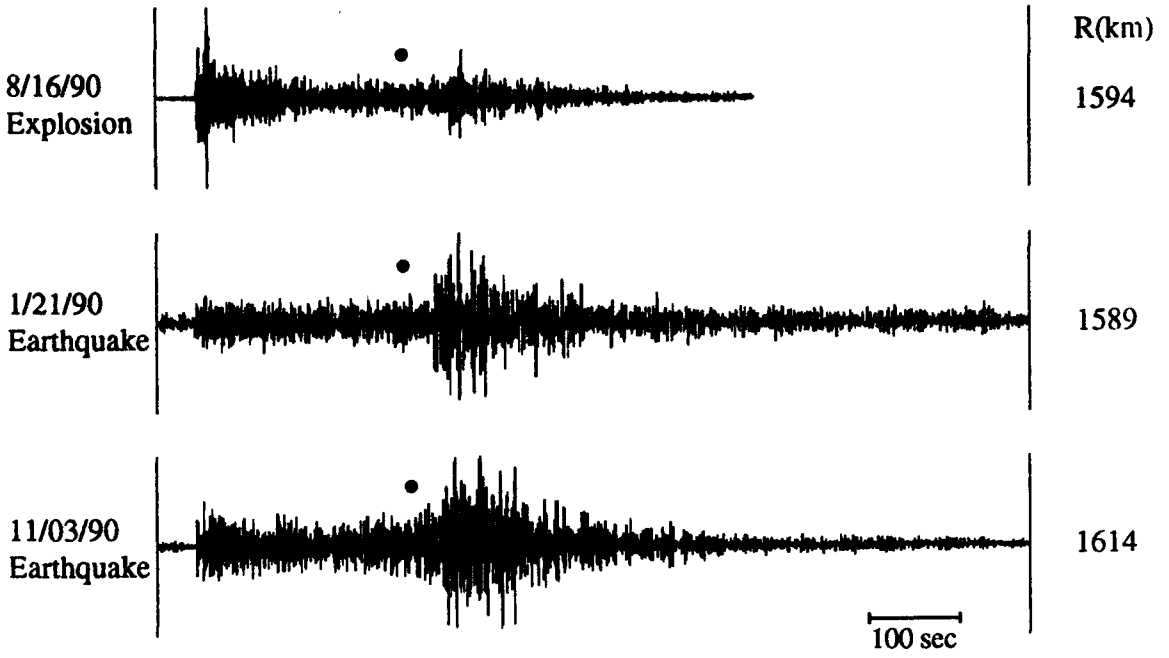

GAR waveforms

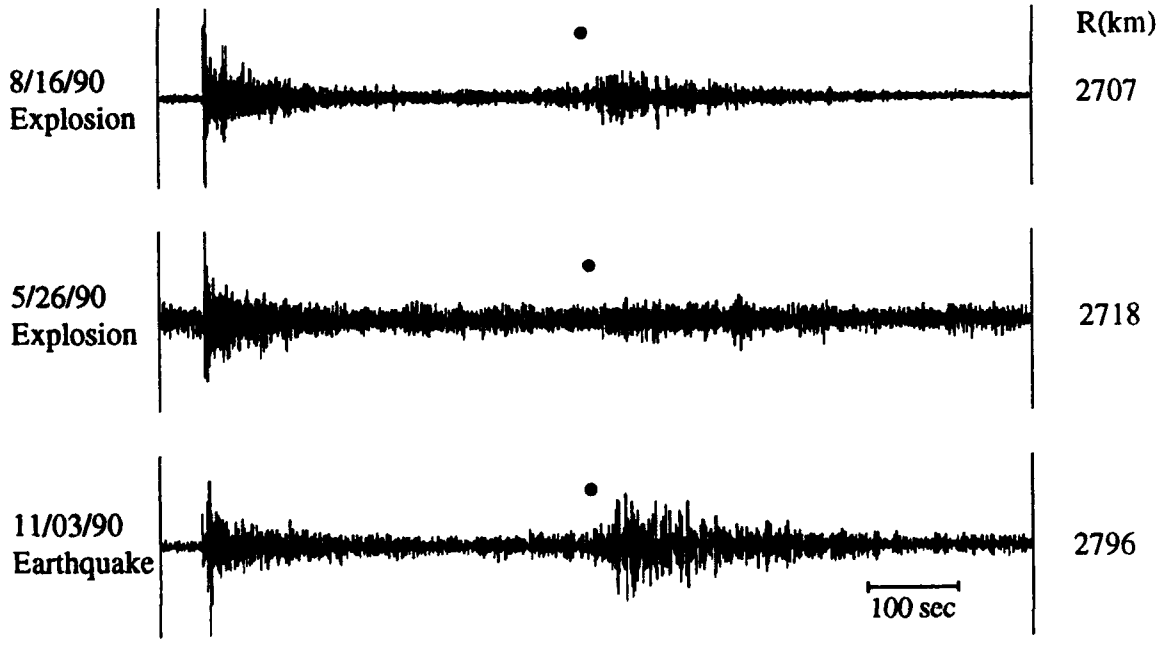

ARU waveforms

Figure 29. High-pass filtered (> 0.2 Hz) vertical-component records from Figure 28 at GAR (top) and ARU (bottom) for nearly co-located events.

some enhancement of these differences may be achieved by additional filtering.

For seismic discrimination the results in Figure 29 suggest that there are differences in the L_g versus regional P excitation between underground nuclear explosions and earthquakes which are related to source differences. However, the observations also indicate that these differences may be harder to identify at larger ranges. For regional seismic monitoring it seems desirable that the network include stations at ranges less than 2000 km from the sources; this range of effective monitoring is likely to be a function of the threshold of events which need to be identified.

4.3.2 L_g/P Spectral Ratios

As noted above, our previous analyses of a large database of Eurasian nuclear explosions and earthquakes recorded at the Chinese digital station WMQ had proven highly successful in discriminating these events on the basis of L_g/P spectral differences. However, questions still remained regarding the relative significance of propagation effects on these results. In the preceding section we attempted to allay this concern based on analyses of L_g/P spectral differences for explosions and earthquakes having an approximate reciprocal relationship. An even more direct approach to resolving what effects are related to source differences is presented here using the regional signals from the 08/16/90 Lop Nor nuclear explosion and nearby 01/21/90 and 11/3/90 earthquakes recorded at GAR. Since the explosion and earthquakes are located in such close proximity, the differences in the L_g/P spectral ratios between these events should be caused by the sources. We first show the results of these analyses and then speculate on possible influences of transmission path differences for this area.

We first computed regional phase spectra and L_g/P spectral ratios for the GAR recordings in Figure 29. These spectra are presented in Figures 30 to 33a. The results indicate good signal-to-noise ratios for the Lop Nor

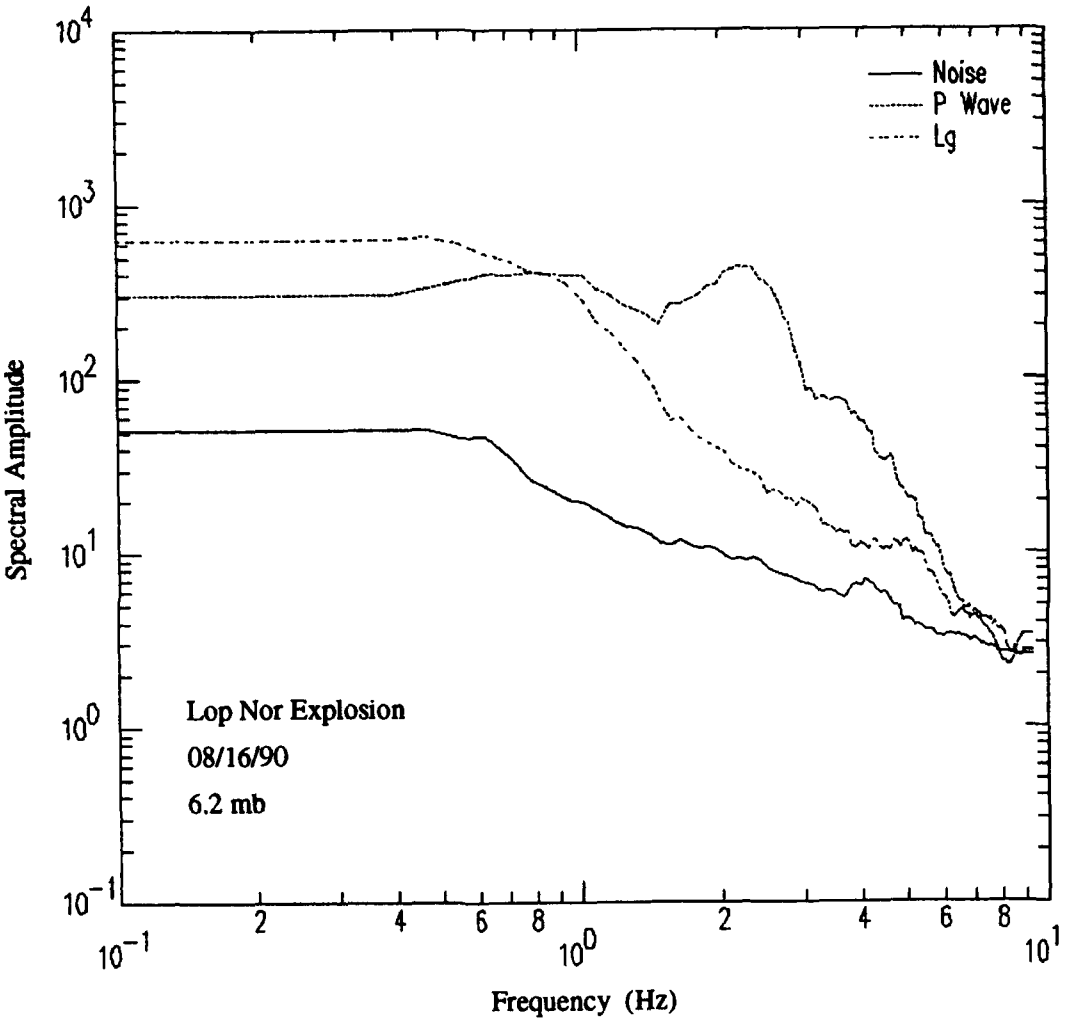

Figure 30. Regional phase spectra for 8/16/90 Lop Nor underground nuclear explosion observed at GAR.

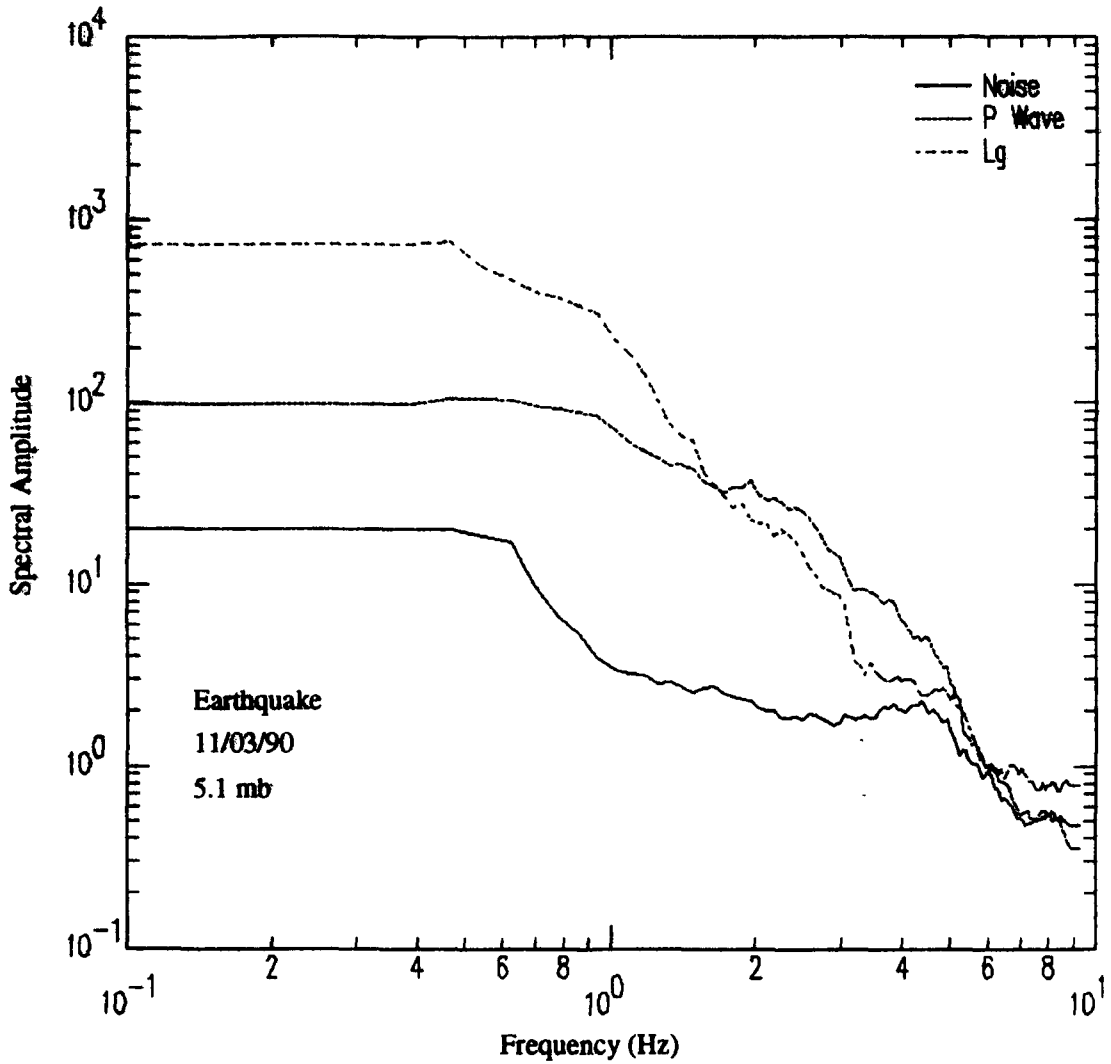

Figure 31. Regional phase spectra for 11/03/90 earthquake observed at GAR.

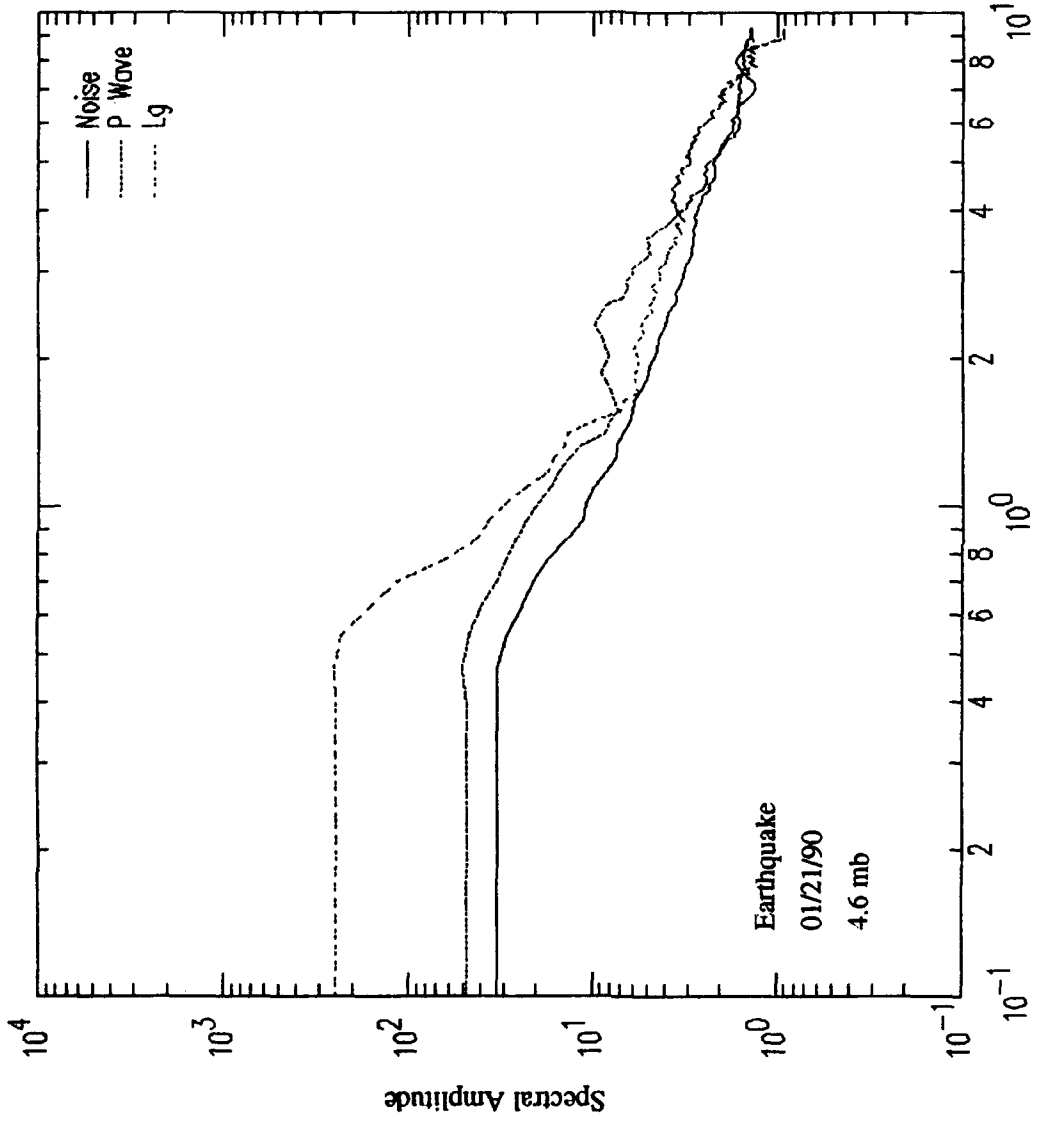

Figure 32. Regional phase spectra for 1/21/90 earthquake observed at GAR.

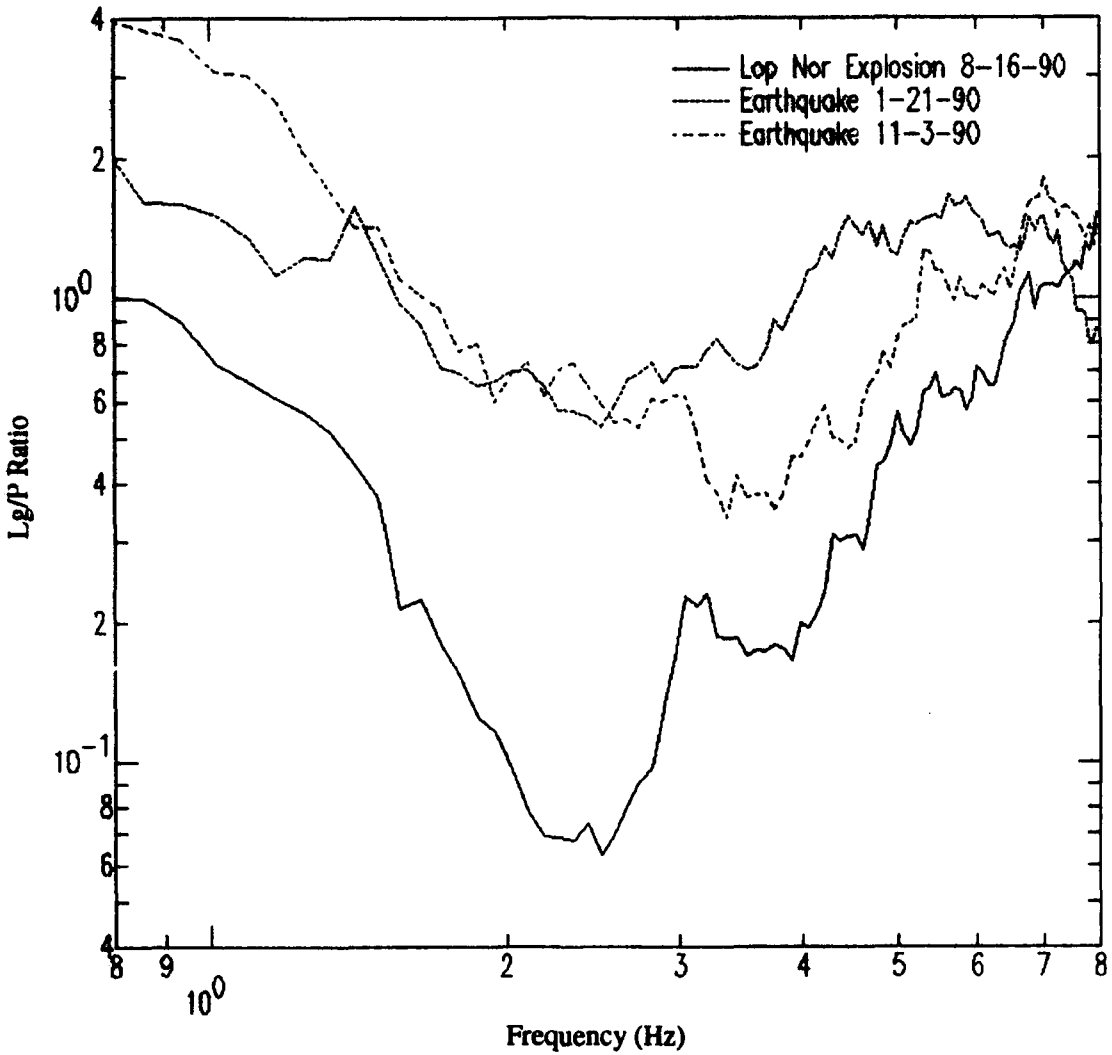

Figure 33a. Lg/P spectral ratios at GAR for Lop Nor nuclear explosion and nearly co-located earthquakes.

explosion and the larger of the two earthquakes up to about 7 to 8 Hz (cf. Figures 30 and 31). However, the smaller earthquake showed noise levels at the P-wave amplitude level from about 4 Hz on up (cf. Figure 32). Nevertheless, we retained this event due to its very close proximity to the Lop Nor test site. The spectra generally show flat portions at low frequencies, below about 0.5 Hz followed by a monotonic decay toward higher frequencies. The regional P-wave spectrum for the Lop Nor explosion (cf. Figure 30) is exceptional in that a lobe of energy appears to extend to higher frequencies above the normal corner.

The L_g/P spectral ratios at GAR for all three of the events are compared in Figure 33a. We first note that the L_g/P spectral ratios for the earthquakes near Lop Nor recorded at GAR are very similar in character to those of the near-GAR earthquakes recorded at WMQ which we analyzed in the reciprocal experiment in a preceding subsection (cf. Figure 26 above). This remarkable similarity provides additional credence to our reciprocity argument. Although fluctuations in the ratios at GAR appear to be somewhat greater than those observed for stations WMQ and ARU, the earthquake ratios lie well above the explosion spectral ratio over the entire frequency band. The earthquake ratios remain between about 0.5 and 3 over the band. The explosion spectral ratios show a more rapid, monotonic decline above 1 Hz out to a frequency between 2 and 3 Hz where they again start to increase. As a result, the greatest difference between the explosion and earthquake L_g/P spectral ratios for these GAR records occurs at between 2 and 3 Hz. The difference in this frequency band is about a factor of ten. This occurrence apparently coincides with the high-frequency lobe in the regional P-wave spectrum from the Lop Nor explosion described earlier (cf. Figure 30). The cause of this observation is unknown at this time. One possibility is a local recording site effect associated with the Surkhov river valley; although enhancement of the P-wave signals in this frequency band is not very strong for explosions arriving at GAR from other azimuths or for the earthquakes near Lop Nor for which the P waves into GAR would have very similar paths to that of the Lop Nor explosion. Another possibility is a near-source effect (e.g., crustal amplification) which affects the explosion P

but may not influence the deeper earthquake sources. While this effect may enhance the differences in the L_g/P spectral ratios between the Lop Nor explosion and nearly co-located earthquake recorded at GAR, the more general difference by a factor of two to four which persists over the broader frequency band appears to provide a robust discriminant which is less likely to be masked by site or propagation effects.

Additional evidence that the observed differences in the L_g/P spectral ratios are more closely related to source factors is provided by the observations at station ARU from the nearly co-located events. In Figure 33b we show the L_g/P spectral ratios for the 8/16/90 Lop Nor explosion and the 11/03/90 earthquake observed at ARU. Although the S/N level is not as great at ARU as at GAR, particularly for the earthquake, several significant features can be observed nevertheless in the L_g/P spectral ratios. In particular, the L_g/P ratio is greater for the earthquake than for the explosion over a fairly broad band from less than 1 Hz to more than 4 Hz. Within this band L_g/P differences between the earthquake and the explosion exceed factors of ten in some intervals. More importantly, the explosion L_g/P spectral ratio shows a sharp trough in the range 2 to 3 Hz, similar to that seen in Figure 33a for the same explosion at GAR. Thus, out to approximately 4 Hz, the L_g/P spectral ratios at both stations from the Lop Nor explosion exhibit very similar behavior which seems to be best explained as a source or near-source effect. Some of the differences at higher frequencies are probably related to noise or attenuation effects. The L_g/P spectral ratios for the 11/03/90 earthquake shown in Figures 33a and 33b for GAR and ARU are more different, although they do maintain a similar level well above the explosion ratios over a broad band. Differences in the spectral ratios between stations for the earthquake may be related to greater noise contamination in the ratios for the smaller magnitude earthquake at the more distant station. However, propagation factors and radiation pattern in the earthquake source may also play some role.

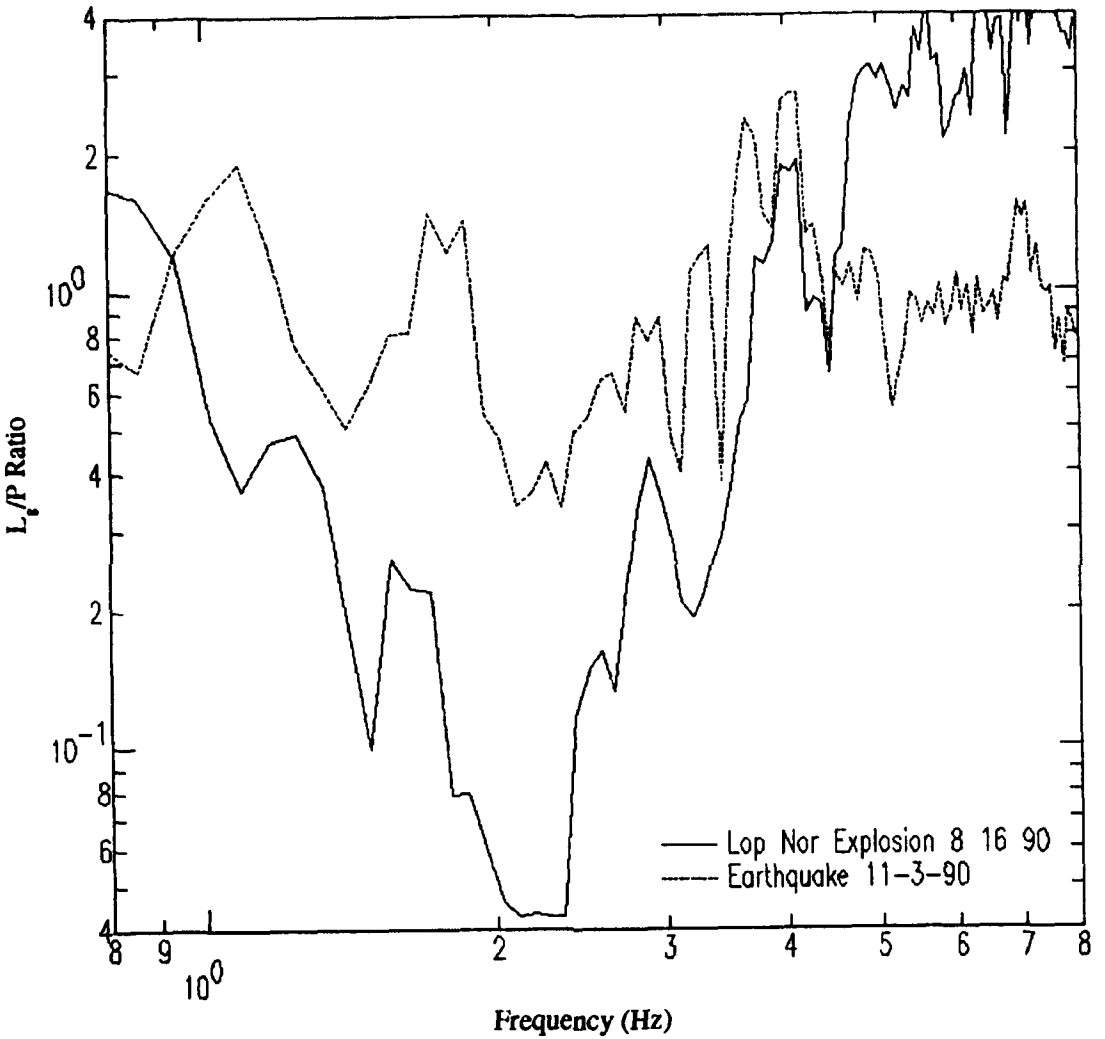

Figure 33b. L_g/P spectral ratios at ARU for Lop Nor nuclear explosion and nearly co-located earthquake.

Therefore, the results from both stations, GAR and ARU, observing the Lop Nor explosions and nearly co-located earthquakes appear to strongly support the conclusion that differences in L_g/P spectral ratios can be related to source or near-source phenomenology. The observations suggest that the differences may be enhanced in certain frequency bands and that more distant stations seem to provide a more restricted frequency window for seeing such differences.

4.3.3 Additional Analysis of Propagation Effects on L_g/P Spectral Ratios

To obtain additional insight into effects of transmission on the robustness of the L_g/P spectral ratio discriminant and to compare these results more directly with similar observations from Semipalatinsk test site events, we also examined data from the 09/14/88 JVE explosion recorded at GAR. L_g/P spectral ratios for the Lop Nor and JVE explosions are compared in greater detail in Figure 34. These two explosions had roughly comparable teleseismic body-wave magnitudes, and the difference in the range to GAR is about 200 km (with the Semipalatinsk test site being nearer). We observe that the spectral ratio from the JVE explosion is considerably larger than that of the Lop Nor explosion over nearly the entire frequency band. The difference is approximately a factor of six at low frequencies and decreases towards higher frequencies. The simplest explanation for the difference would appear to be the difference in the transmission path to GAR for the two events. We note that the L_g/P spectral ratio for the JVE at GAR is very nearly the same as those for the near-Lop Nor earthquakes at GAR. This suggests that care needs to be exercised in applying spectral ratios as discriminants and in accounting for propagation differences.

We can analyze the potential sensitivities of the L_g/P spectral ratio as a discriminant in terms of the effects of differences in transmission path Q on the results. If there were no differences in Q for the whole region

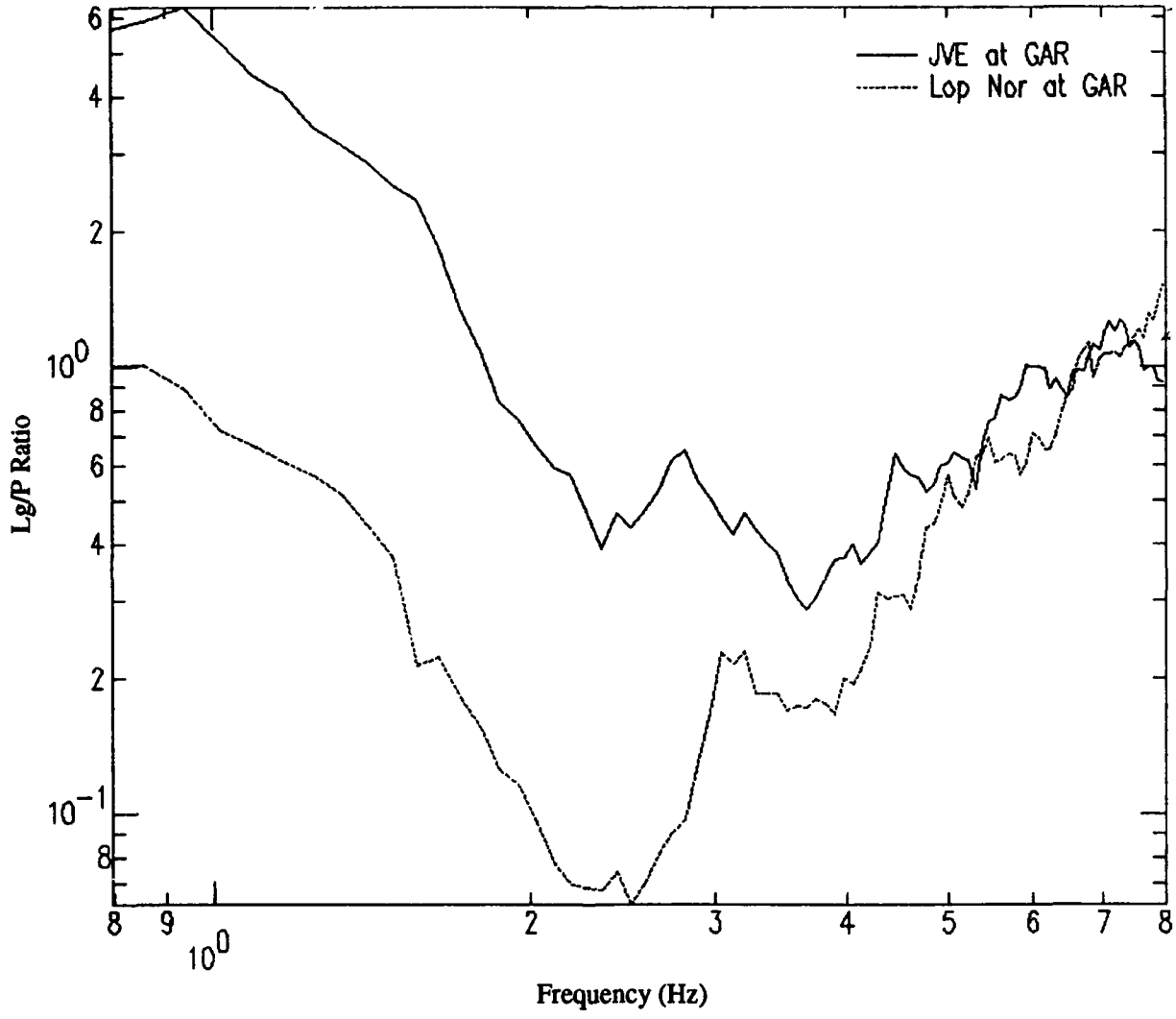

Figure 34. Lg/P spectral ratios at GAR for similar-sized underground nuclear explosions near Semipalatinsk (JVE) and Lop Nor.

encompassed by Semipalatinsk, GAR, Lop Nor and WMQ, we would certainly expect the spectral ratios to be more similar. The observed differences point toward differing propagation or near-station effects. We, therefore, examined for a small data set what differences in Q would be required to bring the spectral ratios for the two stations into better agreement.

The regional phase spectra can be corrected for a constant Q model using a factor of the form $\exp\left\{\frac{\pi R f}{Q C}\right\}$ where f is the frequency of the signal, R is source-receiver distance in km, C is the group velocity and Q is the non-dimensional quality factor. We will assume that the spectral ratio computation for a given path should approximately cancel out path effects for those parts of the path which sample the same volume of the earth. Thus, in the case of the L_g/P spectral ratios, the portions of the earth's crust near both source and receiver through which the P-wave travels should be essentially similar to that which the L_g wave samples. However, the portion of the P-wave path which lies in the mantle or along the crust-mantle interface would be different than that for L_g. We corrected the L_g spectrum using a constant Q model, derived in previous analyses (cf. Bennett *et al.*, 1990a), and then derived an effective Q for the P wave which would result in L_g/P spectral ratios that would match those calculated. It should be noted that this derived effective Q for the P wave includes the Q due to both crustal and mantle propagation, which cannot be separated without data from an independent Q estimate for one or the other. It represents the Q differences attributable to the portions of the P-wave path which are not common to the L_g path. If much of the P-wave path is through similar material, we should then be able to take these Q estimates to another seismic station and determine what change in Q for L_g would be required to match the L_g/P ratios for a given test site for both receiving stations.

We chose explosions from the region around Semipalatinsk recorded at stations WMQ and GAR for this comparison. From our prior study we had an independent estimate of the Q for L_g over the path between Semipalatinsk and WMQ. This Q value was estimated to be approximately

457. We corrected the L_g amplitude spectrum for L_g between Semipalatinsk and WMQ using this value and varied the effective P-wave Q to reproduce the original, uncorrected L_g/P spectral ratios. We found that a value of about 170 for the effective P-wave Q matched the original spectral ratio well over the frequency band from 0.5 to 8 Hz. Then, applying the Q values for P to the explosion record at GAR and varying the Q for L_g to achieve the best visual fit (cf. Figure 35) between the two spectral ratios produced a value of about 470 for the effective Q of L_g for the Semipalatinsk to GAR path. It should be noted, however, that the L_g/P spectral ratio for GAR above about 4 Hz could not be made to match with any reasonable Q values while keeping the portion below 4 Hz in nominal agreement.

We also analyzed the relative sensitivity of the L_g/P spectral ratios to the Q values for L_g and P. For this analysis L_g Q values were fixed at 450 for both records and the effective Q for P was varied to arrive at a visual match between the L_g/P spectral ratios. We found that, to produce a reasonable match, much larger variations in the Q value for P were required and these often appeared physically unreasonable (viz on the order of 25 to 40). Furthermore, these corrections did not make the fit any better than that achieved by the relatively small variations in the Q for L_g. Based on these analyses we conclude that the L_g/P spectral ratio discriminant is more sensitive to variations in the propagation path affecting L_g than to variations affecting regional P. This observation is further supported by examining the spectral ratio of the regional P observed at GAR to that observed at WMQ from the JVE explosion. This ratio is shown in Figure 36. Over the frequency range from about 1 to 6 Hz, the P/P ratio is essentially constant at a value near one, indicating that there is no substantial Q difference for the two P-wave paths.

All of these observations taken together indicate that the reason for the difference in the observed L_g/P ratios for the JVE at different stations are due to variations in the L_g propagation. In particular, the L_g signals which travel the path from Semipalatinsk to WMQ appear to be deficient in energy between about 4 Hz and 8 Hz. One simple explanation of this could be that

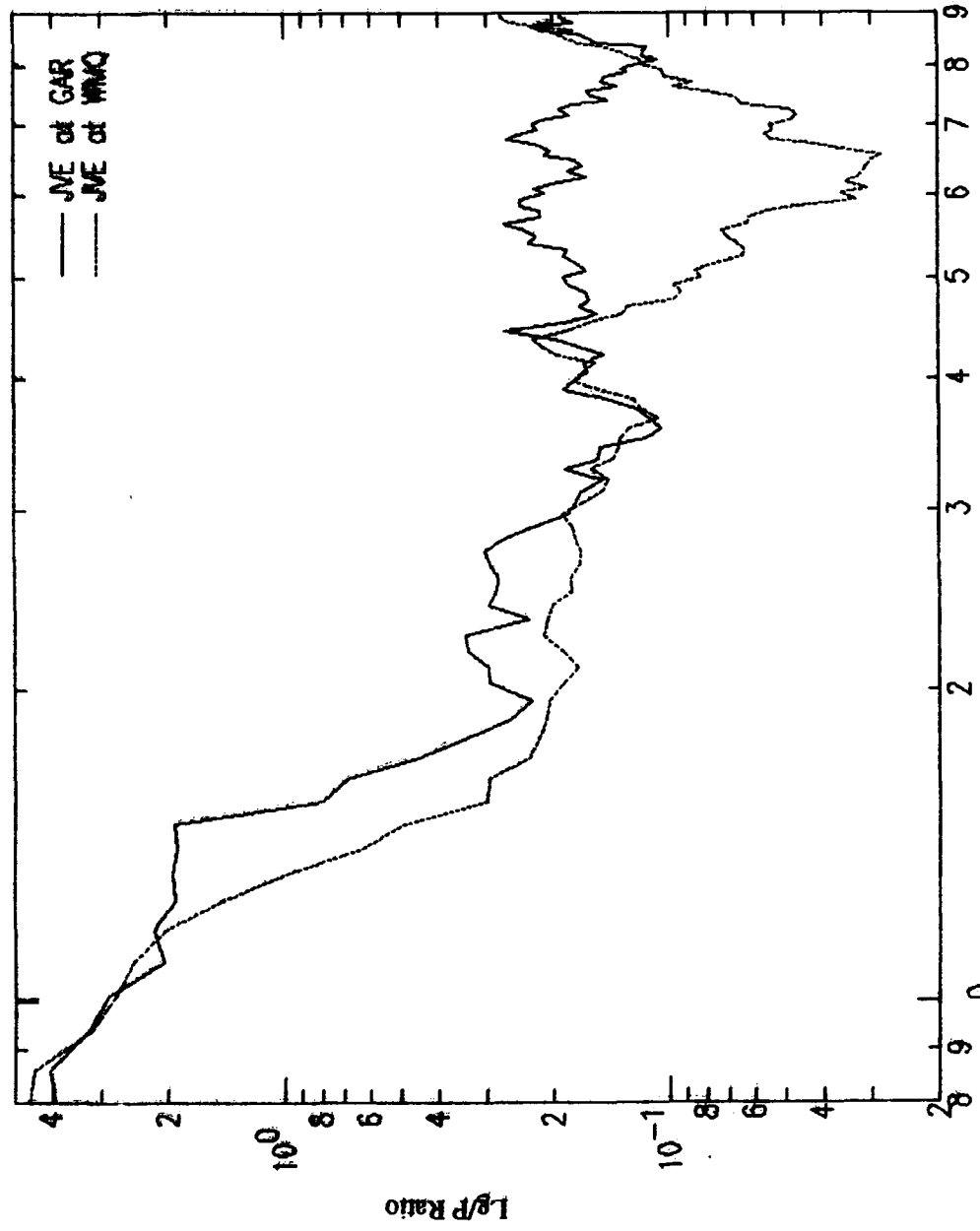

Figure 35. Lg/P spectral ratios at GAR and WMQ for the JVE explosion at Semipalatinsk after corrections for effects of Q on transmission.

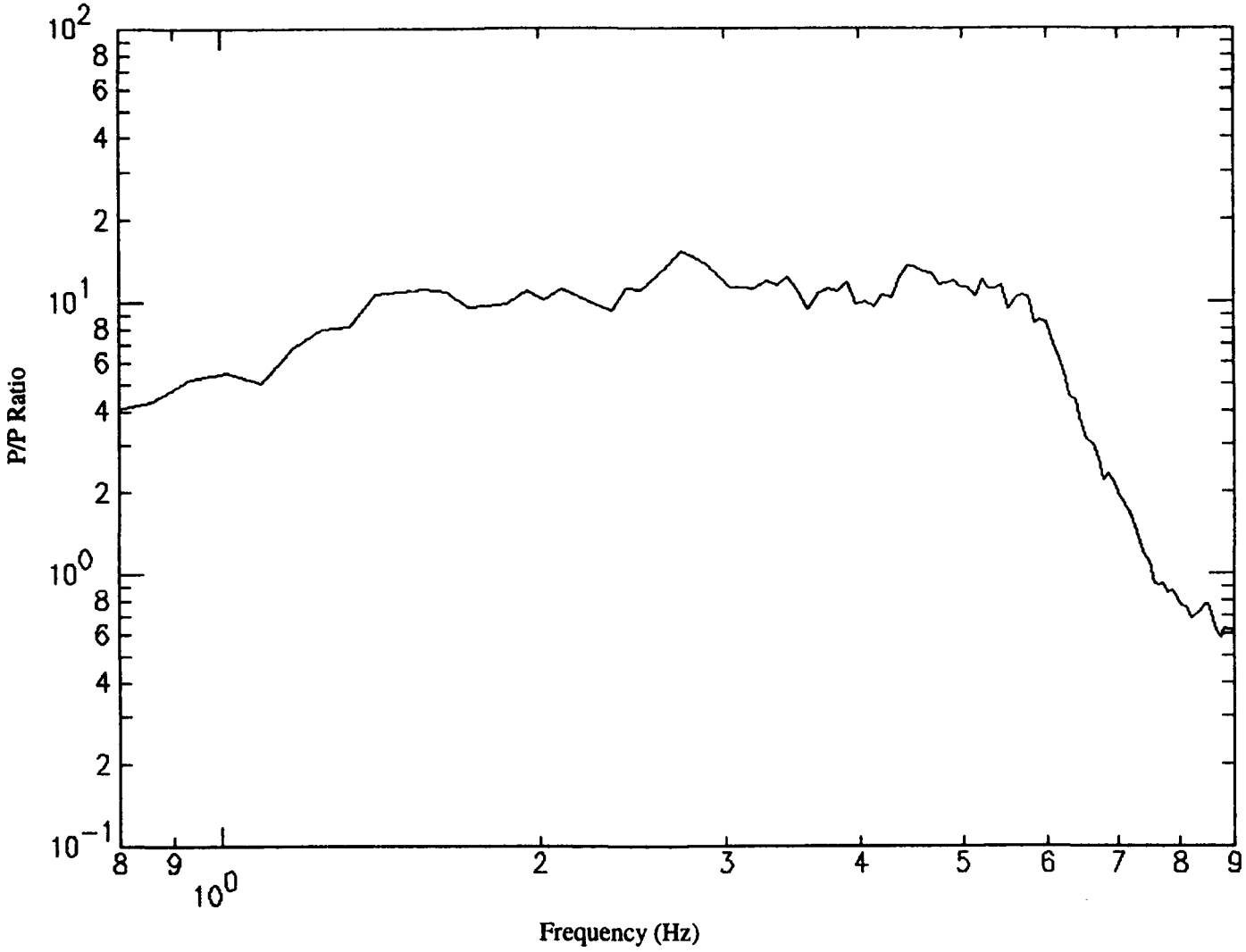

Figure 36. P/P spectral ratio for GAR/WMQ from the JVE explosion at Semipalatinsk.

propagation across the Dzungarian Basin tends to filter out L_g waves in a narrow frequency band centered on 6 Hz. Other variations in the L_g/P ratios, such as the minima near 4 to 5 Hz at GAR, may be site effects. We therefore conclude that, although we seem to have clear evidence of the discrimination potential of L_g/P spectral ratios, the expected behavior of the ratio based on experience from one region should not be extrapolated into a different region without accounting for the effects of seismic wave propagation.

V. REGIONAL DISCRIMINATION ANALYSES OF SELECTED EVENTS NEAR THE SEMIPALATINSK TEST SITE

5.1 Background

As has been described in previous reports (cf. Rodean, 1979; OTA, 1988; Bennett *et al.*, 1989), the region surrounding the Soviet underground nuclear explosion test site near Semipalatinsk is generally aseismic with respect to natural earthquake activity. Seismic discrimination for events in this or similar areas presents a special problem. In such regions methods cannot be tested using a strictly case-based approach which requires direct comparison of seismic signals from events of different types located within the same source region. Instead, a model-based procedure which relies on experience from calibrated source regions can be applied to event identification.

With regard to regional seismic discrimination, in previous reports (cf. Bennett *et al.*, 1989, 1990a, 1991) and in preceding sections of this report, S-CUBED has defined and tested a variety of regional discriminants based on relative amplitude and spectral comparisons of regional phase signals from explosions and earthquakes. Based on our prior analyses, we have concluded that the differences observed in regional phase spectral ratios (viz L_g/P) are related in large measure to source differences. An important test of this regional discrimination model would be its performance on events in the vicinity of the Semipalatinsk test site.

In this section we evaluate the performance of the relative amplitude and spectral comparisons of regional phase signals for two event sets. The first set includes a typical underground nuclear explosion at the Semipalatinsk test site (viz 02/12/89) with a magnitude of 5.8 m_b and an earthquake located at 51.0°N 84.2°E on the same date with a magnitude of

4.6 m_b. This earthquake is the closest natural event to the Semipalatinsk test site for which we have good regional signals in the database (viz at station WMQ). The second event set which we analyzed included two events of more comparable magnitudes with a slightly larger separation of epicenters which produced good regional phase signals at all six stations (viz WMQ, GAR, ARU, HIA, KIV and OBN). The explosion in this latter set is the JVE shot (viz 09/14/88) at Balapan with a magnitude of 6.3 m_b and an earthquake (viz 06/14/90) located at 47.9°N 85.1°E with a magnitude of 6.1 m_b.

5.2 Discrimination of Events Near Semipalatinsk Recorded at WMQ

In our previous regional discrimination analyses of underground nuclear explosions and earthquakes recorded at WMQ (cf. Bennett *et al.*, 1990a), we used explosions at the Semipalatinsk test site and earthquakes coming from a variety of locations principally along the southern Soviet border and in western China. Although the earthquakes tend to have somewhat different propagation paths than the explosions, by including earthquakes from a variety of locations and azimuths any bias effects related to specific paths from particular source areas should tend to be averaged out. Therefore, observed differences in regional phase signal characteristics, such as those seen in L_g/P spectral ratios at WMQ, should be related to source differences.

To further test this concept for events recorded at WMQ, we analyzed the signals from the nuclear explosion-earthquake pair on 02/12/89, described above. The two event epicenters are separated by about 400 km as shown in Figure 37. The distances of the explosion and the earthquake from WMQ are 1040 km and 850 km, respectively. Propagation paths from the two events have nearly common segments within the Dzungarian Basin and Foldbelt. The main differences in the paths appear to be in their initial segments where the explosion path traverses the relatively gentle Balkhash-

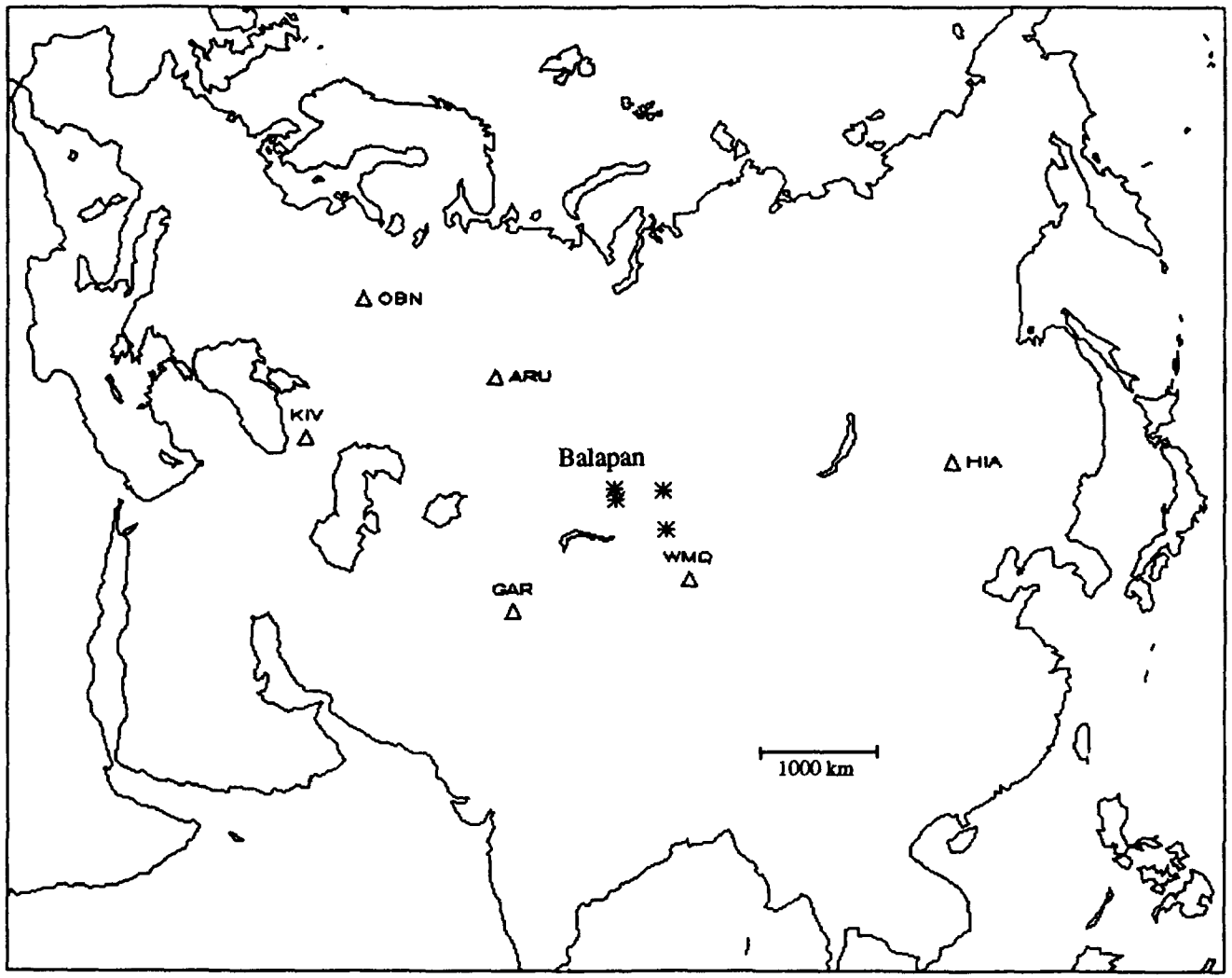

Figure 37. Locations of explosions at the test site near Semipalatinsk (Balapan) and nearby earthquakes used in single-station and network discrimination analyses.

Chingiz Foldbelt while the earthquake path is through the more severe Altay Foldbelt.

Figure 38 shows the vertical-component broad-band records obtained at WMQ for these two events. There are several obvious differences in the regional signals between the events For the explosion the regional P is quite distinct, large and complex. In contrast, for the earthquake the P phase is weak. In both cases the P phase appears to include relatively high-frequency energy and is extended in duration. The L_g signal is the maximum amplitude regional phase on these broad-band recordings for both events; roughly the first 75 seconds of the L_g windows look very similar for the two events. For the explosion the latter portion of the L_g window is much larger and more complex than for the earthquake apparently containing additional high-frequency energy. In addition, the explosion record includes strong, highly-dispersed fundamental-mode Rayleigh waves which are only weakly seen in the earthquake record.

We performed spectral analyses on the regional signals for the records in Figure 38 and computed L_g/P spectral ratios. The procedures in these analyses were the same as those previously performed on the WMQ data and essentially the same as those described in previous sections of this report. The L_g/P spectral ratios for the Semipalatinsk explosion-earthquake pair recorded at WMQ are shown in Figure 39. For the underground nuclear explosion shown at the top, the L_g/P ratio is broadly peaked at a value near ten over the frequency band from 0 to 1 Hz. Above 1 Hz the L_g/P ratio falls off rapidly and monotonically approaching a level near 0.1 at 6 Hz. In contrast, the earthquake L_g/P ratio shown at the bottom of Figure 39 is rather sharply peaked near 0.5 Hz and falls off more gradually toward higher frequencies. The ratio begins to level off in the frequency range 2 to 3 Hz and reaches a minimum level near 0.6 at 6 Hz. Comparison of the two curves shows that the L_g/P spectral ratio for the earthquake lies above that of the explosion over nearly the complete frequency band shown in the figure. The greatest differences appear to occur in the frequency range 2 to 6 Hz where the two curves are separated by a factor of roughly five to six.

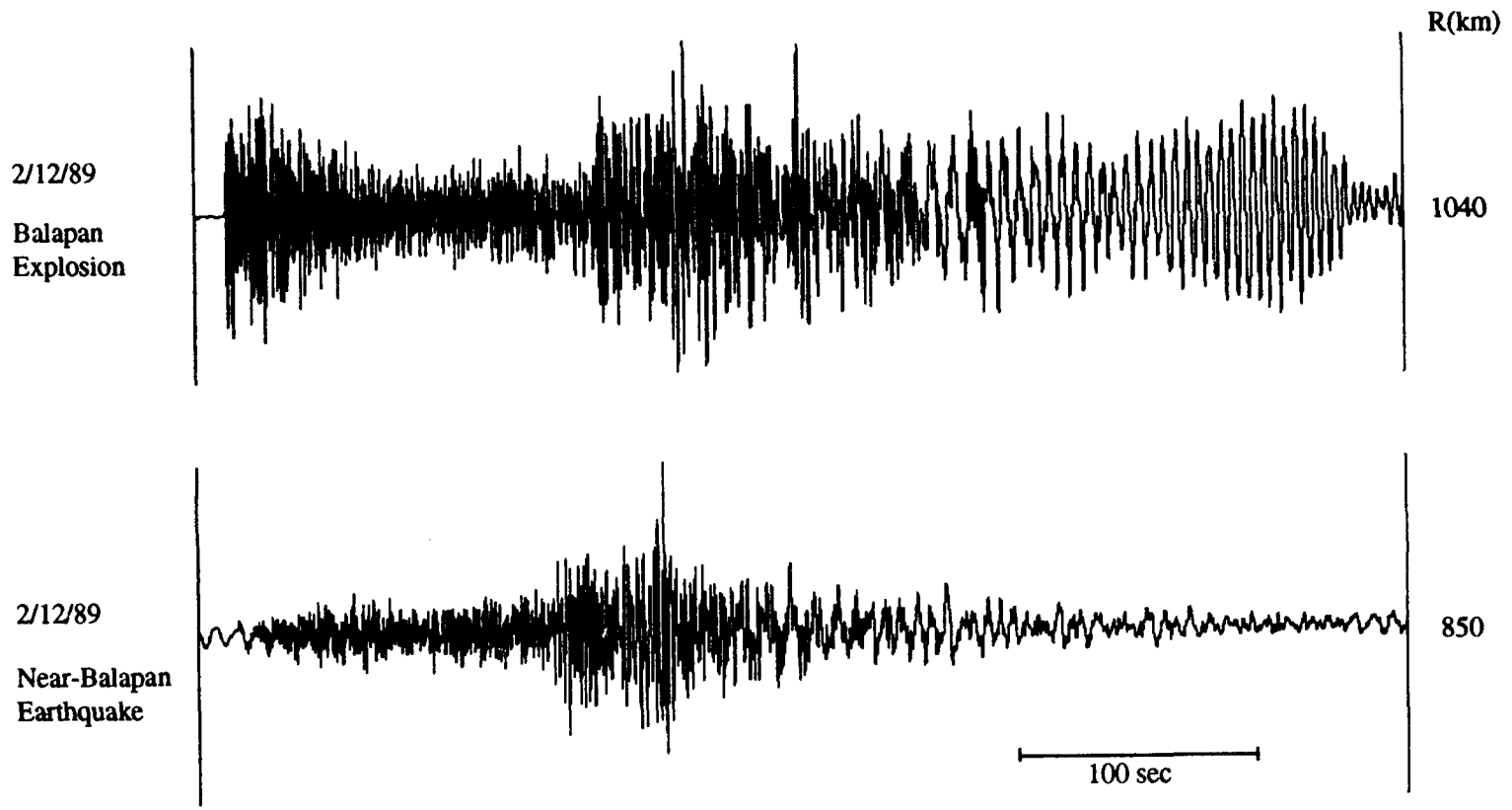

Figure 38. Broad-band, vertical-component records at WMQ from nuclear explosion at Semipalatinsk (Balapan) and nearby earthquake.

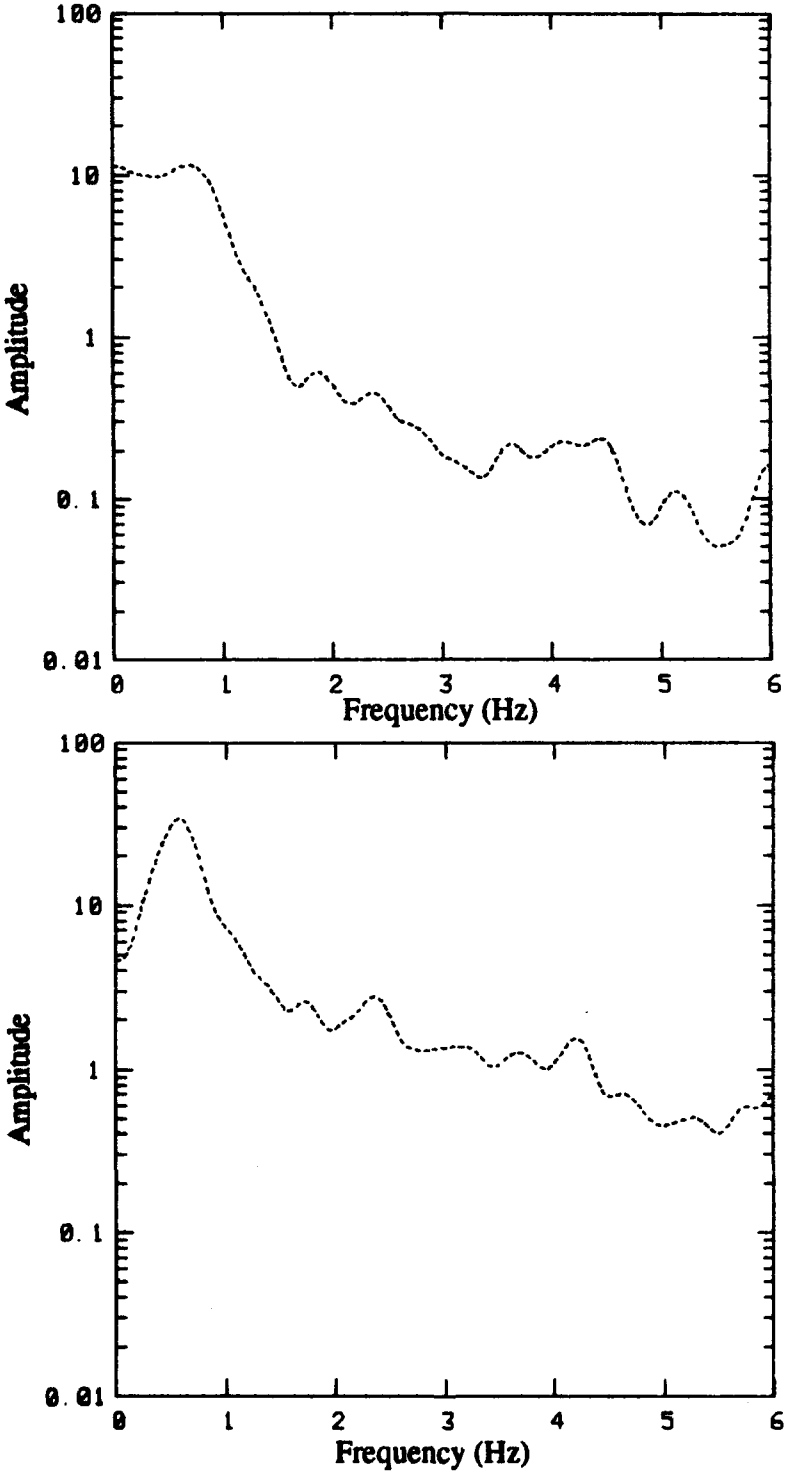

Figure 39. L_g/P spectral ratios at WMQ for Semipalatinsk explosion (top) and nearby earthquake (bottom).

Thus, from the standpoint of regional discrimination, this Semipalatinsk explosion-earthquake pair behave similarly to events previously analyzed. We would conclude from this that Semipalatinsk underground nuclear explosions could be discriminated on the basis of L_g/P spectral ratios from the earthquake nearest the test site, for which high-quality digital data are currently available. Although some propagation path differences still exist even for this pair, based on evidence presented throughout this report, we strongly believe that source effects and not path differences control this observation.

5.3 Discrimination of Events Near Semipalatinsk Recorded at All Regional Stations

Many of the regional discrimination analyses conducted in the past have relied on measurements at only one or, in some cases, a few stations. Considering that earthquake sources are expected to produce radiation patterns in the regional phase signals and that propagation may alter regional signal behavior along particular paths, observations based on only a few stations could lead to non-representative results and uncertainty about the applicability of the techniques. Therefore, it is highly desirable for regional discrimination to incorporate measurements from a network of stations at a wide range of azimuths from the source.

Unfortunately, many of the events in our database have been recorded at a limited number of stations. This is particularly true for many of the smaller events which often produce identifiable regional signals at only one or two of the nearest stations. As noted above, we succeeded in identifying a pair of larger events, including an explosion and an earthquake, which were well recorded at all six stations in our regional network. The two events (viz the 09/14/88 JVE explosion and the 06/14/90 earthquake) in this pair have epicenters separated by approximately 510 km (cf. Figure 37 above).

The distances to the stations range from 500 km to 3400 km, and the greatest azimuthal gap in station coverage is about 130 degrees at northerly azimuths.

Figure 40 shows the broad-band vertical-component records at all six stations for the two events arranged approximately in order of increasing epicentral distance. For the explosion records at the top, the regional P phase is a large signal with a distinct onset at all stations. The P signals in almost all cases include secondary arrivals which contribute to an extended duration which appears quite similar from station to station. In contrast, the P signals for the earthquake (at the bottom) appear relatively weak and emergent at most stations and seem to contain less high-frequency energy than the corresponding explosion signals. The black circles mark the approximate start of the L_g windows at a group velocity of 3.6 km/sec. The L_g signal is apparent in the explosion records at most stations except KIV where its transmission may be blocked by structures related to the Caspian Sea, as described elsewhere in this report. For the earthquake records the L_g is strong at all stations and appears to include a relatively greater proportion of low-frequency energy compared to the explosions, except at the nearest station, WMQ. The lower-frequency L_g signals are even seen for the path to KIV suggesting that the Caspian Sea structures are more effective in blocking higher frequency L_g signals.

With regard to discrimination the L_g/P amplitude ratios seen on the broad-band records are in almost all cases larger for the earthquake records than for the explosions. The only ambiguities are the signals at the two nearer stations, WMQ and GAR, where the L_g/P ratios are of similar size for both events. This observation suggests that broad-band single-station measurements may not always provide reliable regional discrimination, and we may need to apply more sophisticated spectral techniques or use measurements from a broader regional network of stations. There is considerable variability in the broad-band L_g/P ratios between stations which is influenced no doubt to a large measure by propagation path differences. Thus, L_g/P ratios are in the range from 0.12 to 2.42 for the explosion records and in the range from 1.32 to 32.7 for the earthquake records.

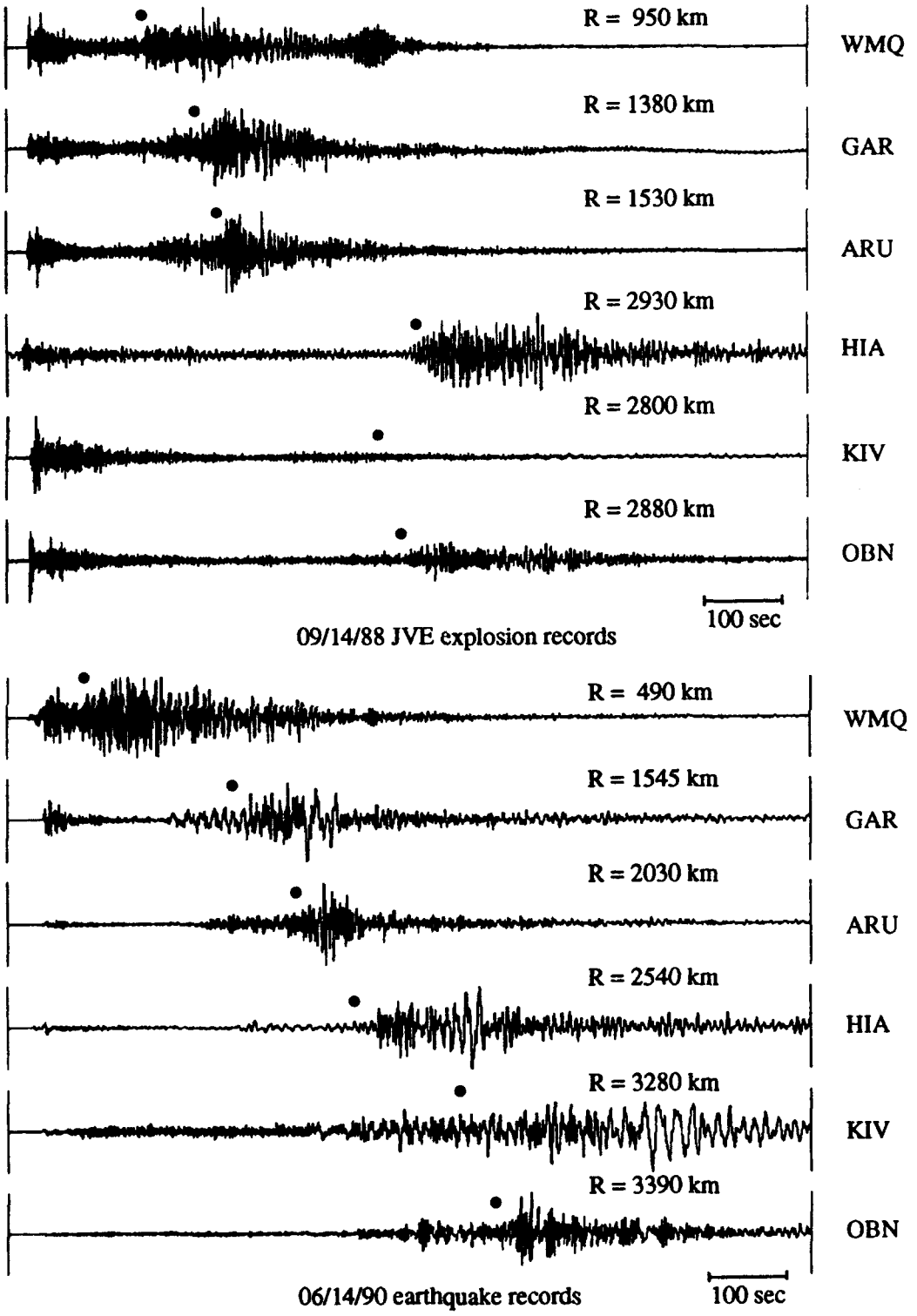

Figure 40. Broad-band, vertical-component records at all network stations for Semipalatinsk JVE explosion and nearby earthquake.

Averaged over all six stations, the L_g/P ratio is much larger for the earthquake than for the explosion, 11.1 versus 1.31.

We computed regional phase spectra and L_g/P spectral ratios for each of the six station records for the JVE explosion and the 06/14/90 earthquake. The L_g/P spectral ratios at each station for the two events are compared in Figures 41-46. Although the spectral ratios vary considerably in appearance from station to station, there are several noteworthy consistencies. In nearly all cases the L_g/P spectral ratios start out at values near ten in the frequency range below 1 Hz. A notable exception is the KIV spectral ratio for the JVE explosion in Figure 45. There the simplest explanation would seem to be blockage of the L_g by geologic structure associated with the Caspian Sea. However, there does seem to be L_g energy in this same frequency band at KIV for the earthquake which has only a slightly different propagation path crossing the Caspian Sea. It is also somewhat surprising that the L_g/P ratio in this band is relatively low for the earthquake at WMQ considering the proximity of the source and station. Perhaps this latter observation is caused by a relatively strong crustal P phase from the earthquake. Another consistency in the L_g/P ratios is that they tend to fall off monotonically above about 0.5 Hz. This is true for both the explosions and the earthquakes, but for the earthquakes the decrease tends to be more gradual. At three of the more distant stations (viz HIA, KIV and OBN) the L_g/P ratios tend to reach a minimum near 2 Hz and then increase.

With regard to differences in the L_g/P spectral ratios between the explosion and the earthquake at individual stations, perhaps the clearest difference is at WMQ where the L_g/P ratio for the earthquake lies well above that for the explosion at frequencies above about 1 Hz. This behavior is generally consistent with the experience we have reported previously as well as elsewhere in this report. L_g/P ratios are also seen to be larger for the earthquakes than the explosions over relatively broad bands at stations ARU, KIV, OBN and HIA. However, at these stations there are also intermediate frequency bands in which the L_g/P ratios overlap. The least difference in the L_g/P spectral ratios for the JVE and 06/14/90 earthquake

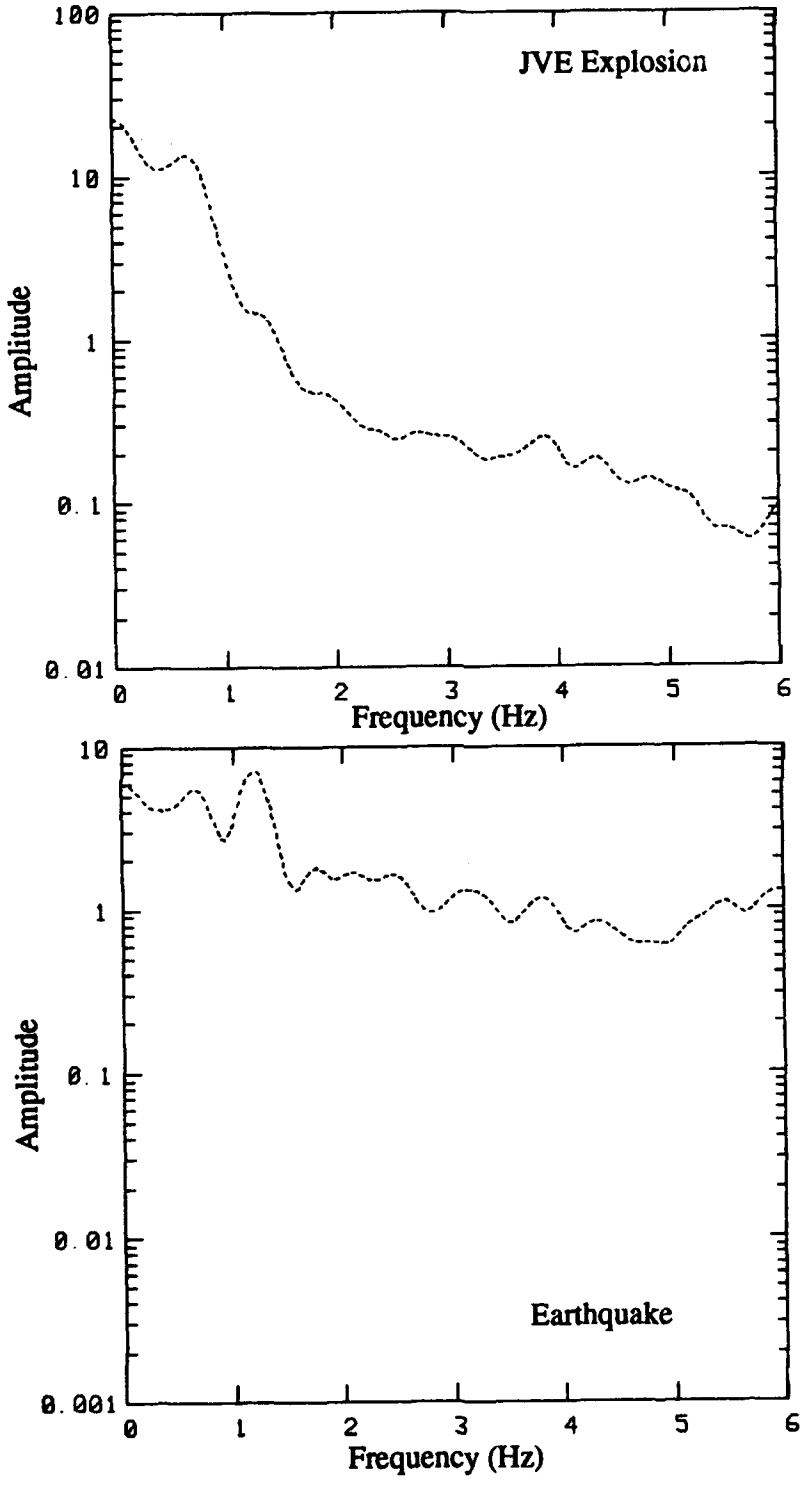

Figure 41. L_g/P spectral ratios at WMQ for Semipalatinsk JVE explosion (top) and nearby earthquake (bottom).

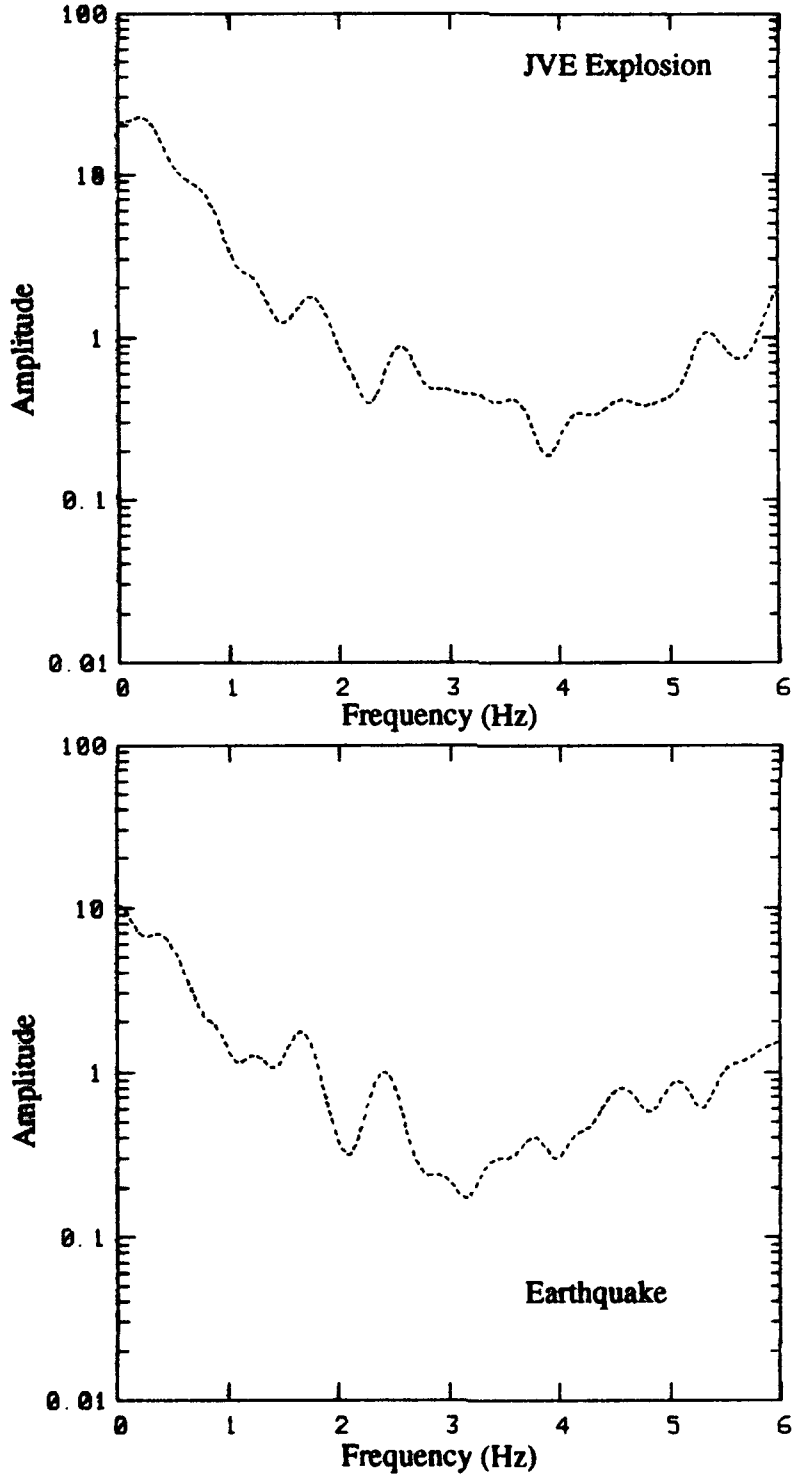

Figure 42. L_g/P spectral ratios at GAR for Semipalatinsk JVE explosion and nearby earthquake.

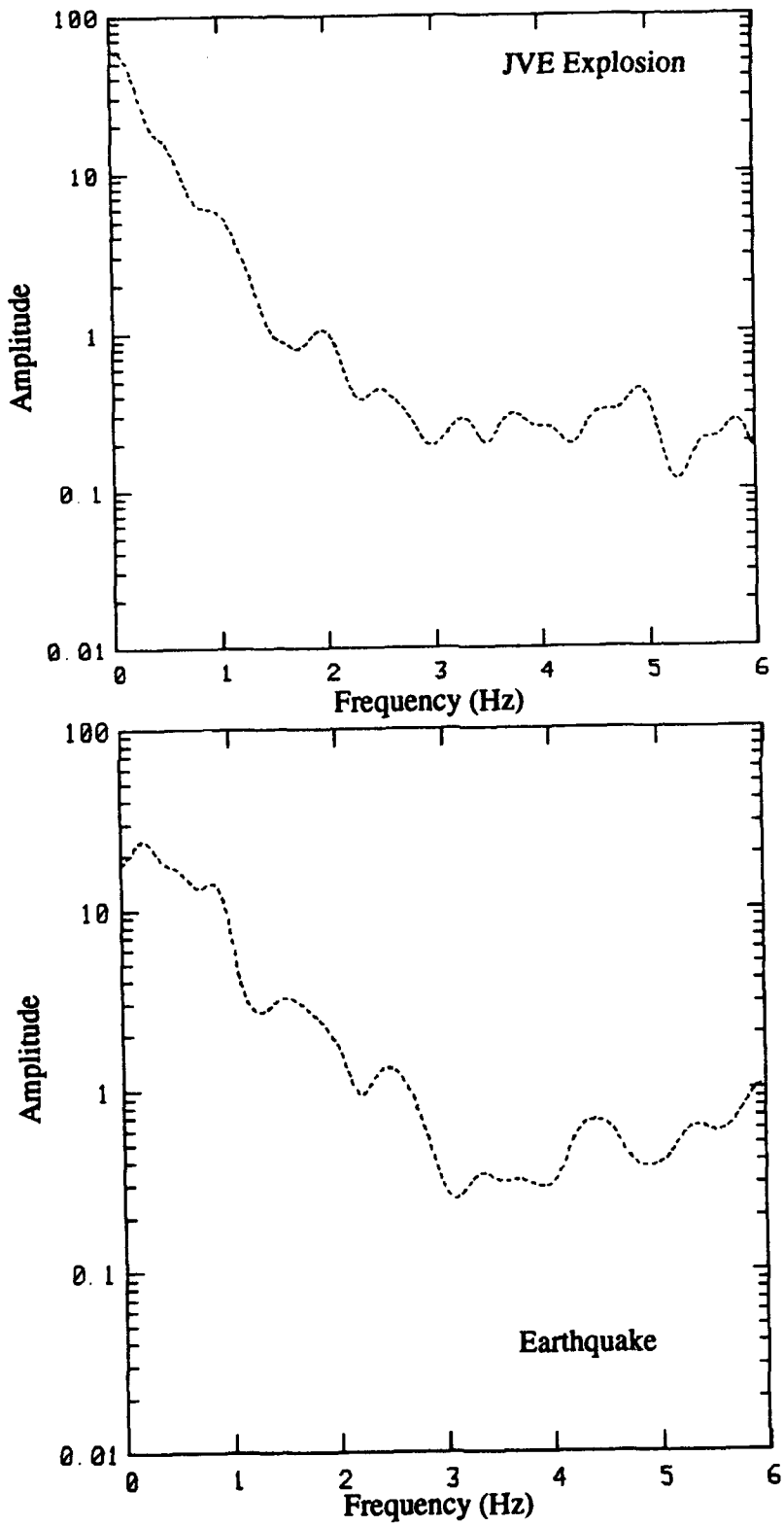

Figure 43. L_g/P spectral ratios at ARU for Semipalatinsk JVE explosion (top) and nearby earthquake (bottom).

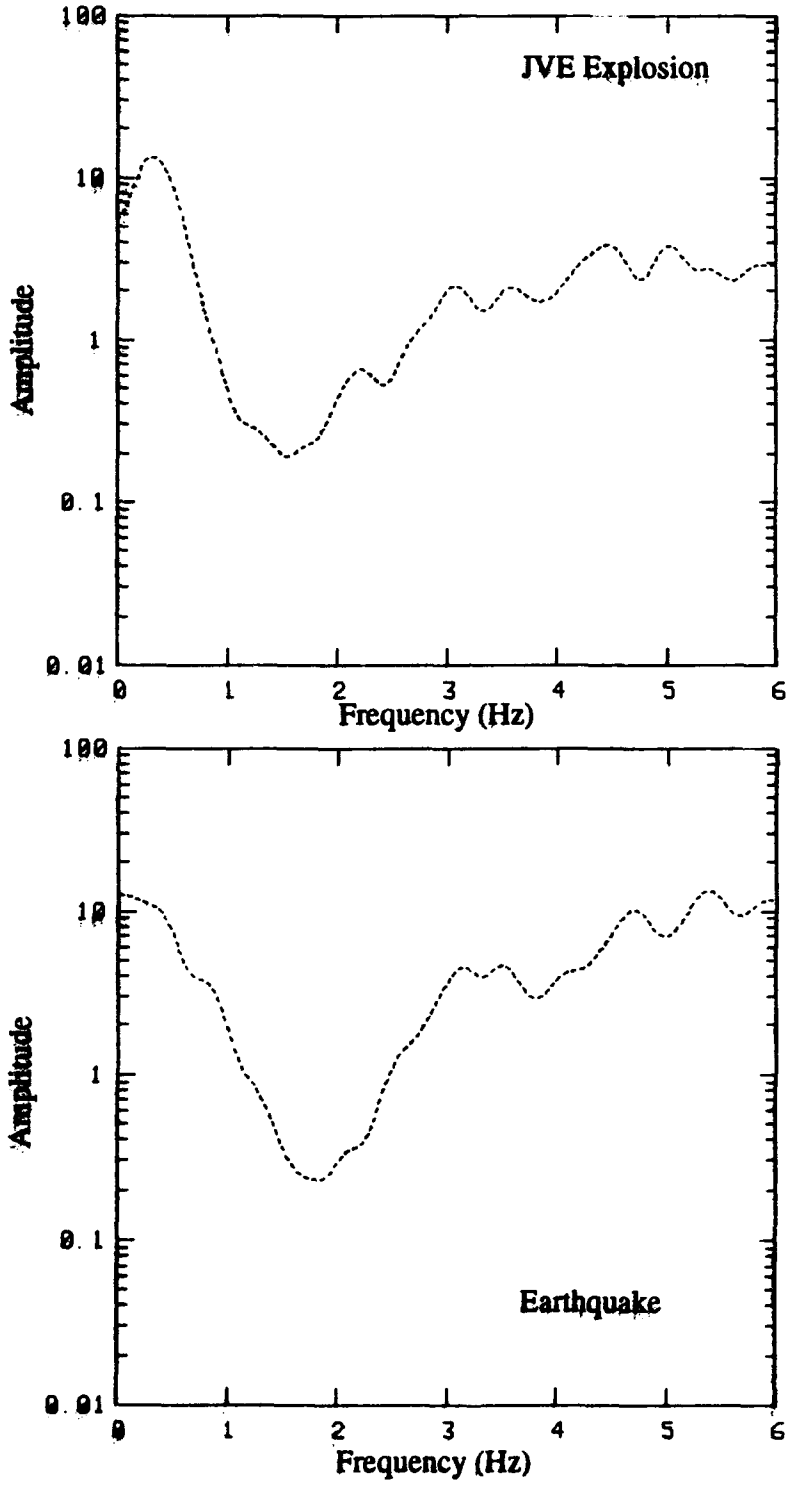

Figure 44. L_g/P spectral ratios at HIA for Semipalatinsk JVE explosion (top) and nearby earthquake (bottom).

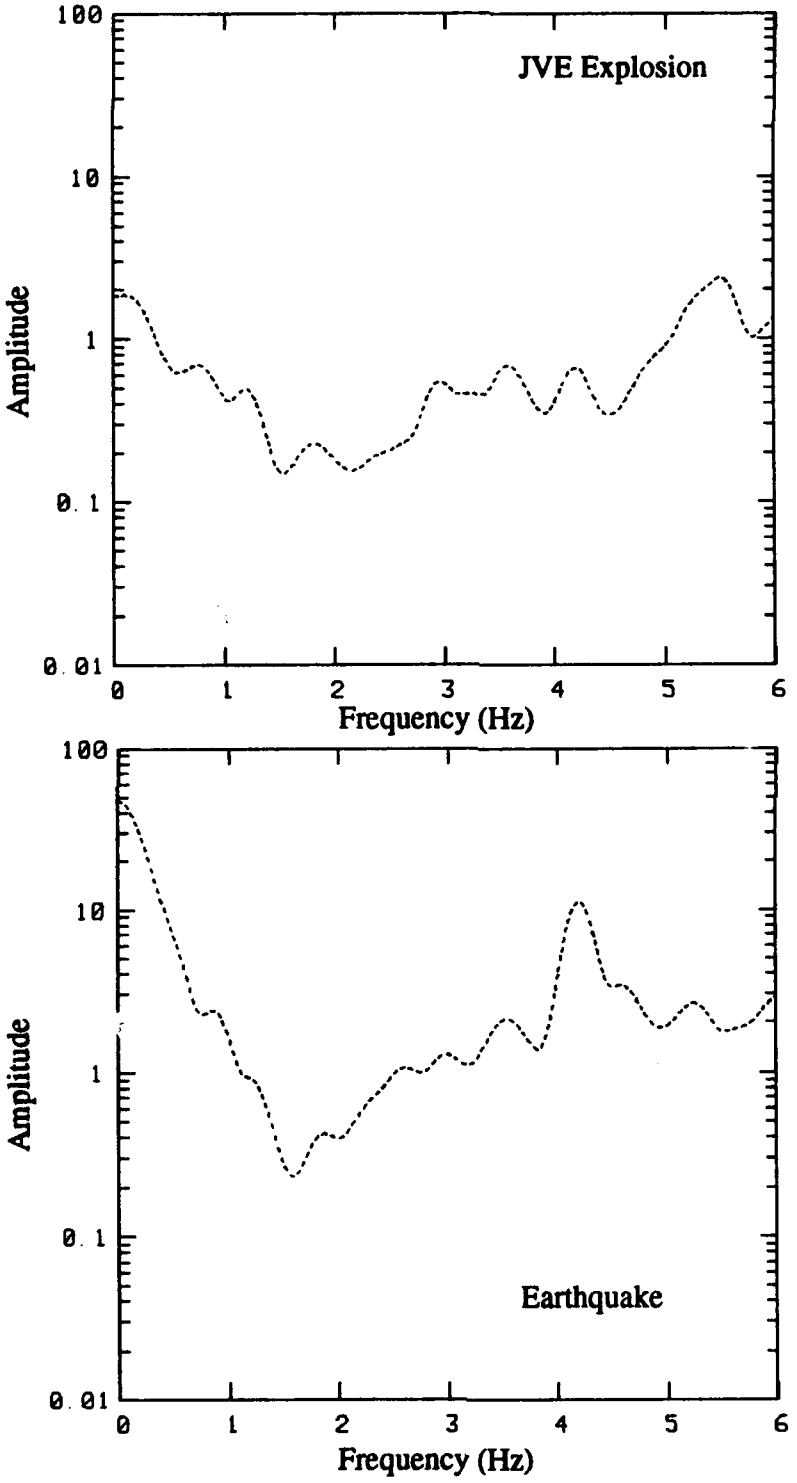

Figure 45. L_g/P spectral ratios at KIV for Semipalatinsk JVE explosion and nearby earthquake.

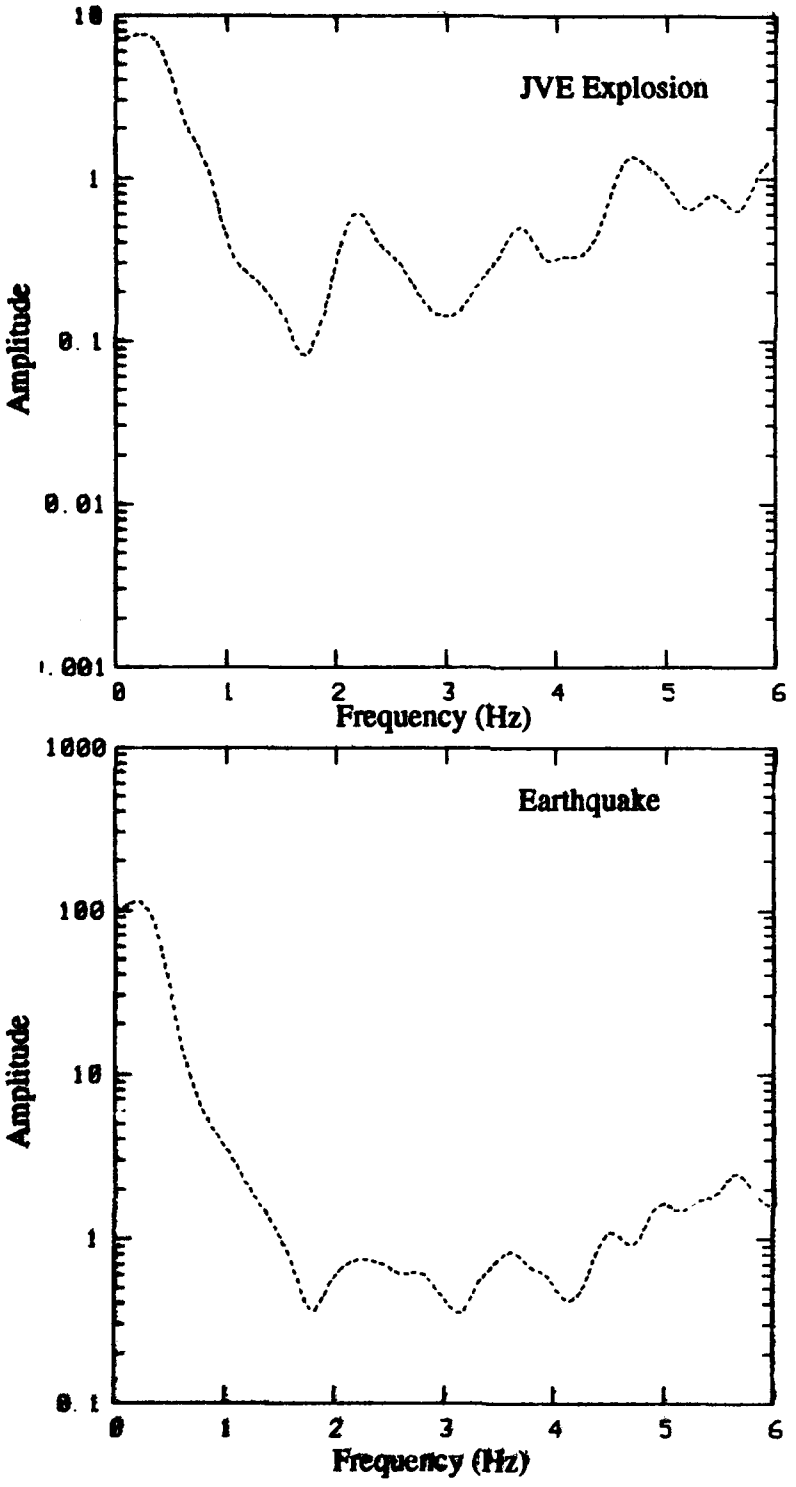

Figure 46. L_g/P spectral ratios at OBN for Semipalatinsk JVE explosion and nearby earthquake.

occurs at GAR. Based on the comparison in Figure 42, these two events would be impossible to discriminate at GAR on the basis of L_g/P spectral ratios. However, looking back at the regional waveforms at GAR for these two events (cf. Figure 40 above), there would appear to be significant differences in the frequency content of the individual regional phases L_g, S and P phases for these events which could assist in their identification.

Therefore, with regard to regional discrimination, we would conclude from the large network observations of the 09/14/88 JVE explosion and the 06/14/90 earthquake that L_g/P spectral ratios may not always be effective as discriminants at a lone station. However, by analyzing the results from a network of regional stations, the L_g/P spectral ratios should be successful. In addition, it would be worthwhile to consider alternative regional discriminant measures at those stations where L_g/P ratios may fail.

VI. CONCLUSIONS AND RECOMMENDATIONS

6.1 Conclusions

Over the past several years, S-CUBED has conducted a research program under DARPA sponsorship aimed at increasing the discrimination capability offered by regional seismic monitoring. This research has produced a number of important findings and a valuable regional database for use in future work. In particular, early investigations of NTS explosions and nearby earthquakes, recorded at VELA array and Lawrence Livermore National Laboratory stations, discovered a new discriminant for nuclear explosions and earthquakes based on spectral differences detected in their regional signals. In subsequent studies we have extended and adapted this spectral-based regional discriminant to events in the former Soviet Union and Eurasia using the various available seismic data sources, including most recently, CDSN and Soviet IRIS station data. The large digital database accumulated in the course of the S-CUBED research program includes approximately 2000 high-quality regional waveforms for some 400 events in a wide variety of tectonic settings. This database could provide a valuable resource for testing the performance of alternative regional discriminant measures and their sensitivity to the tectonic environment.

The most recent phase of our research program presented in this report has provided several significant findings with regard to the behavior of regional seismic signals from Eurasian events and the feasibility of extending regional seismic discrimination techniques into those areas. In particular, our results show that regional stations in Eurasia can furnish valuable data for use in identification of events in these areas. A properly designed network of such stations could permit monitoring of seismic activity throughout the region to a very low threshold depending on the number of stations and their proximity to the sources.

First, with regard to the database, our studies have shown that good quality regional P and L_g signals can be observed out to fairly large regional distances for events throughout much of Eurasia as recorded at the Soviet IRIS and CDSN stations. The database currently assembled includes 38 underground nuclear explosions and 68 regional earthquakes. In some instances L_g signals are discernible on the records to ranges in excess of 4000 km for paths crossing the Eurasian continent. On the other hand, some tectonic structures are seen to block, or severely attenuate, L_g signals. Our data show regions of blockage surrounding the Caspian and Black seas and possibly extending in some areas along the southern border of the former Soviet Union. We have performed several types of regional discrimination measurements on these data and have concluded that in most cases the measurements can be separated on the basis of source type. We believe the database as a whole provides a valuable resource for testing and refining a wide variety of potential regional discrimination techniques for application to Eurasian events. In addition, the database can be used to develop modifications to regional discrimination techniques which may be needed to permit their reliable extension into distinct tectonic regions within the Eurasian continent.

With regard to specific regional discriminant measurements, we have found that the observations in this report strongly support broadband L_g/P amplitude and L_g/P spectral ratio measurements as discriminants for events in Eurasia. In particular, the results presented here for different types of events with nearly common propagation paths are convincing evidence that differences in the source types contribute strongly to the distinctions observed in the ratios. For the common path events, we found that the broadband L_g/P ratios were greater for the earthquakes than for the explosions; and the corresponding spectral ratios suggested that these differences were frequently greatest within certain, limited frequency bands. This is not to say that propagation factors do not also affect the L_g/P measurements; we indeed see propagation effects and, in fact, have described in the report how the signal spectra might require adjustment when comparing events with distinct paths. However, on the positive side, we

found that the regional signals observed at the Soviet IRIS stations were remarkably similar for events of a common source type even if the events are somewhat separated. This suggests that regional discriminants which are effective for some events in an area are likely to be effective for others, and the geographical region over which this conclusion applies may be quite large.

In addition to these more general conclusions, we can identify several additional observations regarding the research presented in this report:

- Broadband L_g/P ratios and L_g/P spectral ratios for a large sample of Semipalatinsk explosions and regional earthquakes at ARU agree on average with previous findings that the ratios tend to be larger for earthquakes.

- Selected nearby events in the vicinity of Semipalatinsk show the same tendency for distinction in broadband L_g/P and L_g/P spectral ratios based on source type. However, in some cases the differences at individual stations may be weak or shifted in frequency; so that observations from a multiple station network would permit greater discernment of differences.

- L_g blockage associated with structures near the Caspian Sea appears to extend well beyond the surface geographic expression. It may be possible to use the L_g observations to map the limits of the responsible structure.

- Although transmission across the Caspian structure blocks L_g, the data show L_g is not effectively blocked by the transition from inside to outside the depression. This appears to suggest that transmission into the basin structure is the cause of the blockage.

- Blockage of L_g signals by the Caspian structures may be more effective at higher frequencies, which could explain blockage of explosion L_g but not earthquake L_g crossing at the same azimuth.

- The useful frequency band, with S/N greater than one, for regional P and L_g signals recorded at the Soviet IRIS stations appears to be more limited for smaller events and at larger ranges. This suggests that discriminant measures requiring broader band observations to discern differences will be most effective if the regional network is sufficiently dense that an adequate frequency band of the signal can be detected above the background noise.

- Some stations in the Soviet IRIS and CDSN networks record good regional signals from events beyond the Soviet borders, including Iran, Iraq, Pakistan and China, which suggests these networks would have value for monitoring other areas of Eurasia for clandestine testing.

6.2 Recommendations

The research described in this report has identified several opportunities where further investigation would produce significant improvements in existing capabilities to discriminate Eurasian events using a regional network. Considering the high quality of the regional signals observed at stations in the Soviet IRIS and CDSN networks from Eurasian events, we believe the available database can provide a valuable source for further testing of regional discrimination methods. Additional regional discriminant measurement techniques should be applied to these data and analyzed to test their effectiveness and identify potential problem areas for interpretation of future results.

The analyses presented here and elsewhere show that regional seismic signals may be strongly influenced by propagation path structure. Data

being collected from the Soviet IRIS and CDSN stations should be used to better define the propagation environment for regional phases throughout Eurasia. In particular, regional variations in attenuation properties and possible localized zones of blockage associated with structural discontinuities should be determined. The database which has already been developed here provides coverage throughout much of the Eurasian continental area, which is of interest. Additional analyses should be performed on these data to identify and quantify variations in the transmission properties for regional phases, particularly P and L_g, throughout the area.

The L_g/P ratio and L_g/P spectral ratio discriminant measures need to be refined to provide more quantitative assessments of the probability associated with event categorization. For this purpose we believe that a neural network analysis should be applied to the database with the output assessed in terms of the probability that the event corresponds to a particular source type (viz nuclear explosion or earthquake). In addition, the effectiveness of adjustments to the discriminant measures, based on the variations in the regional propagation properties described above, should be analyzed in the context of this neural network approach.

Finally, the monitoring capability of these high-quality regional networks for events in other areas of Eurasia, which may be of interest from the standpoint of nuclear weapons proliferation, should be assessed. We have already demonstrated that stations in the networks detect strong regional phase signals from events in countries like Iran, Iraq, Pakistan, India and China. Events currently in the database from these and other areas of interest should be supplemented with additional data. A systematic analysis should then be performed to determine detection and identification thresholds for events in the areas of interest.

VII. REFERENCES

Bennett, T. J., and J. R. Murphy (1986). Analysis of Seismic Discrimination Capabilities Using Regional Data from Western United States Events, *Bull. Seism. Soc. Am., 76*, 1069-1086.

Bennett, T. J., D. G. Lambert, J. R. Murphy, J. M. Savino, and C. B. Archambeau (1981). Regional Discrimination Research, S-CUBED Report No. SSS-R-81-5032, VSC Report VSC-TR-81-20.

Bennett, T. J., B. W. Barker, K. L. McLaughlin, and J. R. Murphy (1989). Regional Discrimination of Quarry Blasts, Earthquakes, and Underground Nuclear Explosions, S-CUBED Report No. SSS-TR-89-10385, GL-TR-89-0114, ADA223148.

Bennett, T. J., A. K. Campanella, J. R. Murphy, and J. F. Scheimer (1990a). Regional Discrimination Research and Methodology Implementation: Analyses of CDSN and Soviet IRIS Data, S-CUBED Report No. SSS-TR-90-11757, GL-TR-90-0194, ADA230251.

Bennett, T. J., A. K. Campanella, J. F. Scheimer, and J. R. Murphy (1990b). Regional Discrimination Research and Methodology Implementation: Analyses of CDSN and Soviet IRIS Data, Papers Presented at 12th Annual DARPA/GL Seismic Research Symposium, Key West, Florida, GL-TR-90-0212, ADA226635, 234-240.

Bennett, T. J., A. K. Campanella, J. F. Scheimer, and J. R. Murphy (1991). Regional Discrimination of Soviet Nuclear Explosions, Earthquakes and Mineblasts, Papers Presented at 13th Annual PL/DARPA Seismic Research Symposium, Keystone, Colorado, PL-TR-91-2208, ADA241325, 78-84.

Dysart, P. S., and J. J. Pulli (1990). Regional Seismic Event Classification at the NORESS Array: Seismological Measurements and the Use of Trained Neural Networks, *Bull. Seism. Soc. Am., 80*, 1910-1933.

Given, H. K. (1990). Variations in Broadband Seismic Noise at IRIS/IDA Stations in the USSR with Implications for Event Detection, *Bull. Seism. Soc. Am., 80*, 2071-2088.

Given, H. K. (1991). Heterogeneous Propagation and Blockage of L_g in the Caspian Sea - Caucasus Mountain Area of the USSR, Papers Presented at 13th Annual PL/DARPA Seismic Research Symposium, Keystone, Colorado, PL-TR-91-2208, ADA241325, 211-217.

Kadinsky-Cade, K., M. Barazangi, J. Oliver and B. Isacks (1981). Lateral Variations of High-Frequency Wave Propagation at Regional Distances Across the Turkish-Iranian Plateaus, *J. Geophys. Res.*, *86*, 9377-9396.

Kennett, B. L. N., and S. Mykkeltveit (1984). Guided Wave Propagation in Laterally Varying Media - II. L_g Waves in Northwestern Europe, *Geophys. J. R. Astr. Soc.*, *79*, 257-267.

Murphy, J. R., and T. J. Bennett (1982). A Discrimination Analysis of Short-Period Regional Seismic Data Recorded at Tonto Forest Observatory, *Bull. Seism. Soc. Am.*, *72*, 1351-1366.

Nuttli, O. W. (1981). On the Attenuation of L_g Waves in Western and Central Asia and Their Use as a Discriminant Between Earthquakes and Explosions, *Bull. Seism. Soc. Am.*, *71*, 249-261.

Office of Technology Assessment (1988). Seismic Verification of Nuclear Testing Treaties, U. S. Congress OTA Report No. OTA-ISC-361.

Piwinskii, A. J., and D. L. Springer (1978). Propagation of L_g Waves Across Eastern Europe and Asia, Lawrence Livermore National Laboratory Report, LLNL Report No. UCRL-52494.

Press, F., and M. Ewing (1952). Two Slow Surface Waves Across North America, *Bull. Seism. Soc. Am.*, *42*, 219-228.

Rodean, H. C. (1979). ISC Events from 1964 to 1976 At and Near the Nuclear Testing Ground in Eastern Kazakhstan, Lawrence Livermore National Laboratory Report, LLNL Report No. UCRL-52856.

Ruzaikin, A., I. Nersesov, U. Khalturin, and P. Molnar (1977). Propagation of L_g and Lateral Variations in the Crustal Structure of Asia, *J. Geophys. Res.*, *82*, 307-316.

Taylor, S. R., N. W. Sherman, and M. D. Denny (1988). Spectral Discrimination Between NTS Explosions and Western United States Earthquakes at Regional Distances, *Bull. Seism. Soc. Am.*, 1563-1579.

DISTRIBUTION LIST

Prof. Thomas Ahrens
Seismological Lab, 252-21
Division of Geological & Planetary Sciences
California Institute of Technology
Pasadena, CA 91125

Prof. Keiiti Aki
Center for Earth Sciences
University of Southern California
University Park
Los Angeles, CA 90089-0741

Prof. Shelton Alexander
Geosciences Department
403 Deike Building
The Pennsylvania State University
University Park, PA 16802

Dr. Ralph Alewine, III
DARPA/NMRO
3701 North Fairfax Drive
Arlington, VA 22203-1714

Prof. Charles B. Archambeau
CIRES
University of Colorado
Boulder, CO 80309

Dr. Thomas C. Bache, Jr.
Science Applications Int'l Corp.
10260 Campus Point Drive
San Diego, CA 92121 (2 copies)

Prof. Muawia Barazangi
Institute for the Study of the Continent
Cornell University
Ithaca, NY 14853

Dr. Jeff Barker
Department of Geological Sciences
State University of New York
at Binghamton
Vestal, NY 13901

Dr. Douglas R. Baumgardt
ENSCO, Inc
5400 Port Royal Road
Springfield, VA 22151-2388

Dr. Susan Beck
Department of Geosciences
Building #77
University of Arizona
Tuscon, AZ 85721

Dr. T.J. Bennett
S-CUBED
A Division of Maxwell Laboratories
11800 Sunrise Valley Drive, Suite 1212
Reston, VA 22091

Dr. Robert Blandford
AFTAC/TT, Center for Seismic Studies
1300 North 17th Street
Suite 1450
Arlington, VA 22209-2308

Dr. G.A. Bollinger
Department of Geological Sciences
Virginia Polytechnical Institute
21044 Derring Hall
Blacksburg, VA 24061

Dr. Stephen Bratt
Center for Seismic Studies
1300 North 17th Street
Suite 1450
Arlington, VA 22209-2308

Dr. Lawrence Burdick
Woodward-Clyde Consultants
566 El Dorado Street
Pasadena, CA 91109-3245

Dr. Robert Burridge
Schlumberger-Doll Research Center
Old Quarry Road
Ridgefield, CT 06877

Dr. Jerry Carter
Center for Seismic Studies
1300 North 17th Street
Suite 1450
Arlington, VA 22209-2308

Dr. Eric Chael
Division 9241
Sandia Laboratory
Albuquerque, NM 87185

Prof. Vernon F. Cormier
Department of Geology & Geophysics
U-45, Room 207
University of Connecticut
Storrs, CT 06268

Prof. Steven Day
Department of Geological Sciences
San Diego State University
San Diego, CA 92182

Marvin Denny
U.S. Department of Energy
Office of Arms Control
Washington, DC 20585

Dr. Zoltan Der
ENSCO, Inc.
5400 Port Royal Road
Springfield, VA 22151-2388

Prof. Adam Dziewonski
Hoffman Laboratory, Harvard University
Dept. of Earth Atmos. & Planetary Sciences
20 Oxford Street
Cambridge, MA 02138

Prof. John Ebel
Department of Geology & Geophysics
Boston College
Chestnut Hill, MA 02167

Eric Fielding
SNEE Hall
INSTOC
Cornell University
Ithaca, NY 14853

Dr. Mark D. Fisk
Mission Research Corporation
735 State Street
P.O. Drawer 719
Santa Barbara, CA 93102

Prof Stanley Flatte
Applied Sciences Building
University of California, Santa Cruz
Santa Cruz, CA 95064

Dr. John Foley
NER-Geo Sciences
1100 Crown Colony Drive
Quincy, MA 02169

Prof. Donald Forsyth
Department of Geological Sciences
Brown University
Providence, RI 02912

Dr. Art Frankel
U.S. Geological Survey
922 National Center
Reston, VA 22092

Dr. Cliff Frolich
Institute of Geophysics
8701 North Mopac
Austin, TX 78759

Dr. Holly Given
IGPP, A-025
Scripps Institute of Oceanography
University of California, San Diego
La Jolla, CA 92093

Dr. Jeffrey W. Given
SAIC
10260 Campus Point Drive
San Diego, CA 92121

Dr. Dale Glover
Defense Intelligence Agency
ATTN: ODT-1B
Washington, DC 20301

Dr. Indra Gupta
Teledyne Geotech
314 Montgomery Street
Alexanderia, VA 22314

Dan N. Hagedon
Pacific Northwest Laboratories
Battelle Boulevard
Richland, WA 99352

Dr. James Hannon
Lawrence Livermore National Laboratory
P.O. Box 808
L-205
Livermore, CA 94550

Dr. Roger Hansen
HQ AFTAC/TTR
Patrick AFB, FL 32925-6001

Prof. David G. Harkrider
Seismological Laboratory
Division of Geological & Planetary Sciences
California Institute of Technology
Pasadena, CA 91125

Prof. Danny Harvey
CIRES
University of Colorado
Boulder, CO 80309

Prof. Donald V. Helmberger
Seismological Laboratory
Division of Geological & Planetary Sciences
California Institute of Technology
Pasadena, CA 91125

Prof. Eugene Herrin
Institute for the Study of Earth and Man
Geophysical Laboratory
Southern Methodist University
Dallas, TX 75275

Prof. Robert B. Herrmann
Department of Earth & Atmospheric Sciences
St. Louis University
St. Louis, MO 63156

Prof. Lane R. Johnson
Seismographic Station
University of California
Berkeley, CA 94720

Prof. Thomas H. Jordan
Department of Earth, Atmospheric &
Planetary Sciences
Massachusetts Institute of Technology
Cambridge, MA 02139

Prof. Alan Kafka
Department of Geology & Geophysics
Boston College
Chestnut Hill, MA 02167

Robert C. Kemerait
ENSCO, Inc.
445 Pineda Court
Melbourne, FL 32940

Dr. Max Koontz
U.S. Dept. of Energy/DP 5
Forrestal Building
1000 Independence Avenue
Washington, DC 20585

Dr. Richard LaCoss
MIT Lincoln Laboratory, M-200B
P.O. Box 73
Lexington, MA 02173-0073

Dr. Fred K. Lamb
University of Illinois at Urbana-Champaign
Department of Physics
1110 West Green Street
Urbana, IL 61801

Prof. Charles A. Langston
Geosciences Department
403 Deike Building
The Pennsylvania State University
University Park, PA 16802

Jim Lawson, Chief Geophysicist
Oklahoma Geological Survey
Oklahoma Geophysical Observatory
P.O. Box 8
Leonard, OK 74043-0008

Prof. Thorne Lay
Institute of Tectonics
Earth Science Board
University of California, Santa Cruz
Santa Cruz, CA 95064

Dr. William Leith
U.S. Geological Survey
Mail Stop 928
Reston, VA 22092

Mr. James F. Lewkowicz
Phillips Laboratory/GPEH
Hanscom AFB, MA 01731-5000(2 copies)

Mr. Alfred Lieberman
ACDA/VI-OA State Department Building
Room 5726
320-21st Street, NW
Washington, DC 20451

Prof. L. Timothy Long
School of Geophysical Sciences
Georgia Institute of Technology
Atlanta, GA 30332

Dr. Randolph Martin, III
New England Research, Inc.
76 Olcott Drive
White River Junction, VT 05001

Dr. Robert Masse
Denver Federal Building
Box 25046, Mail Stop 967
Denver, CO 80225

Dr. Gary McCartor
Department of Physics
Southern Methodist University
Dallas, TX 75275

Prof. Thomas V. McEvilly
Seismographic Station
University of California
Berkeley, CA 94720

Dr. Art McGarr
U.S. Geological Survey
Mail Stop 977
U.S. Geological Survey
Menlo Park, CA 94025

Dr. Keith L. McLaughlin
S-CUBED
A Division of Maxwell Laboratory
P.O. Box 1620
La Jolla, CA 92038-1620

Stephen Miller & Dr. Alexander Florence
SRI International
333 Ravenswood Avenue
Box AF 116
Menlo Park, CA 94025-3493

Prof. Bernard Minster
IGPP, A-025
Scripps Institute of Oceanography
University of California, San Diego
La Jolla, CA 92093

Prof. Brian J. Mitchell
Department of Earth & Atmospheric Sciences
St. Louis University
St. Louis, MO 63156

Mr. Jack Murphy
S-CUBED
A Division of Maxwell Laboratory
11800 Sunrise Valley Drive, Suite 1212
Reston, VA 22091 (2 Copies)

Dr. Keith K. Nakanishi
Lawrence Livermore National Laboratory
L-025
P.O. Box 808
Livermore, CA 94550

Dr. Carl Newton
Los Alamos National Laboratory
P.O. Box 1663
Mail Stop C335, Group ESS-3
Los Alamos, NM 87545

Dr. Bao Nguyen
HQ AFTAC/TTR
Patrick AFB, FL 32925-6001

Prof. John A. Orcutt
IGPP, A-025
Scripps Institute of Oceanography
University of California, San Diego
La Jolla, CA 92093

Prof. Jeffrey Park
Kline Geology Laboratory
P.O. Box 6666
New Haven, CT 06511-8130

Dr. Howard Patton
Lawrence Livermore National Laboratory
L-025
P.O. Box 808
Livermore, CA 94550

Dr. Frank Pilotte
HQ AFTAC/TT
Patrick AFB, FL 32925-6001

Dr. Jay J. Pulli
Radix Systems, Inc.
2 Taft Court, Suite 203
Rockville, MD 20850

Dr. Robert Reinke
ATTN: FCTVTD
Field Command
Defense Nuclear Agency
Kirtland AFB, NM 87115

Prof. Paul G. Richards
Lamont-Doherty Geological Observatory
of Columbia University
Palisades, NY 10964

Mr. Wilmer Rivers
Teledyne Geotech
314 Montgomery Street
Alexandria, VA 22314

Dr. George Rothe
HQ AFTAC/TTR
Patrick AFB, FL 32925-6001

Dr. Alan S. Ryall, Jr.
DARPA/NMRO
3701 North Fairfax Drive
Arlington, VA 22209-1714

Dr. Richard Sailor
TASC, Inc.
55 Walkers Brook Drive
Reading, MA 01867

Prof. Charles G. Sammis
Center for Earth Sciences
University of Southern California
University Park
Los Angeles, CA 90089-0741

Prof. Christopher H. Scholz
Lamont-Doherty Geological Observatory
of Columbia University
Palisades, CA 10964

Dr. Susan Schwartz
Institute of Tectonics
1156 High Street
Santa Cruz, CA 95064

Secretary of the Air Force
(SAFRD)
Washington, DC 20330

Office of the Secretary of Defense
DDR&E
Washington, DC 20330

Thomas J. Sereno, Jr.
Science Application Int'l Corp.
10260 Campus Point Drive
San Diego, CA 92121

Dr. Michael Shore
Defense Nuclear Agency/SPSS
6801 Telegraph Road
Alexandria, VA 22310

Dr. Matthew Sibol
Virginia Tech
Seismological Observatory
4044 Derring Hall
Blacksburg, VA 24061-0420

Prof. David G. Simpson
IRIS, Inc.
1616 North Fort Myer Drive
Suite 1440
Arlington, VA 22209

Donald L. Springer
Lawrence Livermore National Laboratory
L-025
P.O. Box 808
Livermore, CA 94550

Dr. Jeffrey Stevens
S-CUBED
A Division of Maxwell Laboratory
P.O. Box 1620
La Jolla, CA 92038-1620

Lt. Col. Jim Stobie
ATTN: AFOSR/NL
Bolling AFB
Washington, DC 20332-6448

Prof. Brian Stump
Institute for the Study of Earth & Man
Geophysical Laboratory
Southern Methodist University
Dallas, TX 75275

Prof. Jeremiah Sullivan
University of Illinois at Urbana-Champaign
Department of Physics
1110 West Green Street
Urbana, IL 61801

Prof. L. Sykes
Lamont-Doherty Geological Observatory
of Columbia University
Palisades, NY 10964

Dr. David Taylor
ENSCO, Inc.
445 Pineda Court
Melbourne, FL 32940

Dr. Steven R. Taylor
Los Alamos National Laboratory
P.O. Box 1663
Mail Stop C335
Los Alamos, NM 87545

Prof. Clifford Thurber
University of Wisconsin-Madison
Department of Geology & Geophysics
1215 West Dayton Street
Madison, WS 53706

Prof. M. Nafi Toksoz
Earth Resources Lab
Massachusetts Institute of Technology
42 Carleton Street
Cambridge, MA 02142

Dr. Larry Turnbull
CIA-OSWR/NED
Washington, DC 20505

Dr. Gregory van der Vink
IRIS, Inc.
1616 North Fort Myer Drive
Suite 1440
Arlington, VA 22209

Dr. Karl Veith
EG&G
5211 Auth Road
Suite 240
Suitland, MD 20746

Prof. Terry C. Wallace
Department of Geosciences
Building #77
University of Arizona
Tuscon, AZ 85721

Dr. Thomas Weaver
Los Alamos National Laboratory
P.O. Box 1663
Mail Stop C335
Los Alamos, NM 87545

Dr. William Wortman
Mission Research Corporation
8560 Cinderbed Road
Suite 700
Newington, VA 22122

Prof. Francis T. Wu
Department of Geological Sciences
State University of New York
at Binghamton
Vestal, NY 13901

AFTAC/CA
(STINFO)
Patrick AFB, FL 32925-6001

DARPA/PM
3701 North Fairfax Drive
Arlington, VA 22203-1714

DARPA/RMO/RETRIEVAL
3701 North Fairfax Drive
Arlington, VA 22203-1714

DARPA/RMO/SECURITY OFFICE
3701 North Fairfax Drive
Arlington, VA 22203-1714

HQ DNA
ATTN: Technical Library
Washington, DC 20305

Defense Intelligence Agency
Directorate for Scientific & Technical Intelligence
ATTN: DTIB
Washington, DC 20340-6158

Defense Technical Information Center
Cameron Station
Alexandria, VA 22314 (2 Copies)

TACTEC
Battelle Memorial Institute
505 King Avenue
Columbus, OH 43201 (Final Report)

Phillips Laboratory
ATTN: XPG
Hanscom AFB, MA 01731-5000

Phillips Laboratory
ATTN: GPE
Hanscom AFB, MA 01731-5000

Phillips Laboratory
ATTN: TSML
Hanscom AFB, MA 01731-5000

Phillips Laboratory
ATTN: SUL
Kirtland, NM 87117 (2 copies)

Dr. Michel Bouchon
I.R.I.G.M.-B.P. 68
38402 St. Martin D'Heres
Cedex, FRANCE

Dr. Michel Campillo
Observatoire de Grenoble
I.R.I.G.M.-B.P. 53
38041 Grenoble, FRANCE

Dr. Kin Yip Chun
Geophysics Division
Physics Department
University of Toronto
Ontario, CANADA

Prof. Hans-Peter Harjes
Institute for Geophysic
Ruhr University/Bochum
P.O. Box 102148
4630 Bochum 1, GERMANY

Prof. Eystein Husebye
NTNF/NORSAR
P.O. Box 51
N-2007 Kjeller, NORWAY

David Jepsen
Acting Head, Nuclear Monitoring Section
Bureau of Mineral Resources
Geology and Geophysics
G.P.O. Box 378, Canberra, AUSTRALIA

Ms. Eva Joh... son
Se... r Researc... Officer
National Defense Research Inst.
P.O. Box 27322
S-102 54 Stockholm, SWEDEN

Dr. Peter Marshall
Procurement Executive
Ministry of Defense
Blacknest, Brimpton
Reading FG7-FRS, UNITED KINGDOM

Dr. Bernard Massinon, Dr. Pierre Mechler
Societe Radiomana
27 rue Claude Bernard
75005 Paris, FRANCE (2 Copies)

Dr. Svein Mykkeltveit
NTNT/NORSAR
P.O. Box 51
N-2007 Kjeller, NORWAY (3 Copies)

Prof. Keith Priestley
University of Cambridge
Bullard Labs, Dept. of Earth Sciences
Madingley Rise, Madingley Road
Cambridge CB3 OEZ, ENGLAND

Dr. Jorg Schlittenhardt
Federal Institute for Geosciences & Nat'l Res.
Postfach 510153
D-3000 Hannover 51, GERMANY

Dr. Johannes Schweitzer
Institute of Geophysics
Ruhr University/Bochum
P.O. Box 1102148
4360 Bochum 1, GERMANY